FUNDAMENTALS OF TEXTURE PROCESSING FOR BIOMEDICAL IMAGE ANALYSIS

Adrien Depeursinge, PhD

MICCAI 2015 Tutorial on Biomedical Texture Analysis (BTA), Munich, Oct 5 2015

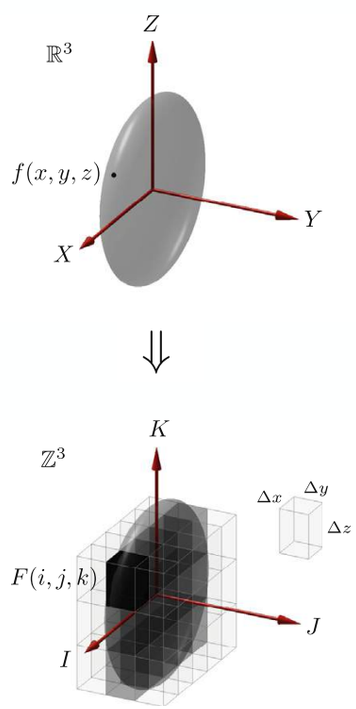

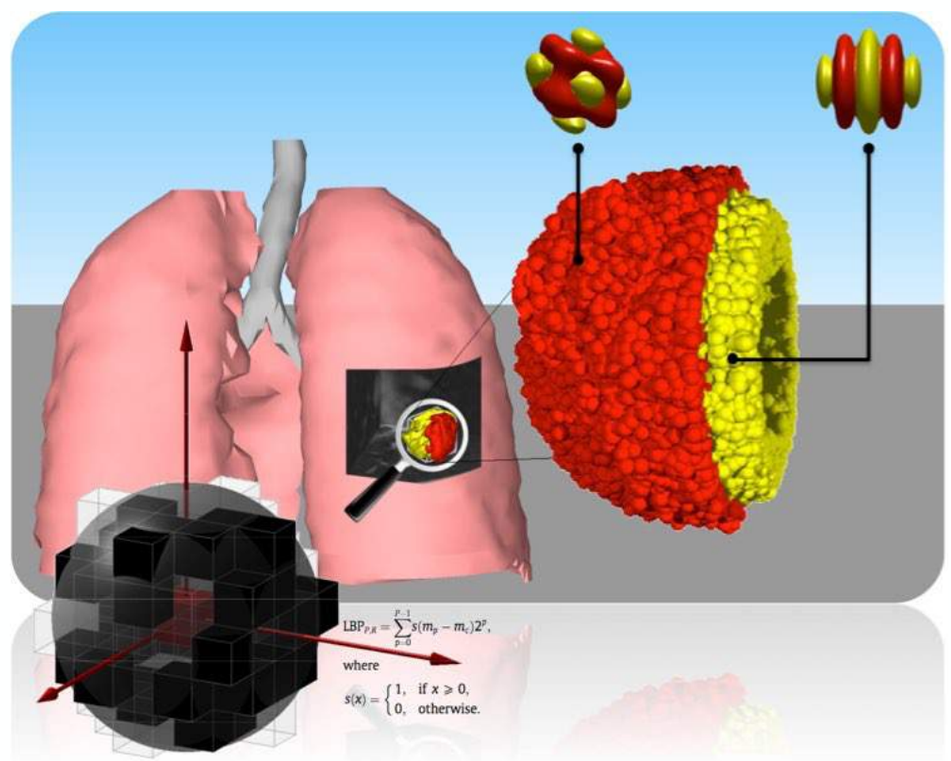

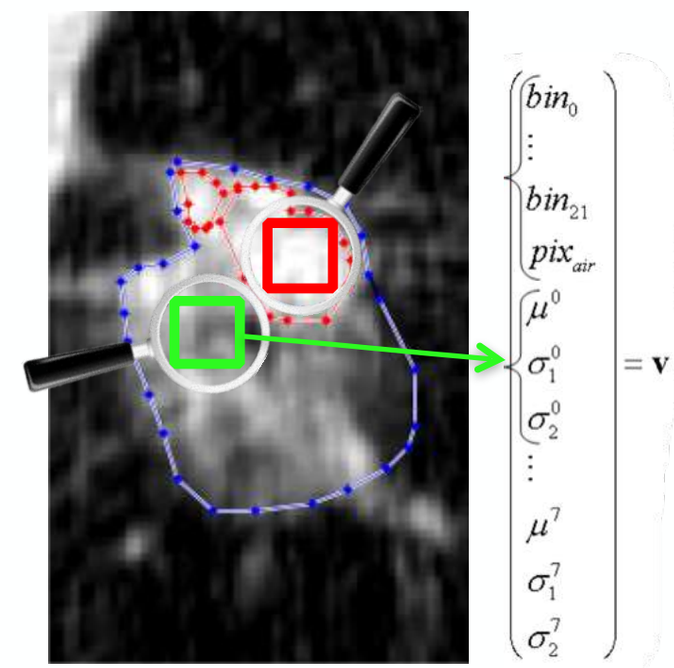

ÉCOLE POLYTECHNIQUE FÉDÉRALE DE LAUSANNE

[BIG]

MICCAI'15 MUNICH

Hes·so VALAIS WALLIS
School of Management & Tourism

OUTLINE

- Biomedical texture analysis: background
- Defining texture processes
  - Notations, sampling and texture functions
- Texture operators, primitives and invariances
  - Multiscale analysis
    - Operator scale and uncertainty principle
    - Region of interest and operator aggregation
  - Multidirectional analysis
    - Isotropic versus directional operators
    - Importance of the local organization of image directions
- Conclusions
- References

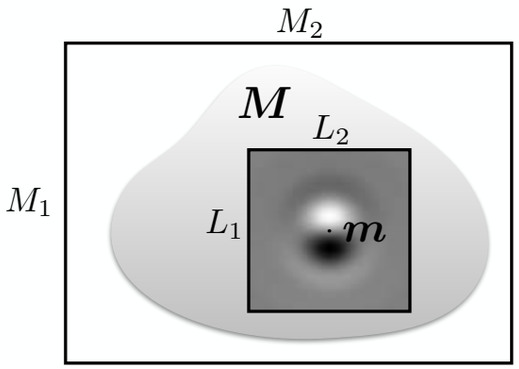

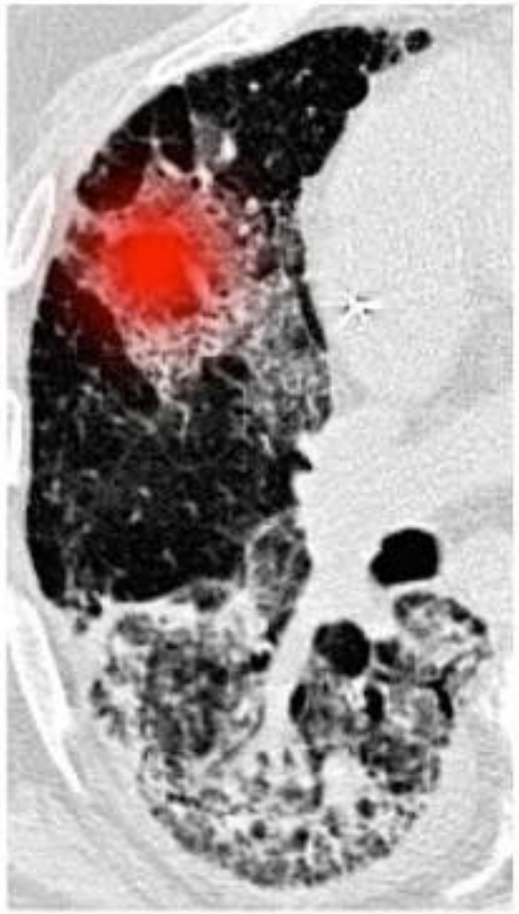

Hes·so VALAIS WALLIS
School of Management & Tourism

Background – Radiomics - Histopatholomics

- Personalized medicine aims at enhancing the patient's quality of life and prognosis
  - Tailored treatment and medical decisions based on the molecular composition of diseased tissue
- Current limitations [Gerlinger2012]
  - Molecular analysis of tissue composition is invasive (biopsy), slow and costly
  - Cannot capture molecular heterogeneity

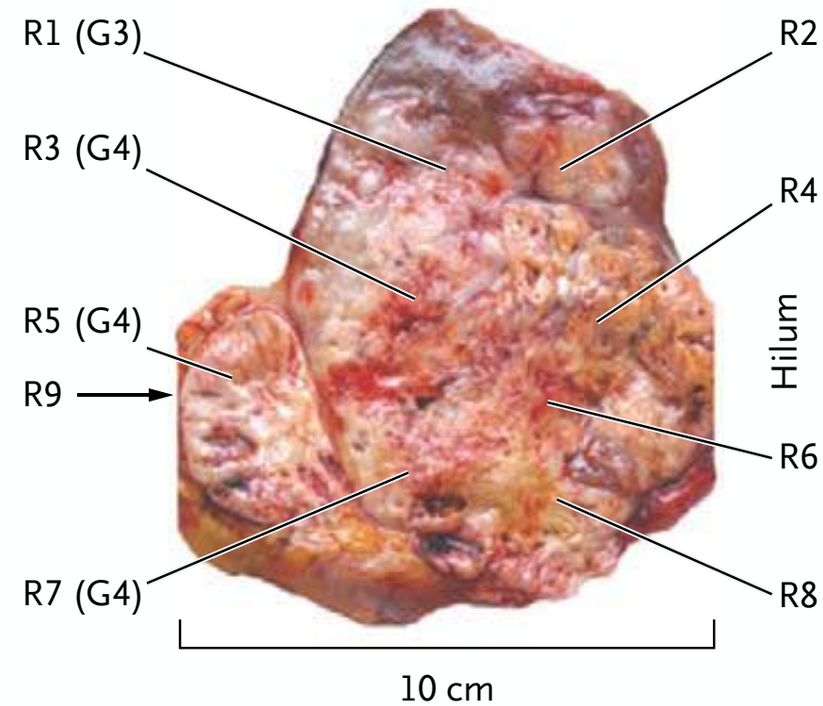

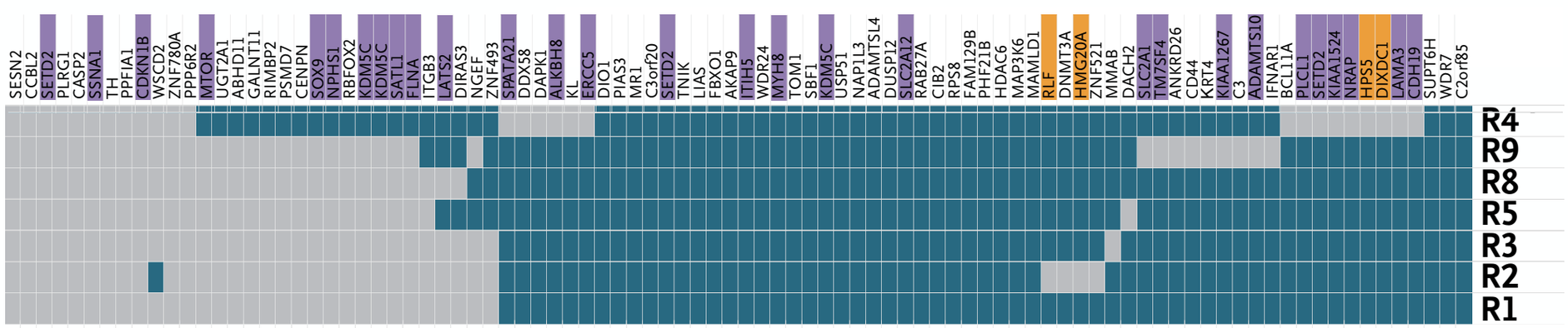

Background – Radiomics - Histopatholomics

- Huge potential for computerized medical image analysis
  - Explore and reveal tissue structures related to tissue composition, function, ….
    - Local quantitative image feature extraction
    - Supervised and unsupervised machine learning

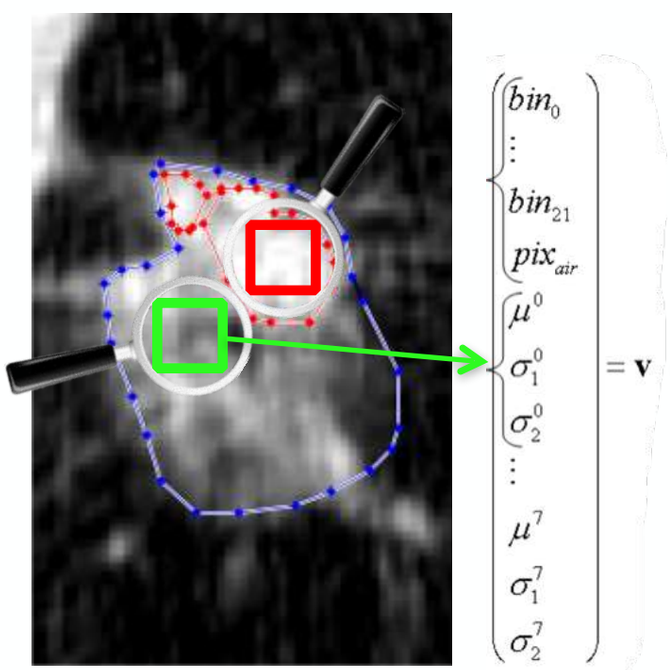

$$\begin{pmatrix} bin_0 \\ \vdots \\ bin_{21} \\ pix_{air} \\ \mu^0 \\ \sigma_1^0 \\ \sigma_2^0 \\ \vdots \\ \mu^7 \\ \sigma_1^7 \\ \sigma_2^7 \end{pmatrix} = \mathbf{v}$$

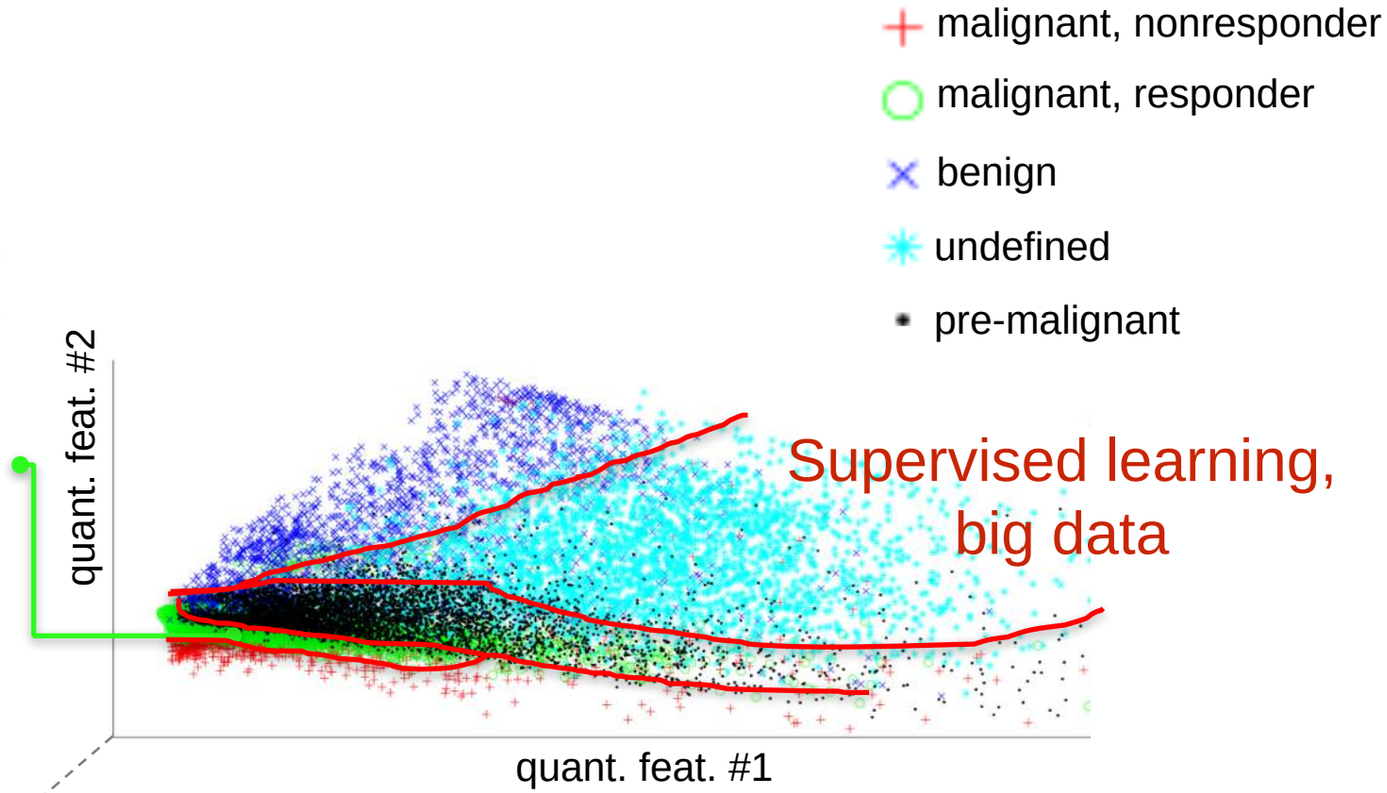

Background – Radiomics - Histopatholomics

- Huge potential for computerized medical image analysis
  - Create imaging biomarkers to predict diagnosis, prognosis, treatment response [Aerts2014]

	Radiomics [Kumar2012]		"Histopatholomics" [Gurcan2009]	
Reuse existing diagnostic images	✓	radiology data[1]	✓	digital pathology
Capture tissue heterogeneity	✓	3D neighborhoods (e.g., 512x512x512)	✓	large 2D regions (e.g., 15,000x15,000)
Analytic power beyond naked eyes	✓	complex 3D tissue morphology	✓	exhaustive characterization of 2D tissue structures
Non-invasive	✓		✗	

[1]e.g., X-ray, Ultrasound, CT, MRI, PET, OCT, …

Background – Radiomics - Histopatholomics

- Huge potential for computerized medical image analysis
  - Explore and reveal tissue structures related to tissue composition, function, ….
    - Local quantitative image feature extraction
    - Supervised and unsupervised machine learning

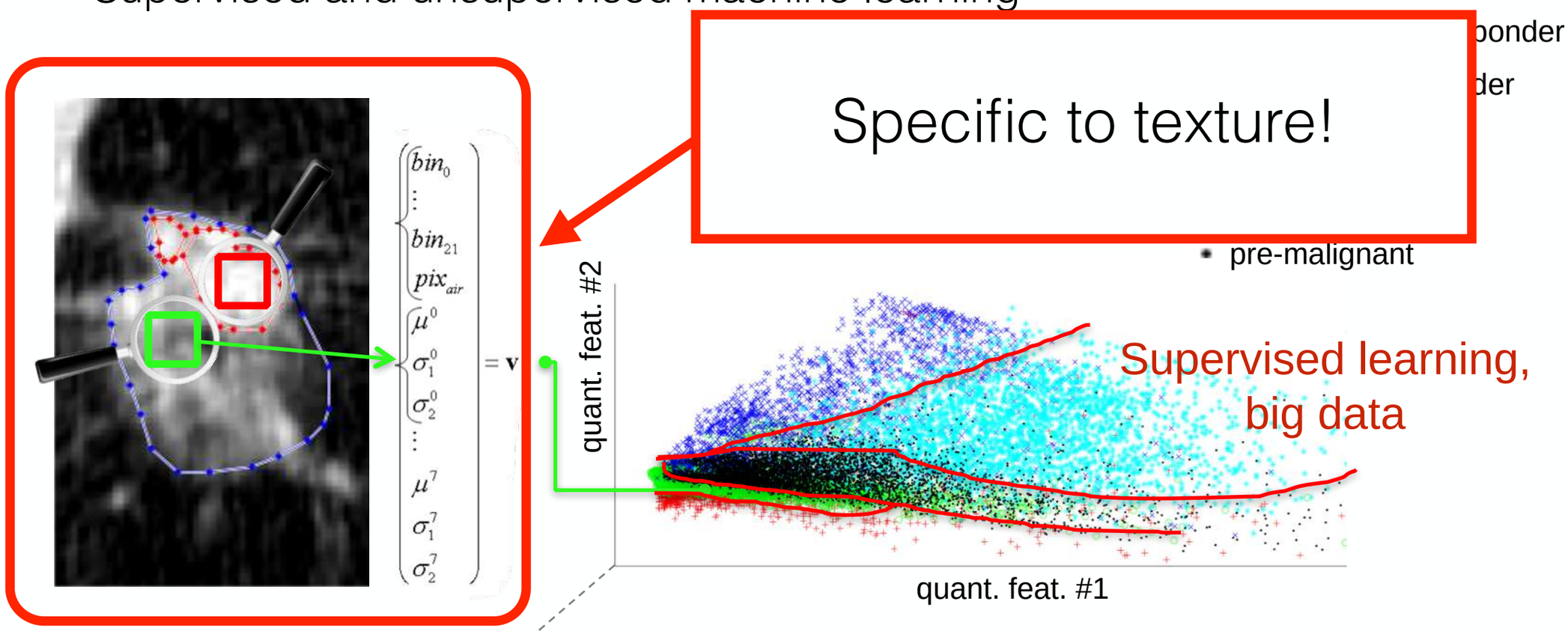

OUTLINE

- Biomedical texture analysis: background
- Defining texture processes
  - Notations, sampling and texture functions
- Texture operators, primitives and invariances
  - Multiscale analysis
    - Operator scale and uncertainty principle
    - Region of interest and operator aggregation
  - Multidirectional analysis
    - Isotropic versus directional operators
    - Importance of the local organization of image directions
- Conclusions
- References

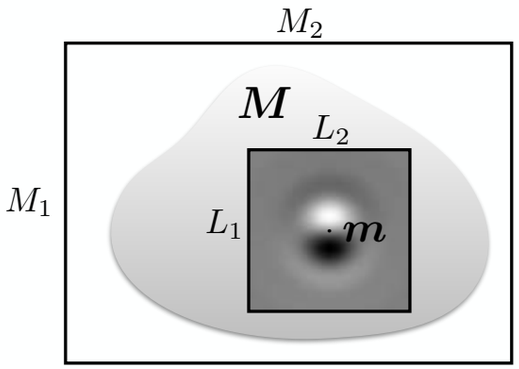

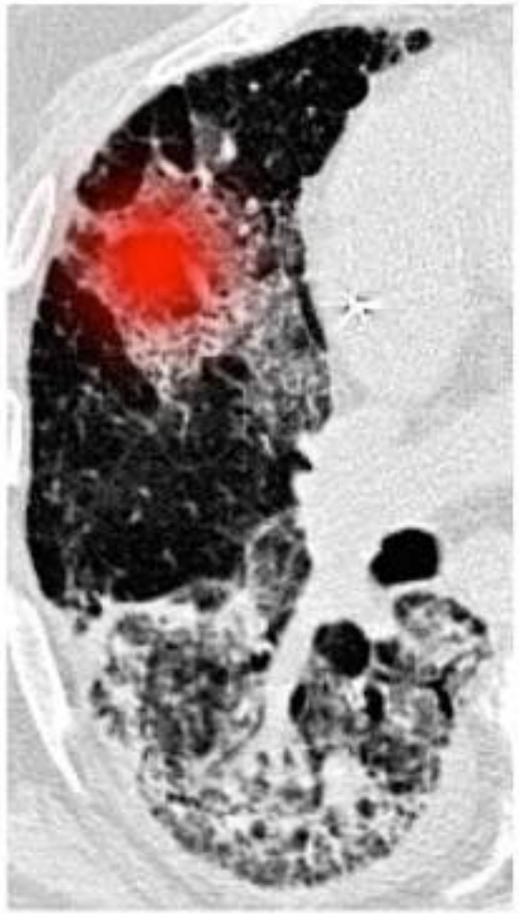

Hes·so VALAIS WALLIS
School of Management & Tourism

Computerized texture analysis

- Definition of texture
  - Everybody agrees that nobody agrees on the definition of “texture” (context-dependent)
    - “coarse”, “edgy”, “directional”, “repetitive”, “random”, …
  - Oxford dictionary: “the feel, appearance, or consistency of a surface or a substance”
  - [Haidekker2011]: “Texture is a systematic local variation of the image values”
  - [Petrou2011]: “The most important characteristic of texture is that it is scale dependent. Different types of texture are visible at different scales”

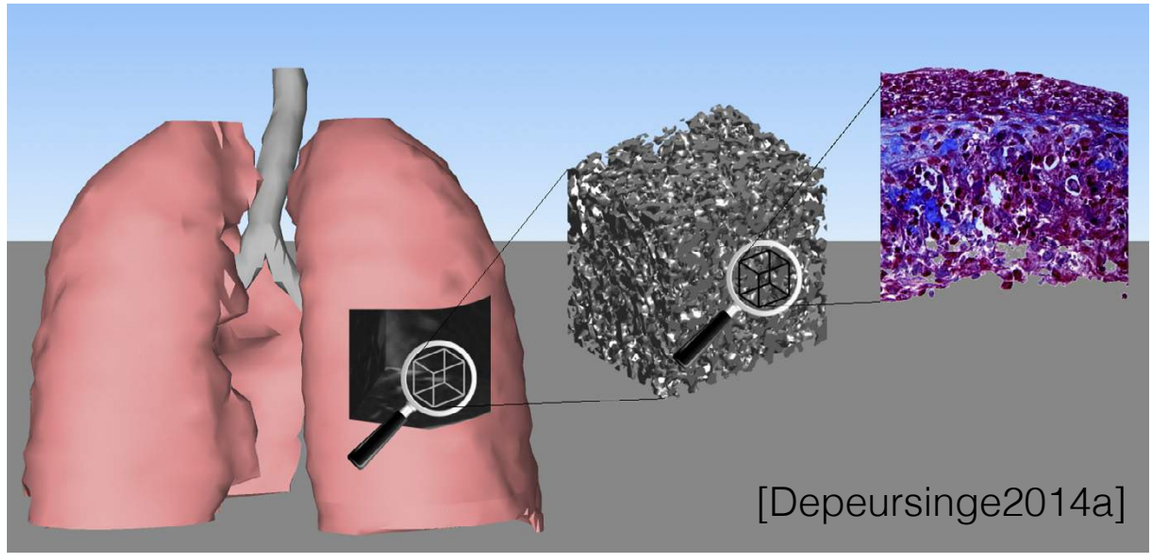

Computerized texture analysis

- Spatial scales and directions in images are fundamental for visual texture discrimination [Blakemore1969, Romeny2011]

scales

directions

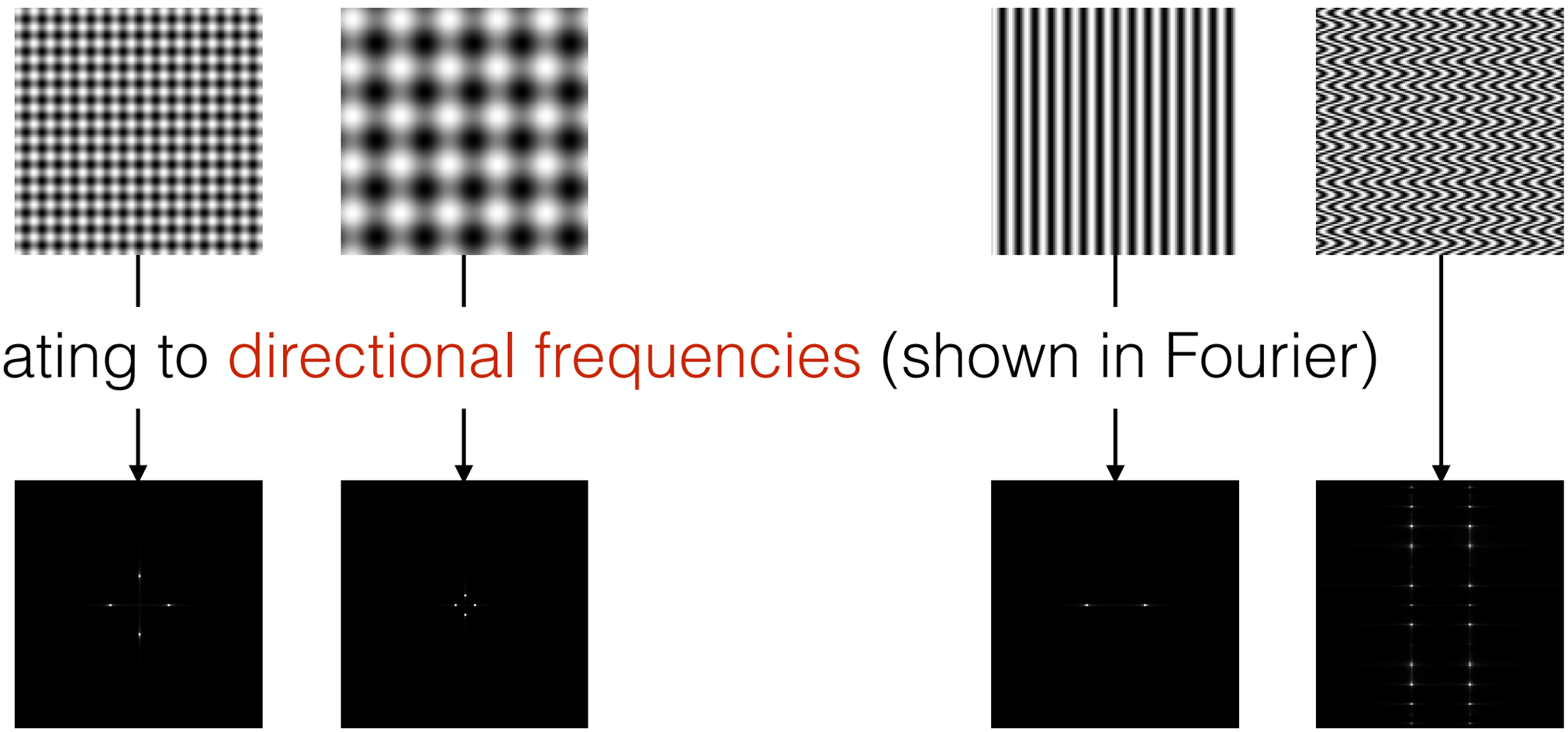

- Relating to directional frequencies (shown in Fourier)

Computerized texture analysis

- Spatial scales and directions in images are fundamental for visual texture discrimination [Blakemore1969, Romeny2011]

scales

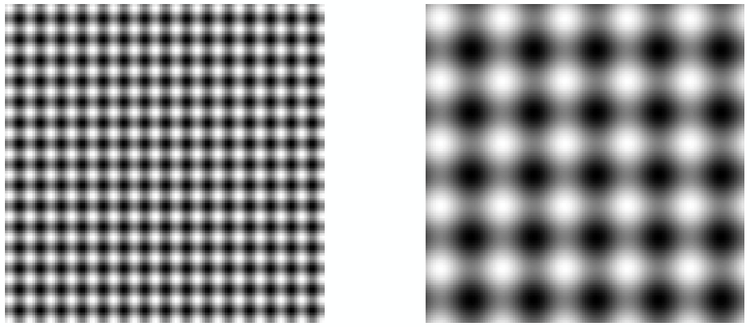

directions

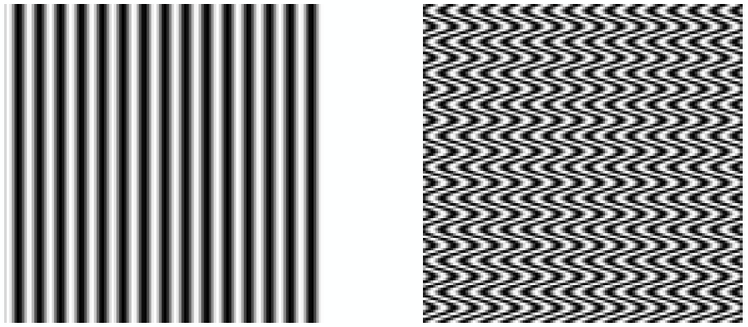

- Most approaches are leveraging these two properties
  - Explicitly: Gray-level co-occurrence matrices (GLCM), run-length matrices (RLE), directional filterbanks and wavelets, Fourier, histograms of gradients (HOG), local binary patterns (LBP)
  - Implicitly: Convolutional neural networks (CNN), scattering transform, topographic independant component analysis (TICA)

NOTATIONS, SAMPLING AND TEXTURE FUNCTIONS

- 2-D continuous texture functions in space and Fourier
  - Cartesian coordinates: $f(\boldsymbol{x}),\ \boldsymbol{x} = \begin{pmatrix} x_1 \\ x_2 \end{pmatrix} \in \mathbb{R}^2, \quad f(\boldsymbol{x}) \xrightarrow{\mathcal{F}} \hat{f}(\boldsymbol{\omega}) = \int_{\mathbb{R}^2} f(\boldsymbol{x}) e^{-j\langle \boldsymbol{\omega}, \boldsymbol{x} \rangle} \mathrm{d}\boldsymbol{x},\ \boldsymbol{\omega} \in \mathbb{R}^2$
  - Polar coordinates: $f(r,\theta), r \in \mathbb{R}^+, \theta \in [0, 2\pi), \quad f(r,\theta) \xrightarrow{\mathcal{F}} \hat{f}(\rho,\phi), \rho \in \mathbb{R}^+, \phi \in [0, 2\pi)$
- 2-D digital texture functions
  - Cartesian coordinates: $f(\boldsymbol{k}), \quad \boldsymbol{k} = \begin{pmatrix} k_1 \\ k_2 \end{pmatrix} \in \mathbb{Z}^2$
  - Polar coordinates: $f(R,\Theta), \quad R \in \mathbb{Z}^+, \Theta \in [0, 2\pi)$
- Sampling (Cartesian)
  - Increments in (k_1, k_2) corresponds to physical displacements in $\mathbb{R}^2$ as

$$\begin{pmatrix} x_1 \\ x_2 \end{pmatrix} = \begin{pmatrix} \Delta x_1 \cdot k_1 \\ \Delta x_2 \cdot k_2 \end{pmatrix}$$

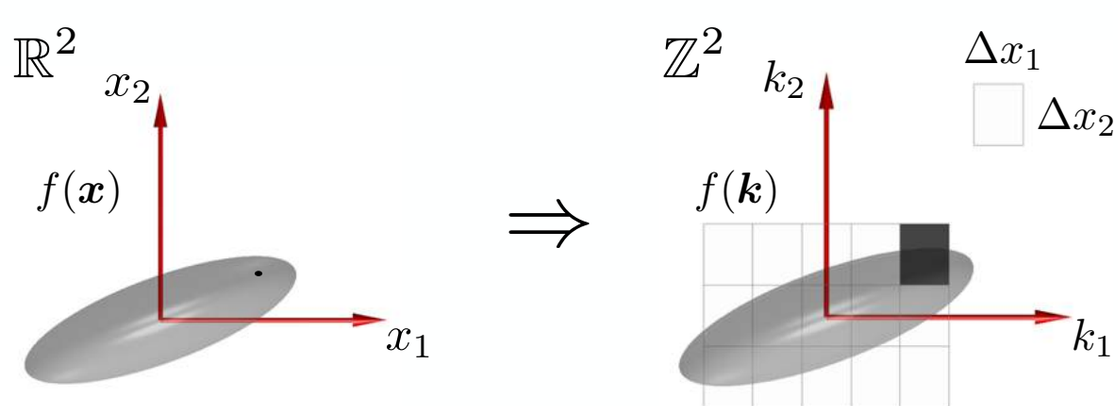

ÉCOLE POLYTECHNIQUE FÉDÉRALE DE LAUSANNE

NOTATIONS, SAMPLING AND TEXTURE FUNCTIONS

- 3-D continuous texture functions in space and Fourier
  - Cartesian coordinates: $f(\boldsymbol{x}),\ \boldsymbol{x} = \begin{pmatrix} x_1 \\ x_2 \\ x_3 \end{pmatrix} \in \mathbb{R}^3, \quad f(\boldsymbol{x}) \xrightarrow{\mathcal{F}} \hat{f}(\boldsymbol{\omega}) = \int_{\mathbb{R}^3} f(\boldsymbol{x}) e^{-j\langle \boldsymbol{\omega}, \boldsymbol{x} \rangle} \mathrm{d}\boldsymbol{x},\ \boldsymbol{\omega} \in \mathbb{R}^3$
  - Polar coordinates: $f(r, \theta, \phi), \quad r \in \mathbb{R}^+, \theta \in [0, 2\pi), \phi \in [0, 2\pi)$
- 3-D digital texture functions
  - Cartesian coordinates: $f(\boldsymbol{k}), \quad \boldsymbol{k} = \begin{pmatrix} k_1 \\ k_2 \\ k_3 \end{pmatrix} \in \mathbb{Z}^3$
  - Polar coordinates: $f(R, \Theta, \Phi), \quad R \in \mathbb{Z}^+, \Theta \in [0, 2\pi), \Phi \in [0, 2\pi)$
- Sampling (Cartesian)
  - Increments in (k_1, k_2, k_3) corresponds to physical displacements in $\mathbb{R}^3$ as

$$\begin{pmatrix} x_1 \\ x_2 \\ x_3 \end{pmatrix} = \begin{pmatrix} \Delta x_1 \cdot k_1 \\ \Delta x_2 \cdot k_2 \\ \Delta x_3 \cdot k_3 \end{pmatrix}$$

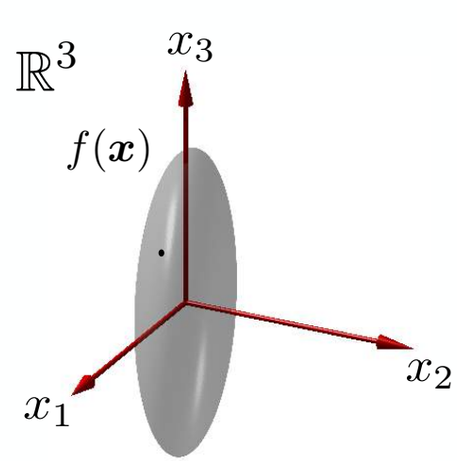

$\Rightarrow$

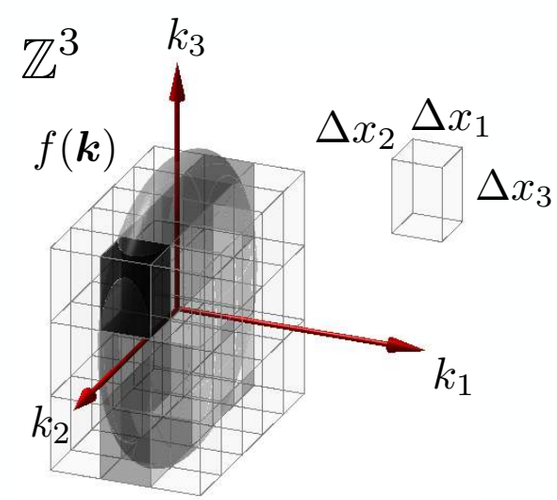

ÉCOLE POLYTECHNIQUE FÉDÉRALE DE LAUSANNE

NOTATIONS, SAMPLING AND TEXTURE FUNCTIONS

- We consider a texture function $f(\boldsymbol{x})$ as a realization of a spatial stochastic process of $\mathbb{R}^d$

$$\{X_{\boldsymbol{m}}, \boldsymbol{m} \in \mathbb{R}^{M_1 \times \cdots \times M_d}\}$$

where $X_{\boldsymbol{m}}$ is the value at the spatial position indexed by $\boldsymbol{m}$

  - The values of $X_{\boldsymbol{m}}$ follow one or several probability density functions $f_{\boldsymbol{X}_m}(q)$

- Examples

moving average Gaussian

$\boldsymbol{m} \in \mathbb{R}^{128 \times 128}$

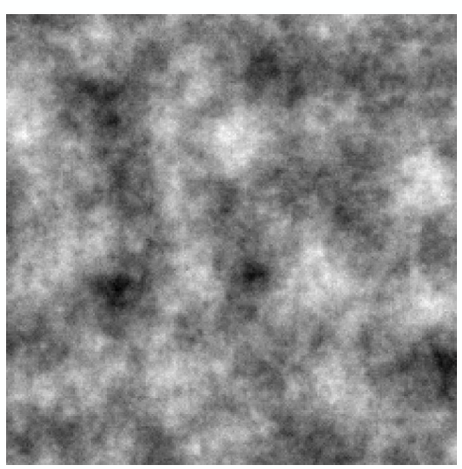

pointwise Poisson

$\boldsymbol{m} \in \mathbb{R}^{32 \times 32}$

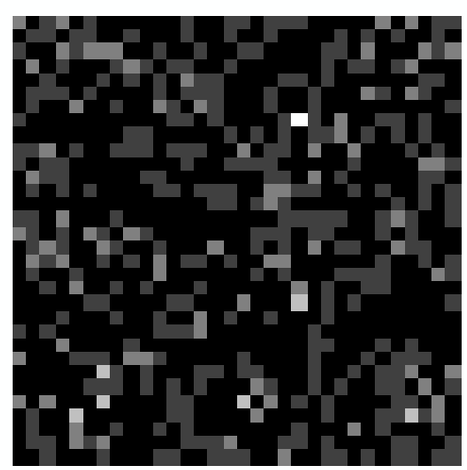

biomedical: lung fibrosis in CT

$\boldsymbol{m} \in \mathbb{R}^{84 \times 84}$

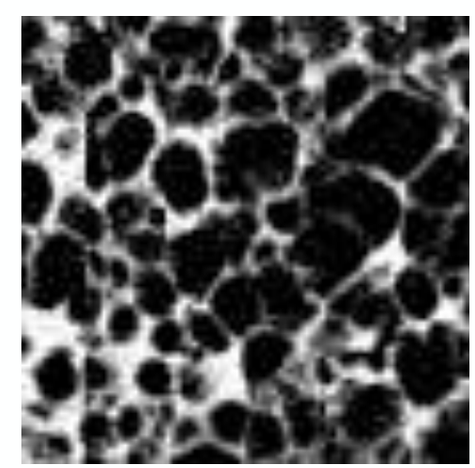

NOTATIONS, SAMPLING AND TEXTURE FUNCTIONS

- Stationarity of spatial stochastic processes
  - A spatial process $\{X_{\boldsymbol{m}}, \boldsymbol{m} \in \mathbb{R}^{M_1 \times \cdots \times M_d}\}$ is stationary if the probability density functions $f_{\boldsymbol{X}_m}(q)$ are equivalent for all $\boldsymbol{m}$

- Example: heteroscedastic moving average Gaussian process

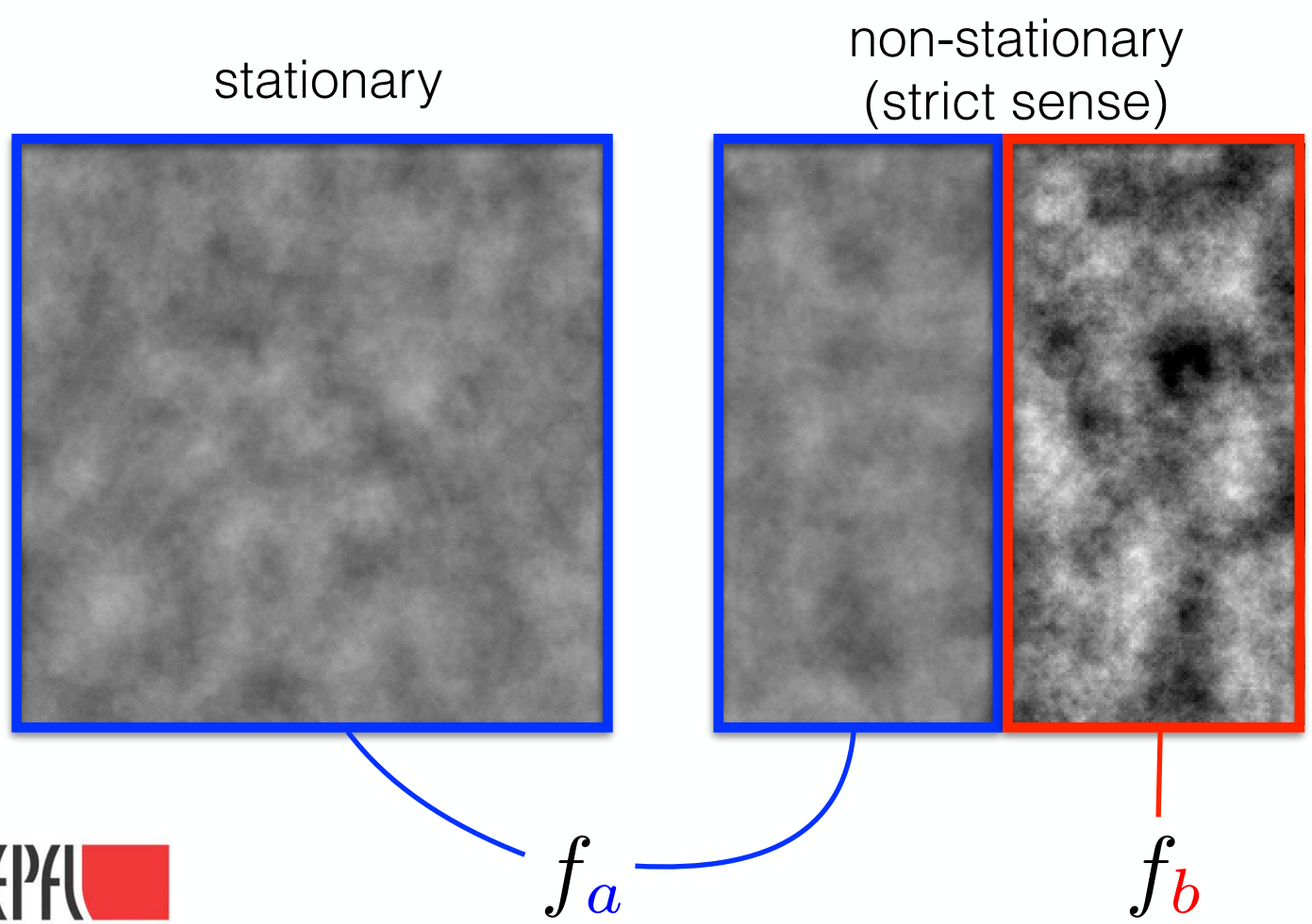

$$f_{a,\boldsymbol{X}_m}(q) = \frac{1}{1\sqrt{2\pi}} e^{-\frac{(q-0)^2}{2\,1^2}}$$

$$f_{b,\boldsymbol{X}_m}(q) = \frac{1}{3\sqrt{2\pi}} e^{-\frac{(q-0)^2}{2\,3^2}}$$

NOTATIONS, SAMPLING AND TEXTURE FUNCTIONS

- Stationarity of textures and human perception / tissue biology
  - Strict/weak process stationarity and texture class definition is not equivalent

Outex “canvas039”: stationary?

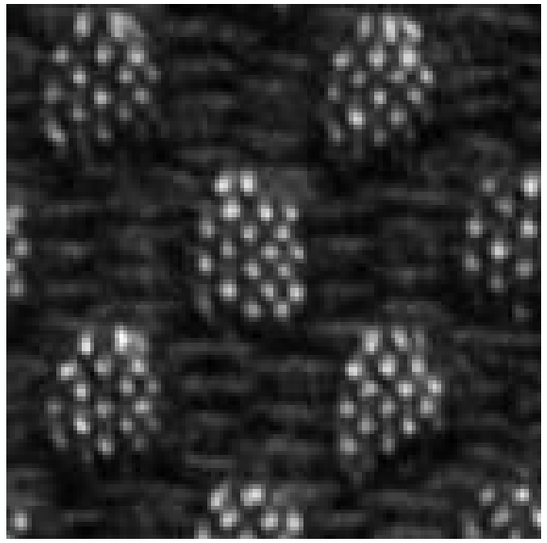

brain glioblastoma in T1-MRI: stationary?

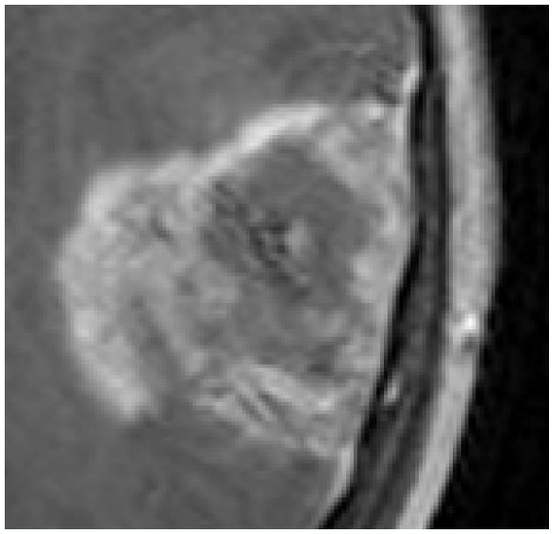

- Image analysis tasks when textures are considered as
  - Stationary (wide sense): texture classification
  - Non-stationary: texture segmentation

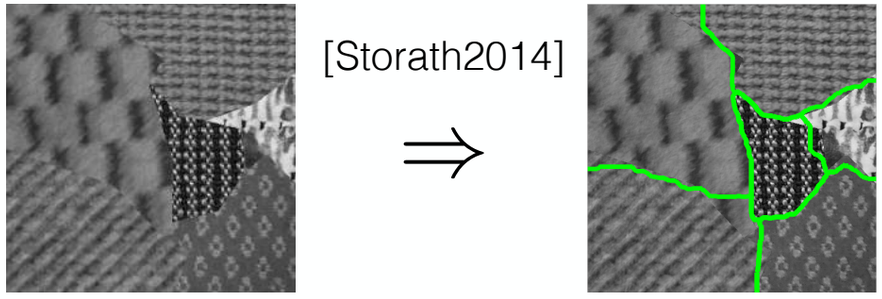

ÉCOLE POLYTECHNIQUE FÉDÉRALE DE LAUSANNE

OUTLINE

- Biomedical texture analysis: background
- Defining texture processes
  - Notations, sampling and texture functions
- Texture operators, primitives and invariances
  - Multiscale analysis
    - Operator scale and uncertainty principle
    - Region of interest and operator aggregation
  - Multidirectional analysis
    - Isotropic versus directional operators
    - Importance of the local organization of image directions
- Conclusions
- References

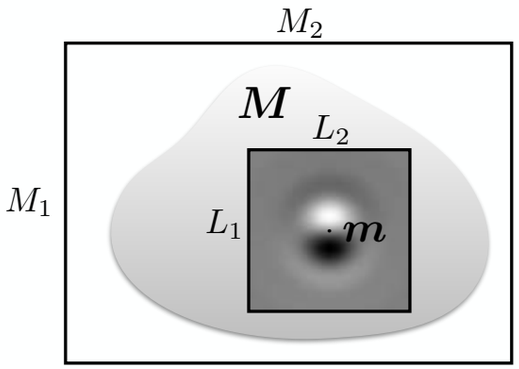

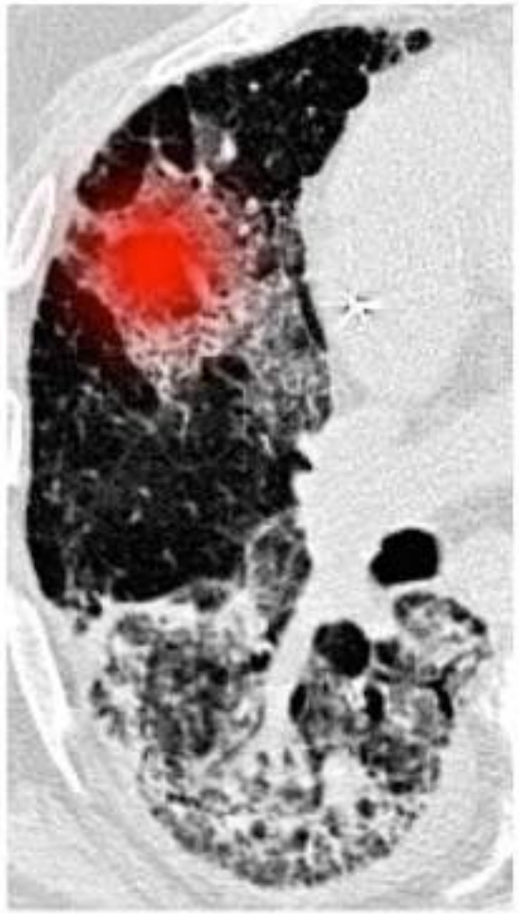

Hes·so VALAIS WALLIS
School of Management & Tourism

TEXTURE OPERATORS AND PRIMITIVES

- Texture operators
  - A d-dimensional texture analysis approach is characterized by a set of N local operators centered at the position $\boldsymbol{m}$

$$g_n(\boldsymbol{x}, \boldsymbol{m}): \quad \mathbb{R}^{M_1 \times \cdots \times M_d} \mapsto \mathbb{R}^P, \quad n = 1, \ldots, N$$

  - g_n is local in the sense that each element $\big(g_n(\boldsymbol{x}, \boldsymbol{m})\big)_{p=1,\ldots,P}$ only depends on a $L_1 \times \cdots \times L_d$ subregion of $\boldsymbol{x}$

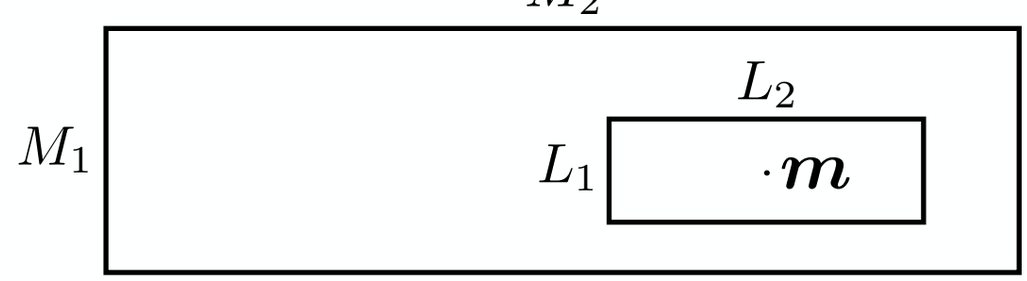

    - The subregion $L_1 \times \cdots \times L_d$ is the support of g_n
  - g_n can be linear (e.g., wavelets) or non-linear (e.g., median, GLCMs, LBPs)
  - For each position $\boldsymbol{m}$, g_n maps the texture function $f(\boldsymbol{x})$ into a P-dimensional space

$$g_n(f(\boldsymbol{x}), \boldsymbol{m}): \quad \mathbb{R}^{M_1 \times \cdots \times M_d} \mapsto \mathbb{R}^P$$

Texture operators and primitives

- From texture operators to texture measurements (i.e., features)
  - The operator $g_n(\boldsymbol{x}, \boldsymbol{m})$ is typically applied to all positions $\boldsymbol{m}$ of the image by "sliding" its window $L_1 \times \cdots \times L_d$ over the image
  - Regional texture measurements $\boldsymbol{\mu} \in \mathbb{R}^P$ can be obtained from the aggregation of $g_n(f(\boldsymbol{x}), \boldsymbol{m})$ over a region of interest $\boldsymbol{M}$

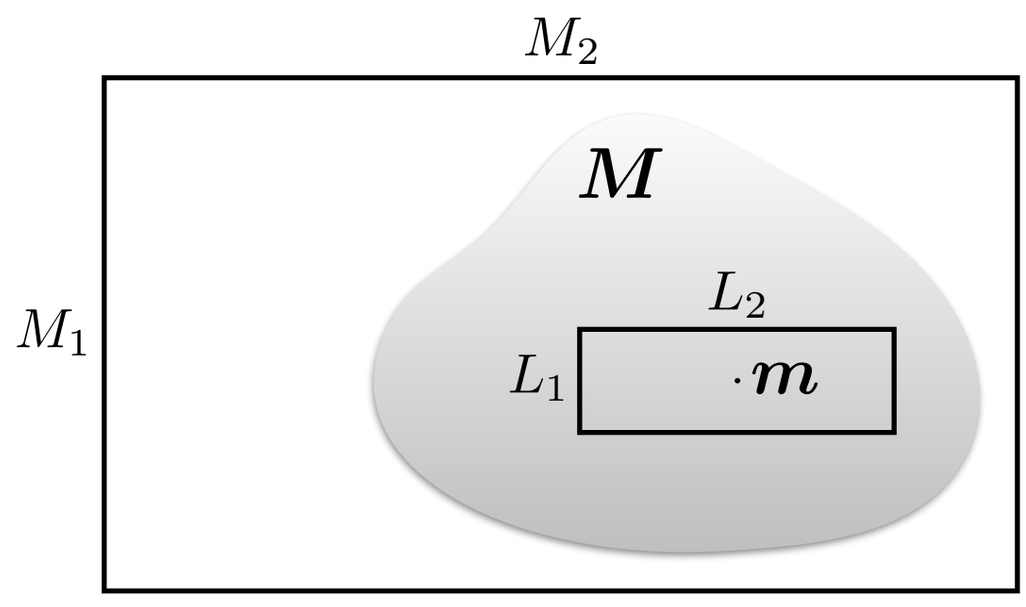

  - For instance, integration can be used to aggregate $g_n(f(\boldsymbol{x}), \boldsymbol{m})$ over $\boldsymbol{M}$
    - e.g., average:

$$\boldsymbol{\mu} = \begin{pmatrix} \mu_1 \\ \vdots \\ \mu_P \end{pmatrix} = \frac{1}{|\boldsymbol{M}|} \int_{\boldsymbol{M}} \left(g_n(f(\boldsymbol{x}), \boldsymbol{m})\right)_{p=1,\ldots,P} \mathrm{d}\boldsymbol{m}$$

Texture operators and primitives

- Texture primitives
  - A “texture primitive” (also called “texel”) is a fundamental elementary unit (i.e., a building block) of a texture class [Haralick1979, Petrou2006]

texture primitives

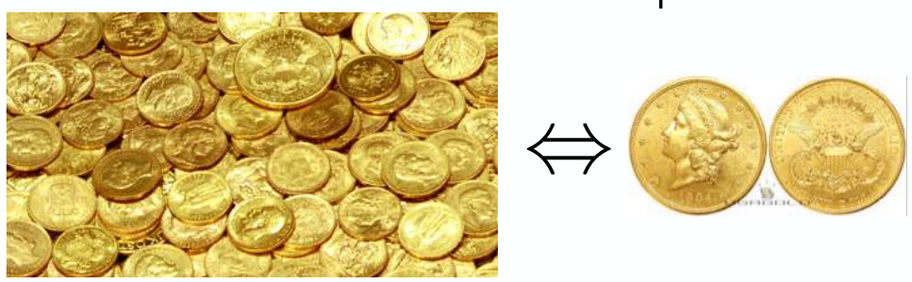

texture primitive

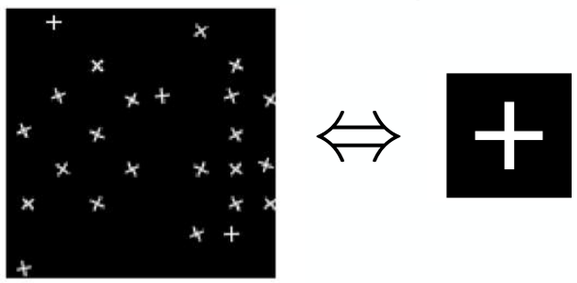

  - Intuitively, given a collection of texture functions f_j, an appropriate set of texture operators g_n must be able to:

    (i) Detect and quantify the presence of all distinct primitives in $f_{j=1,\ldots,J}$

    (ii) Characterize the spatial relationships between the primitives (e.g., geometric transformations, density) when aggregated

primitive f_1 f_2 primitive

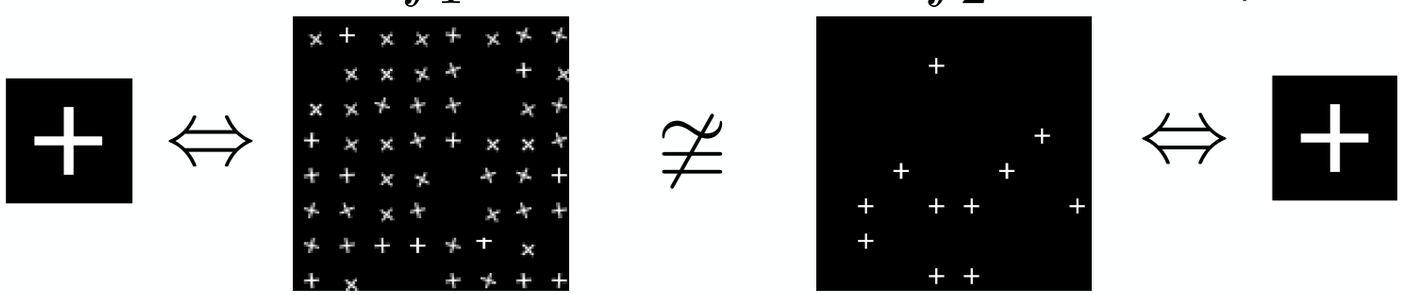

Texture operators and primitives

- General-purpose texture operators
  - In general, the texture primitives are neither well-defined, nor known in advance (e.g., biomedical tissue)

2-D lung tissue in CT images
[Depeursinge2012a]

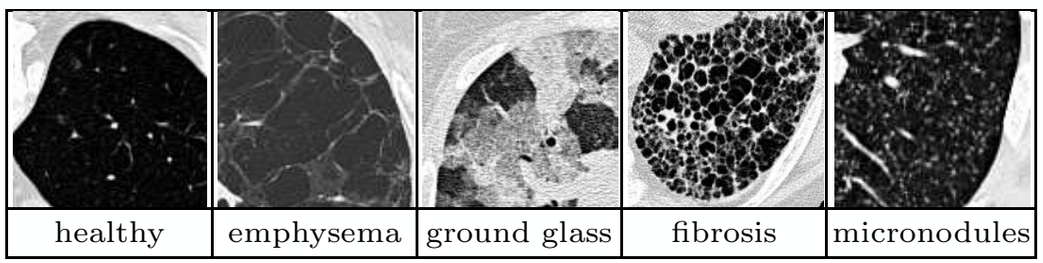

3-D normal and osteoporotic bone in μCT [Dumas2009]

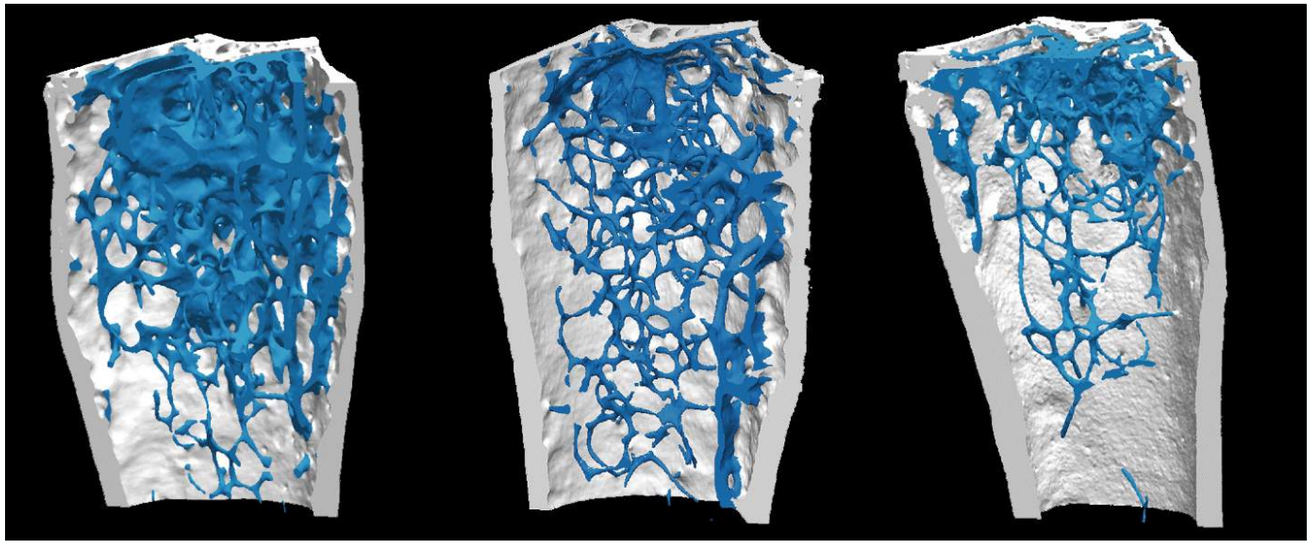

- General-purpose operator sets are useful to estimate the primitives
- How to build such operator sets?

TEXTURE OPERATORS AND PRIMITIVES

- General-purpose texture operators
  - The exhaustive analysis of spatial scales and directions is computationally expensive when the support $L_1 \times \cdots \times L_d$ of the operators is large: choices are required
    - Directions (e.g., GLCMs, RLE, HOG)

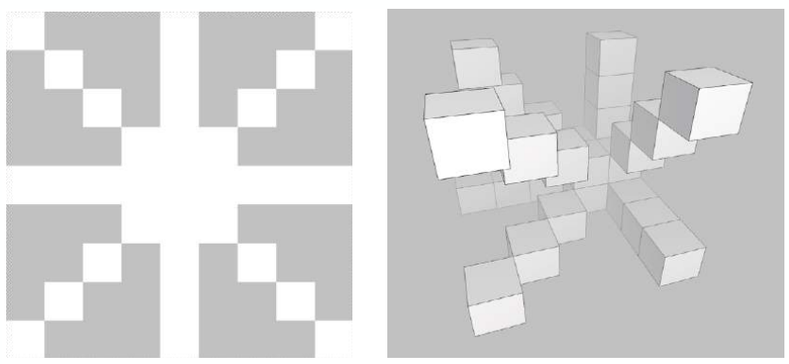

2-D 3-D (one quadrant)

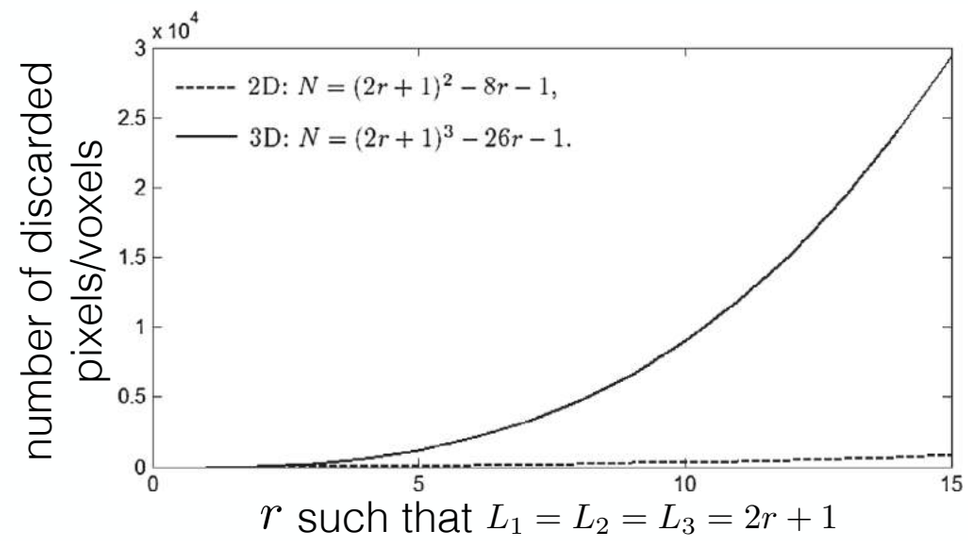

    - Scales

2-D GLCMs with various spatial distances d [Haralick1979]

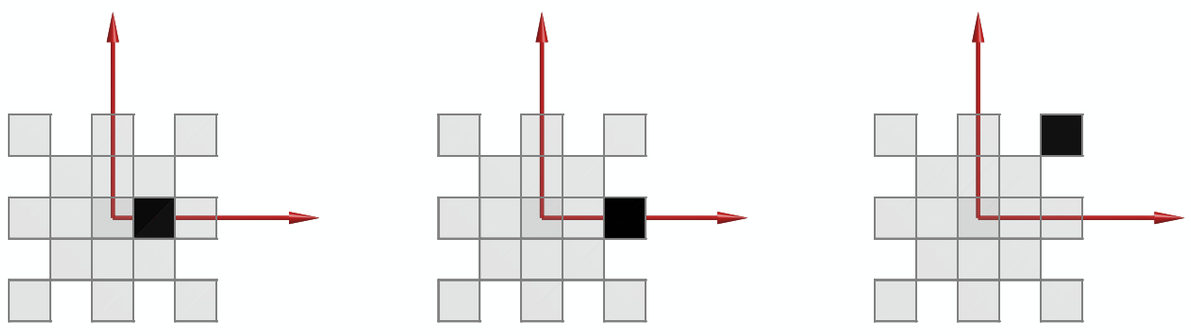

$d = 1 \quad (\Delta_{k_1} = 1, \Delta_{k_2} = 0)$ $d = 2 \quad (\Delta_{k_1} = 2, \Delta_{k_2} = 0)$ $d = 2\sqrt{2} \quad (\Delta_{k_1} = 2, \Delta_{k_2} = 2)$

2-D isotropic dyadic wavelets in Fourier [Chenouard2011]

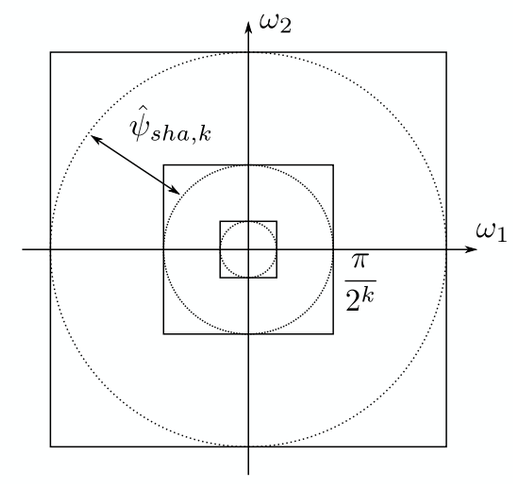

ÉCOLE POLYTECHNIQUE FÉDÉRALE DE LAUSANNE

Invariance of texture operators

- Invariances of the texture operators to geometric transformations can be desirable
  - E.g., scaling, rotations and translations

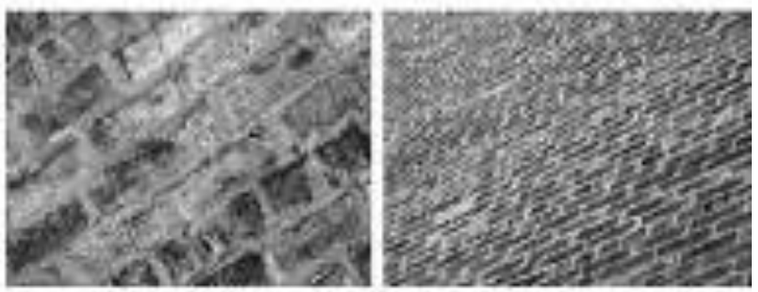

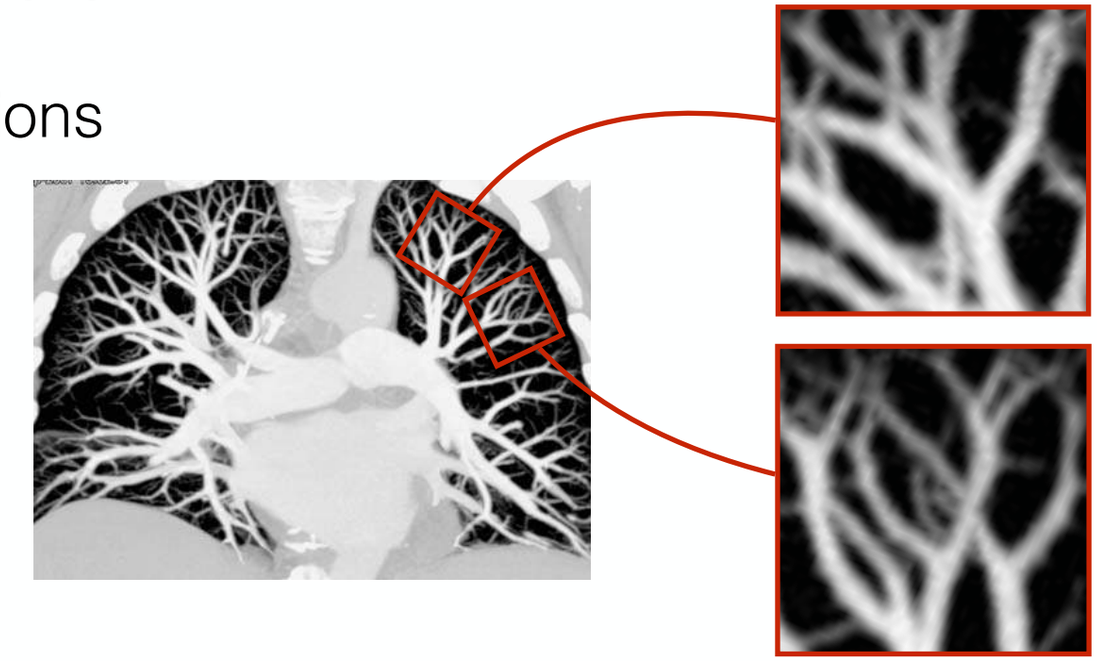

- Invariances of texture operators can be enforced
  - Example with 2-D Euclidean transforms (i.e., rotation and translation)

$$g(f(\boldsymbol{x}), \boldsymbol{m}) = g(f(\boldsymbol{R}_{\theta_0}\boldsymbol{x} - \boldsymbol{x}_0), \boldsymbol{m}), \quad \forall \boldsymbol{x}_0 \in \mathbb{R}^2,\ \theta_0 \in [0, 2\pi)$$

with the rotation matrix $\boldsymbol{R}_{\theta_0} = \begin{pmatrix} \cos\theta_0 & -\sin\theta_0 \\ \sin\theta_0 & \cos\theta_0 \end{pmatrix}$

Invariance of texture operators

- Computer vision versus biomedical imaging

	Computer vision	Biomedical image analysis
translation	translation-invariant	translation-invariant
rotation	rotation-invariant	rotation-invariant
scale	scale-invariant	multi-scale

[Lazebnik2005]

[Gurcan2009]

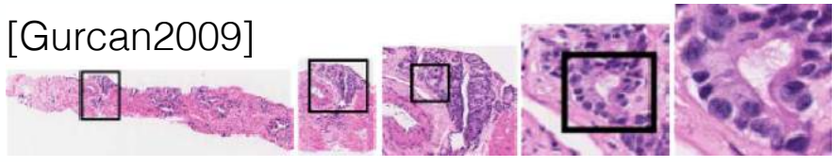

OUTLINE

- Biomedical texture analysis: background
- Defining texture processes
  - Notations, sampling and texture functions
- Texture operators, primitives and invariances
  - Multiscale analysis
    - Operator scale and uncertainty principle
    - Region of interest and operator aggregation
  - Multidirectional analysis
    - Isotropic versus directional operators
    - Importance of the local organization of image directions
- Conclusions
- References

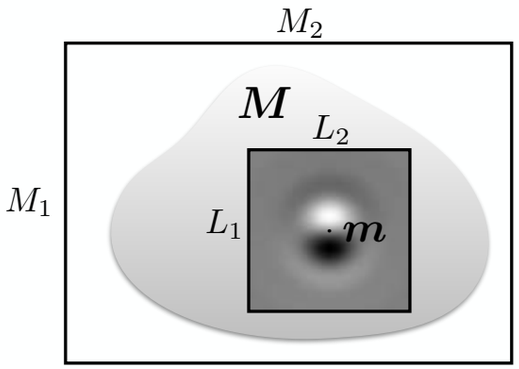

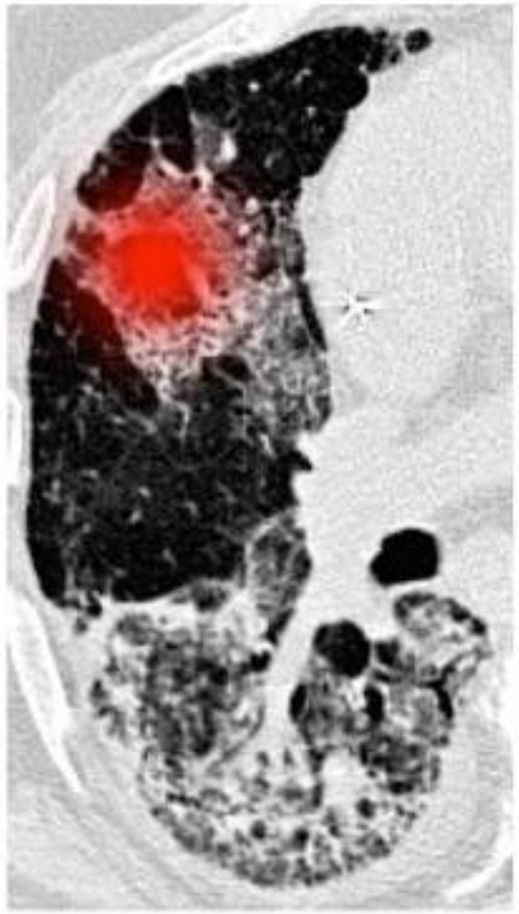

Hes·so VALAIS WALLIS
School of Management & Tourism

MULTISCALE TEXTURE OPERATORS

- Inter-patient and inter-dimension scale normalization
  - Most medical imaging protocols yield images with various sampling steps $(\Delta x_1, \Delta x_2, \Delta x_3)$
  - Inter-patient scale normalization is required to ensure the correspondance of spatial frequencies

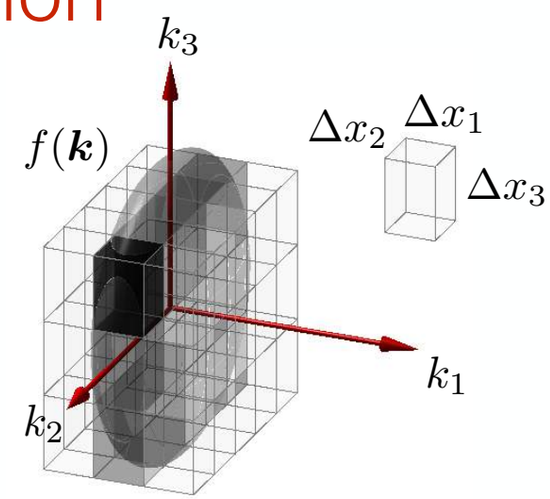

$\Delta x_1 = \Delta x_2 = 0.4\text{mm}$

spatial

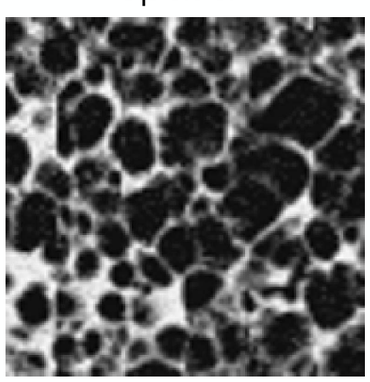

Fourier

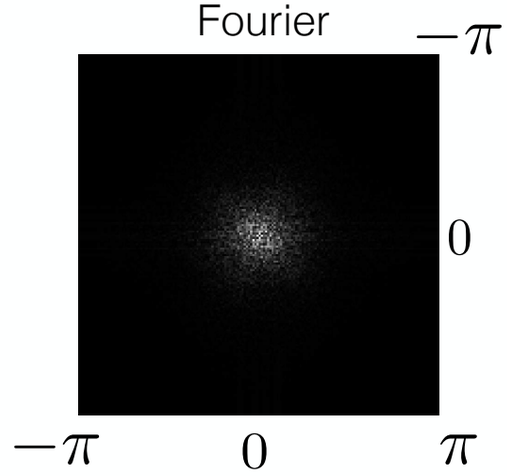

$\Delta x_1 = \Delta x_2 = 1.6\text{mm}$

spatial

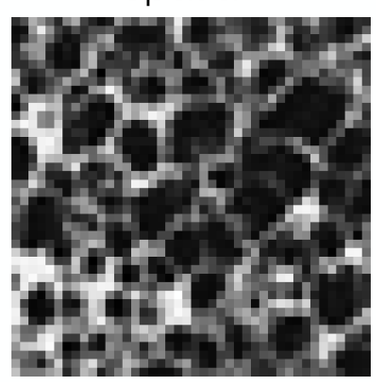

Fourier

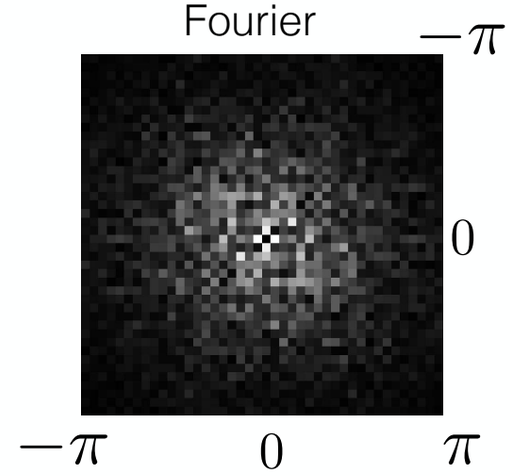

GLCMs

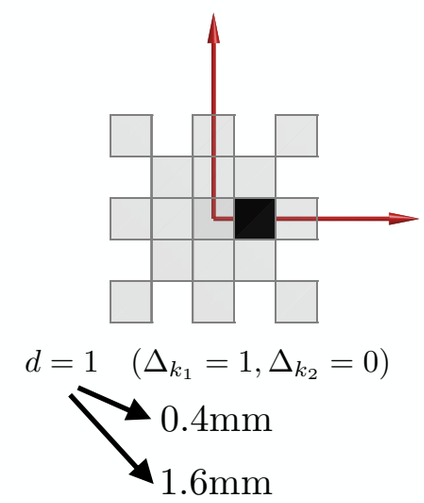

  - Inter-dimension scale normalization is required to ensure isotropic scale/directions definition

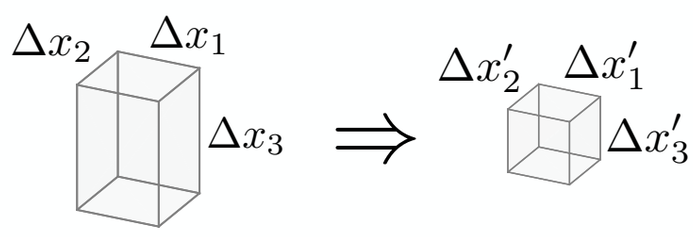

MULTISCALE TEXTURE OPERATORS

- Which scales for texture measurements?
- Two aspects:

A. How to define the size(s) of the operator(s) $L_1^n \times \cdots \times L_d^n$?

B. How to define the size of the region of interest $\boldsymbol{M}$?

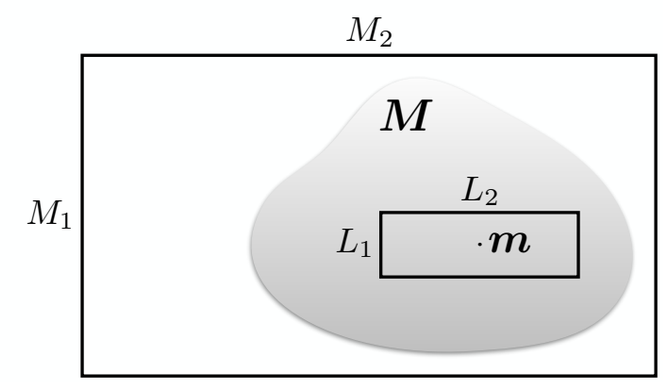

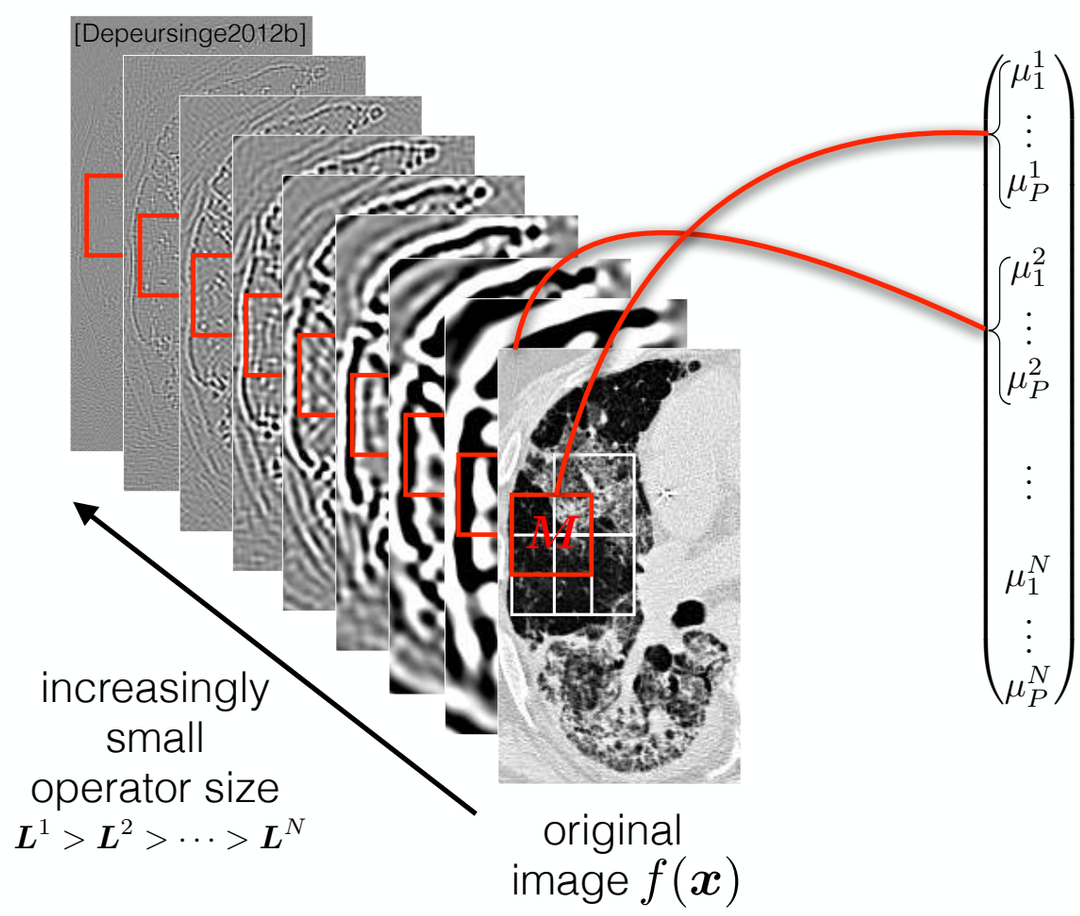

$= \boldsymbol{\mu}_{\boldsymbol{M}}$: concatenated measurements from multiscale operators $g_{n=1,\ldots,N}(f(\boldsymbol{x}), \boldsymbol{m})$ aggregated over $\boldsymbol{M}$

MULTISCALE TEXTURE OPERATORS

- Which scales for texture measurements?
- Two aspects:

A. How to define the size(s) of the operator(s) $L_1^n \times \cdots \times L_d^n$?

B. How to define the size of the region of interest $\boldsymbol{M}$?

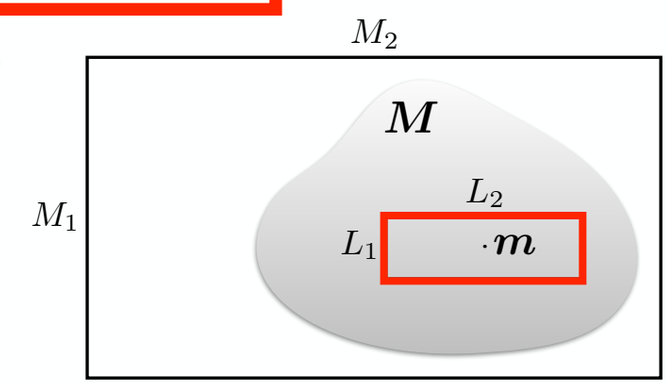

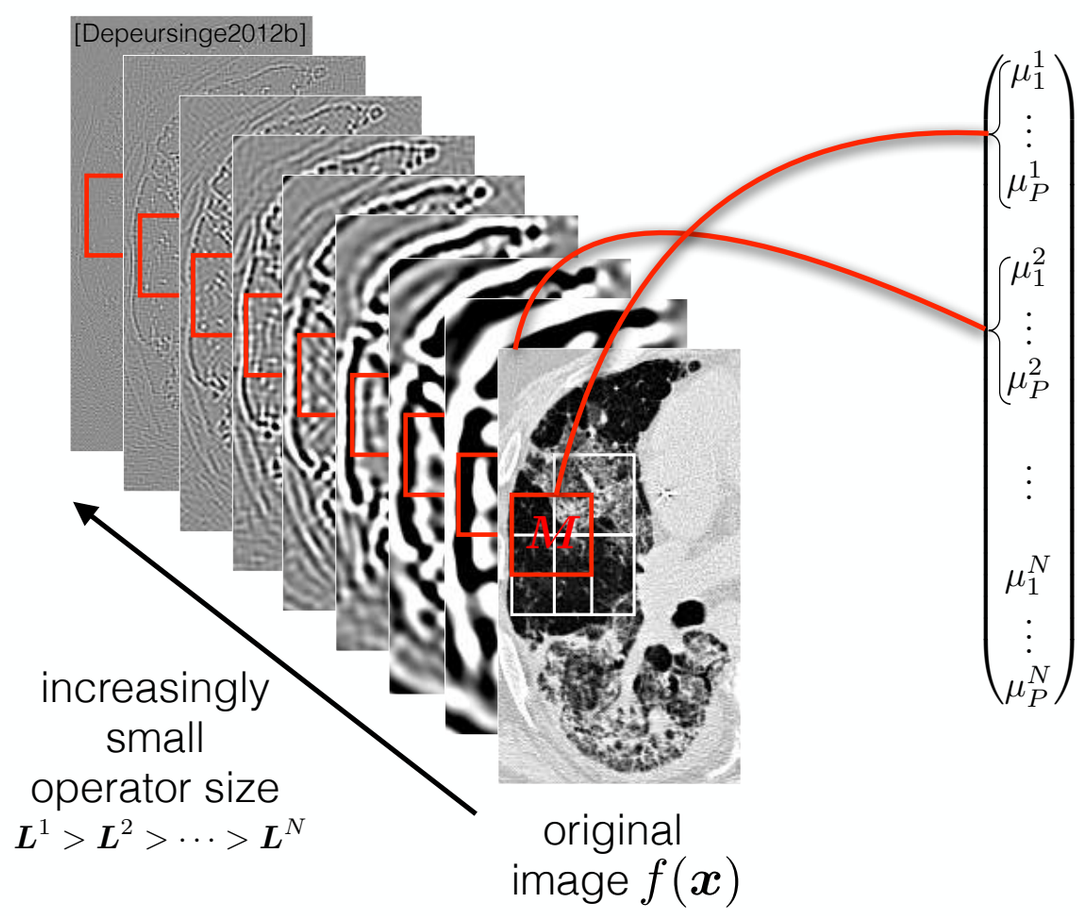

$= \boldsymbol{\mu}_{\boldsymbol{M}}$: concatenated measurements from multiscale operators $g_{n=1,\ldots,N}(f(\boldsymbol{x}), \boldsymbol{m})$ aggregated over $\boldsymbol{M}$

MULTISCALE TEXTURE OPERATORS

- Size and spectral coverage of operators
  - Uncertainty principle: operators cannot be well located both in space and Fourier [Petrou2006]
  - In 2D, the trade-off between the spatial support (i.e., $L_1 \times L_2$) and frequency support (i.e., $\Omega_1 \times \Omega_2$) of the operators is given by

$$L_1^2\,\Omega_1^2\,L_2^2\,\Omega_2^2 \geq \frac{1}{16}$$

$f(\boldsymbol{x})$ $\xrightarrow{\mathcal{F}}$ $\hat{f}(\boldsymbol{\omega})$

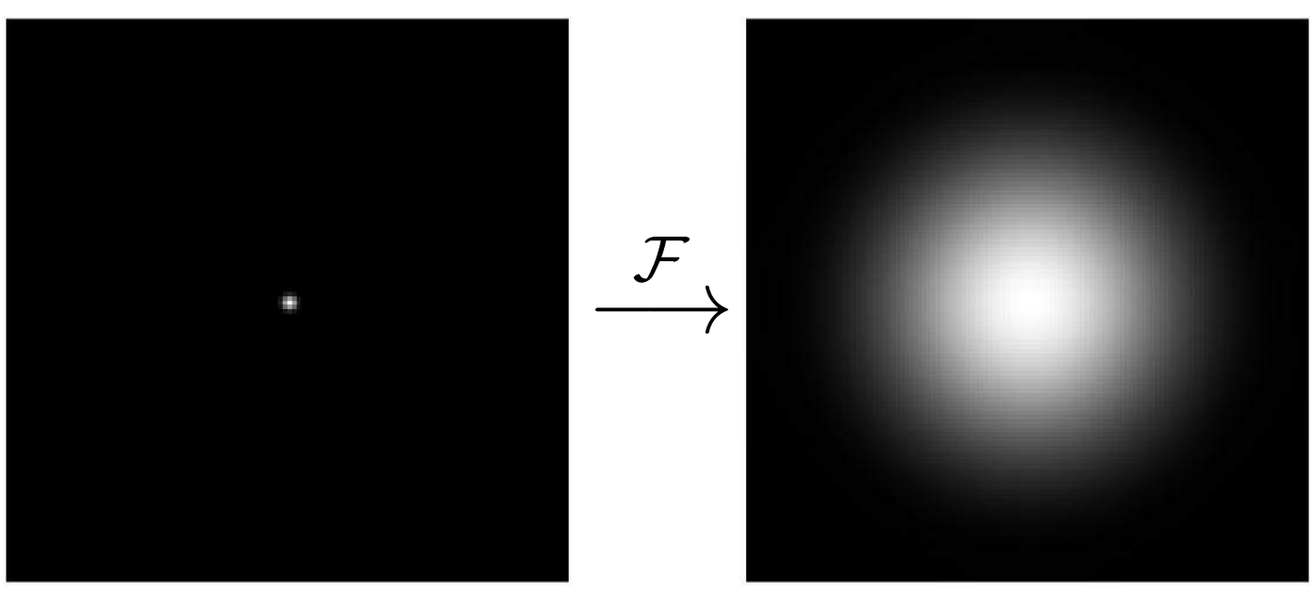

MULTISCALE TEXTURE OPERATORS

- Size and spectral coverage of operators
  - Becomes a problem in the case of non-stationary texture:

accurate spatial localization $\Leftrightarrow$ poor spectrum characterization

Gaussian window: $\sigma = 3.2\mathrm{mm}$

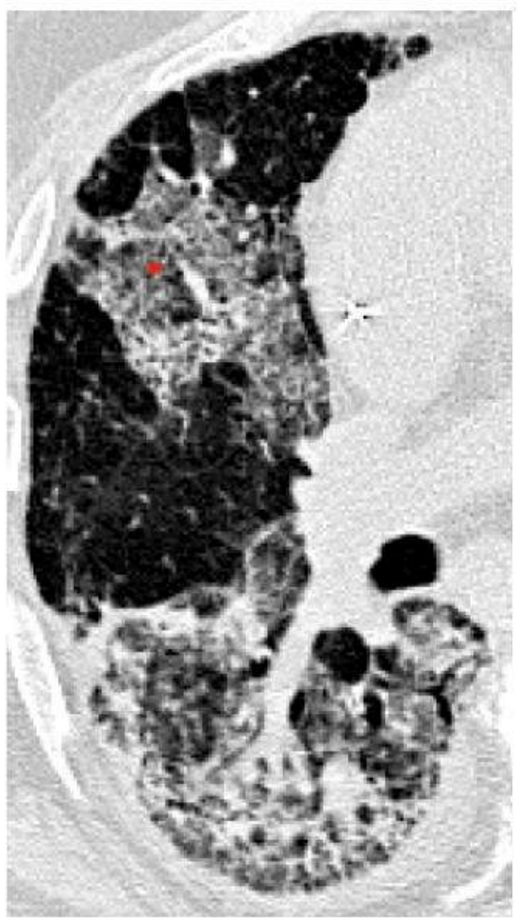

$\xrightarrow{\mathcal{F}}$

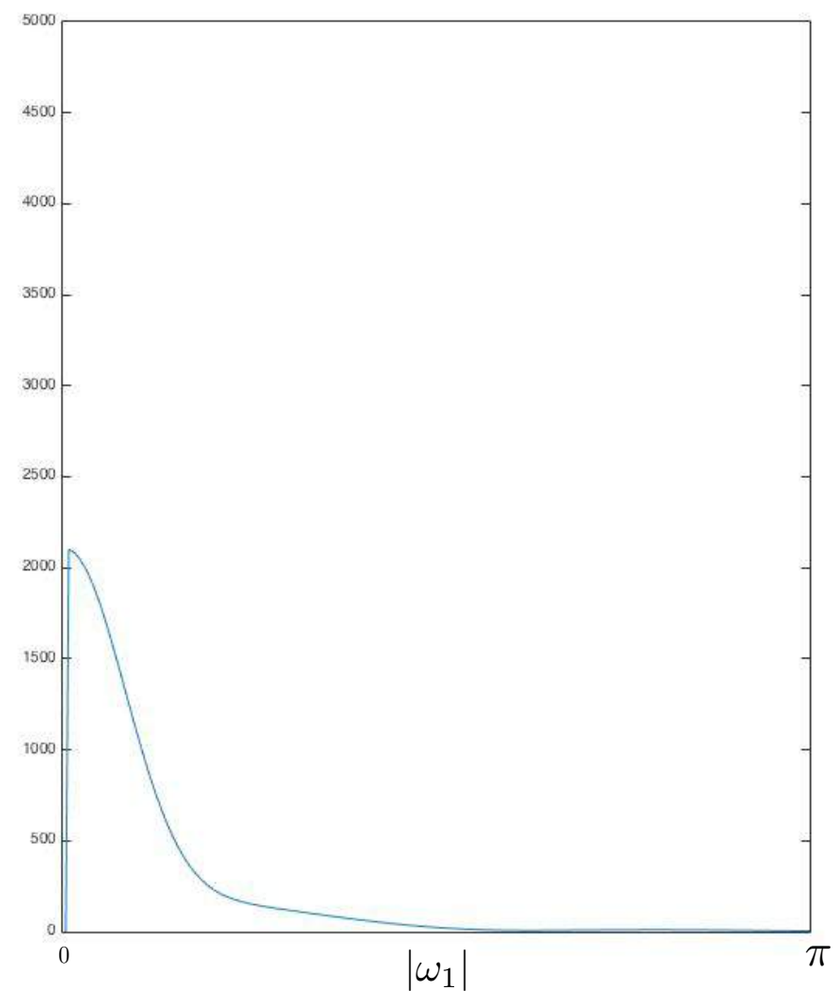

MULTISCALE TEXTURE OPERATORS

- Size and spectral coverage of operators
  - Becomes a problem in the case of non-stationary texture:

accurate spatial localization $\Leftrightarrow$ poor spectrum characterization

Gaussian window: $\sigma = 38.4\text{mm}$

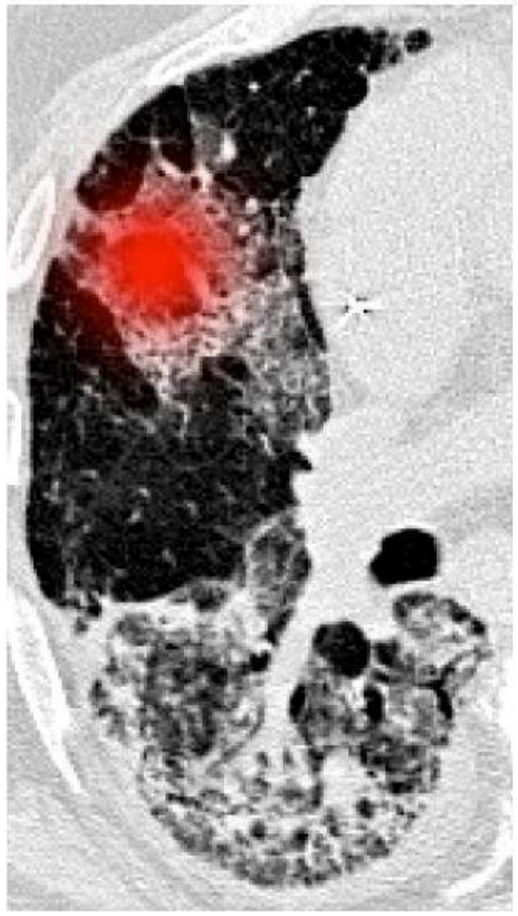

$\xrightarrow{\mathcal{F}}$

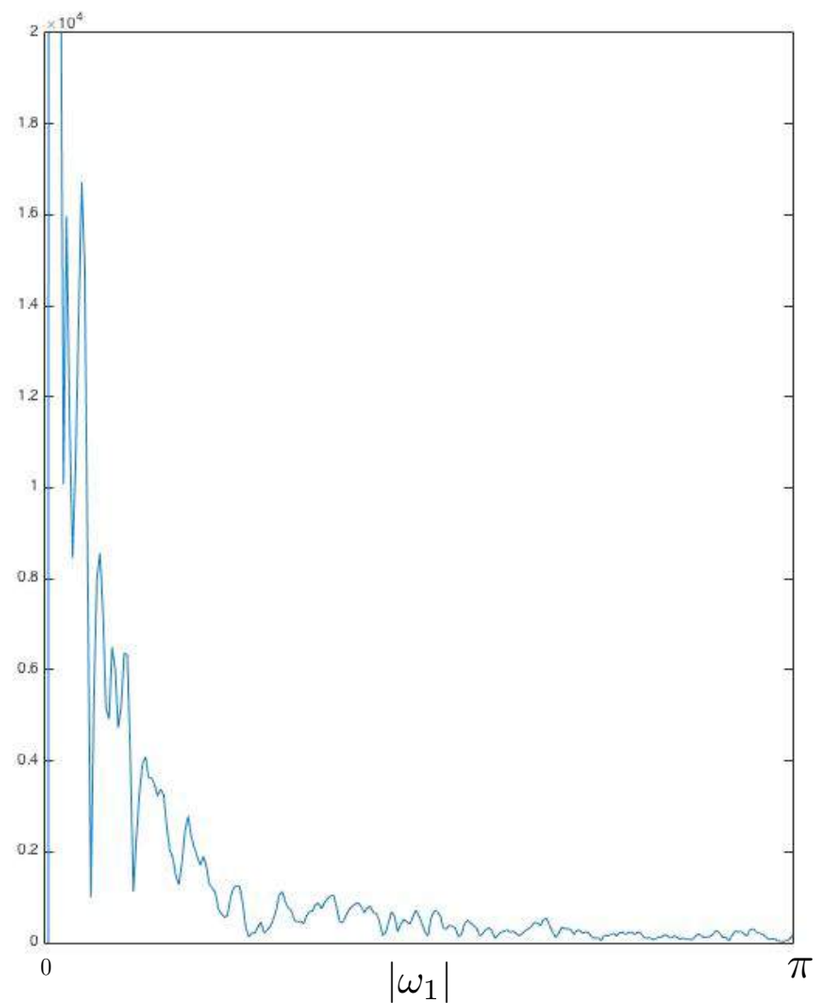

MULTISCALE TEXTURE OPERATORS

- Size and spectral coverage of operators
  - Becomes a problem in the case of non-stationary texture:

accurate spatial ⇌ poor spectrum

The spatial support should have the minimum size that allows rich enough texture-specific spectral characterization

Gaussian window: $\sigma = 38.4\text{mm}$

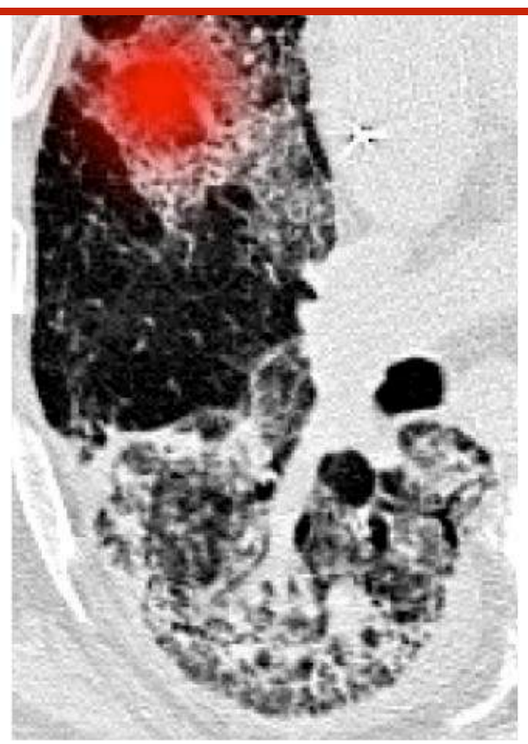

$\xrightarrow{\mathcal{F}}$

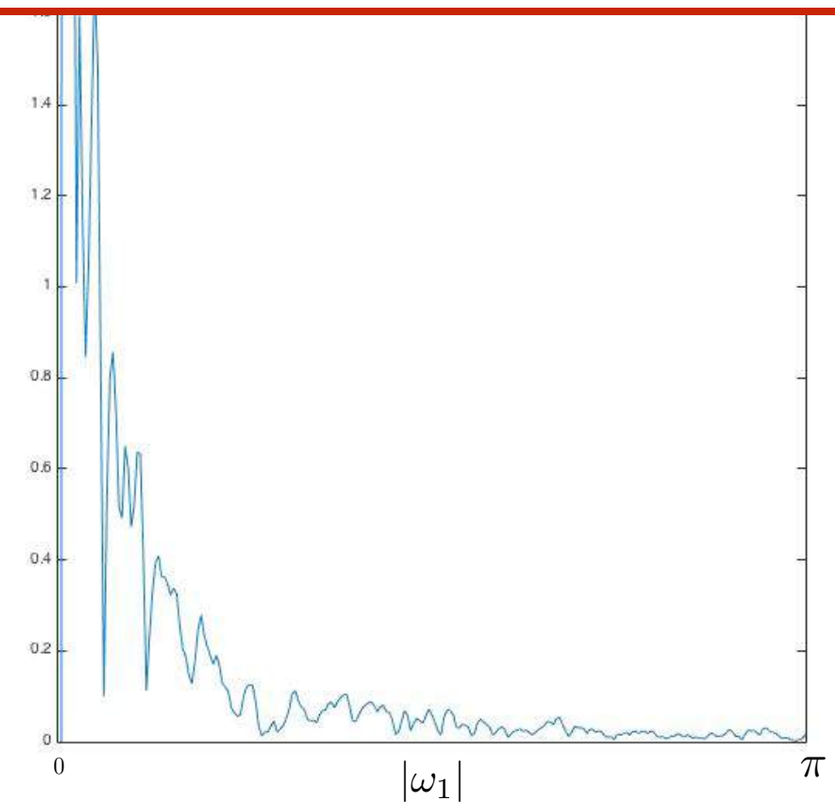

MULTISCALE TEXTURE OPERATORS

- Other consequence:
  - Large influence of proximal objects when the support of operators is larger than the region of interest

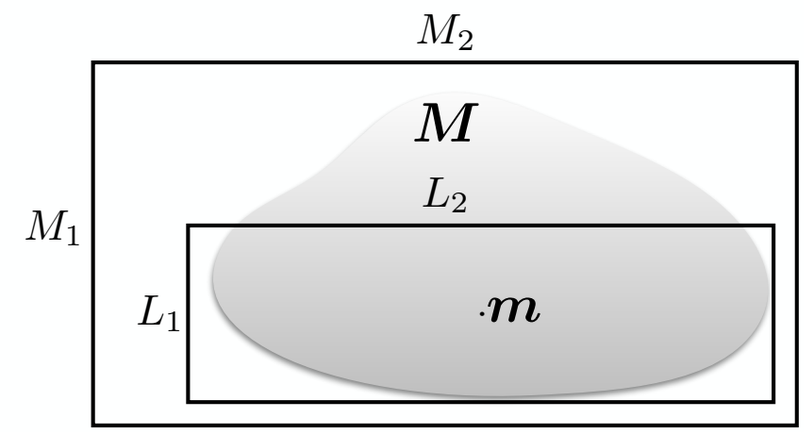

  - Example with band-limited operators (2D isotropic wavelets) and lung boundary [Ward2015, Depeursinge2015a]

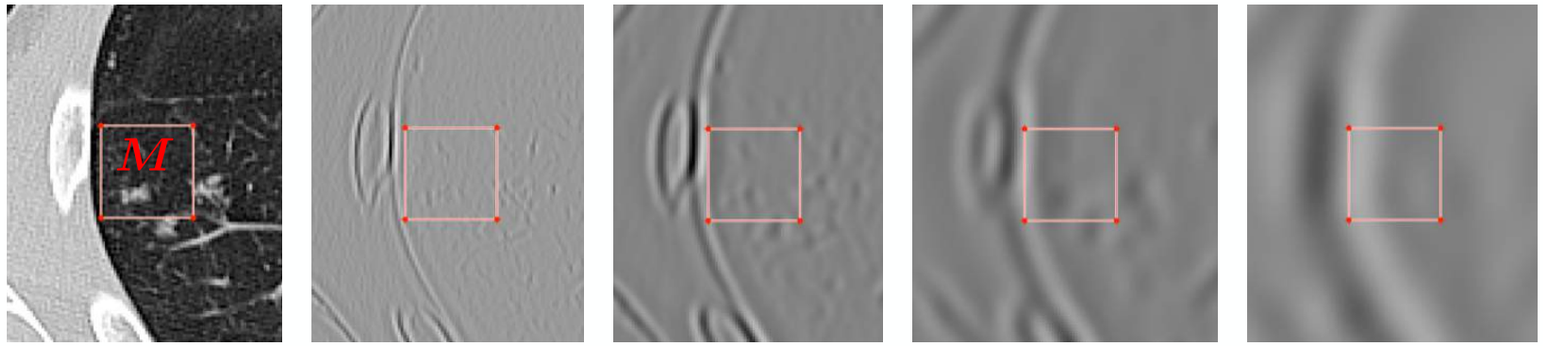

  - Tuning the shape/bandwidth was found to have a strong influence on lung tissue classification accuracy

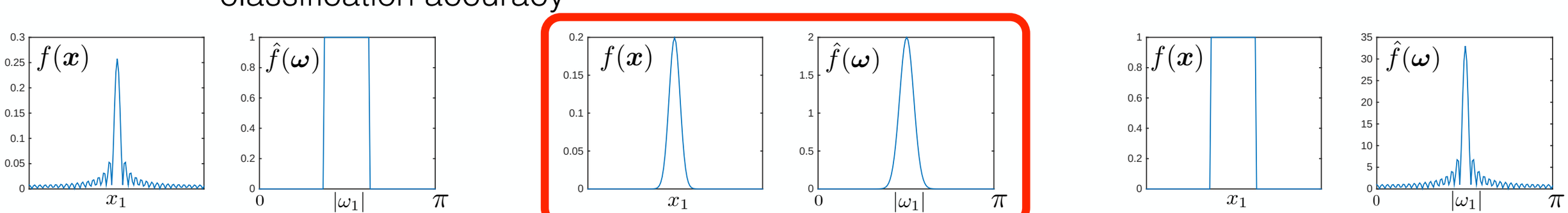

better spatial localization

worse spectral localization

MULTISCALE TEXTURE OPERATORS

- Which scales for texture measurements?
- Two aspects:

A. How to define the size(s) of the operator(s) $L_1^n \times \cdots \times L_d^n$?

B. How to define the size of the region of interest $\boldsymbol{M}$?

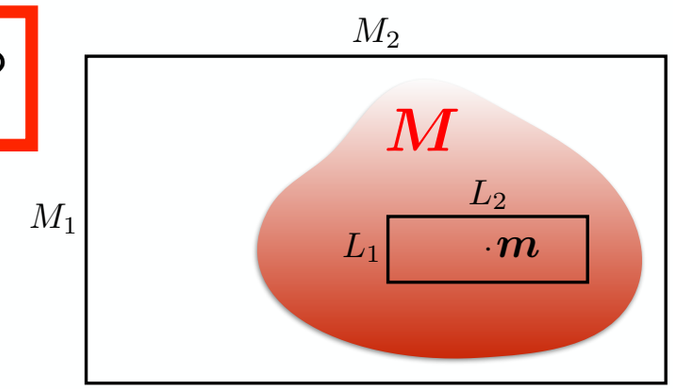

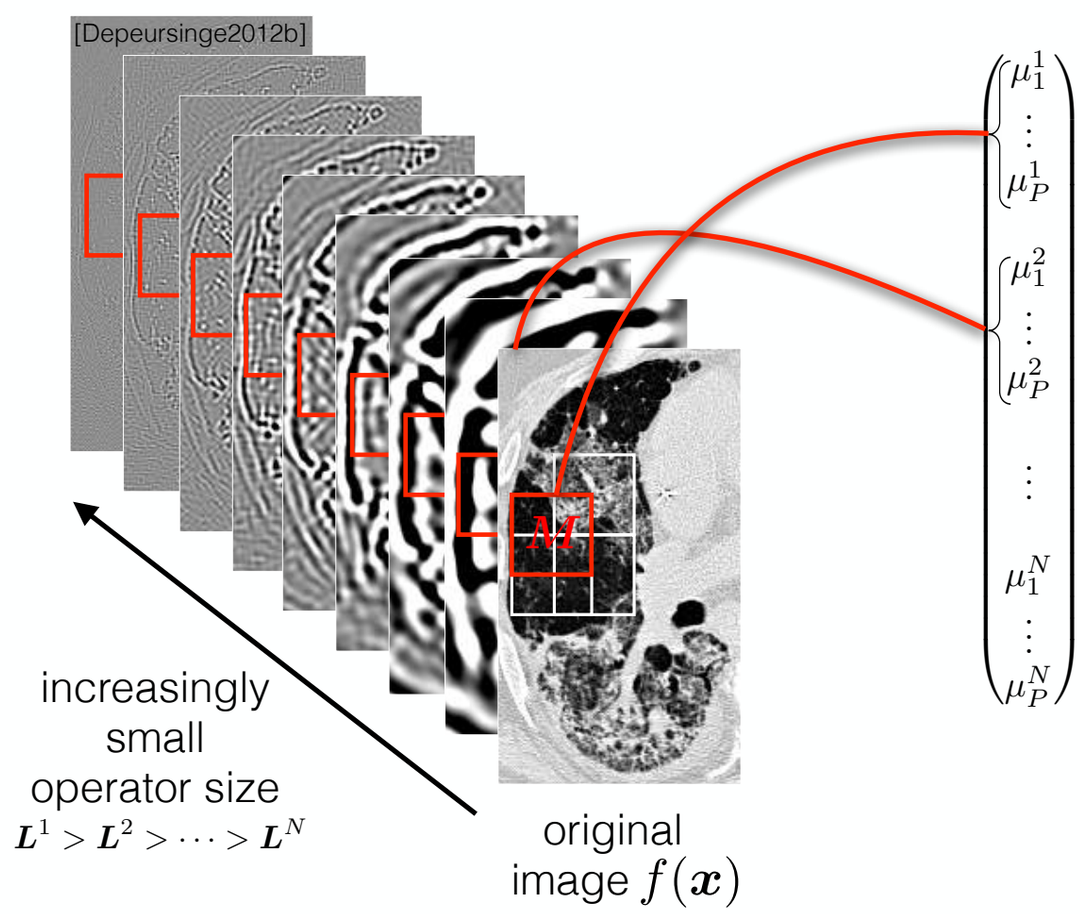

$= \boldsymbol{\mu}_{\boldsymbol{M}}$: concatenated measurements from multiscale operators $g_{n=1,\ldots,N}(f(\boldsymbol{x}), \boldsymbol{m})$ aggregated over $\boldsymbol{M}$

MULTISCALE TEXTURE OPERATORS

- How large must be the region of interest $\boldsymbol{M}$?
  - No more than enough to evaluate texture stationarity in terms of human perception / tissue biology

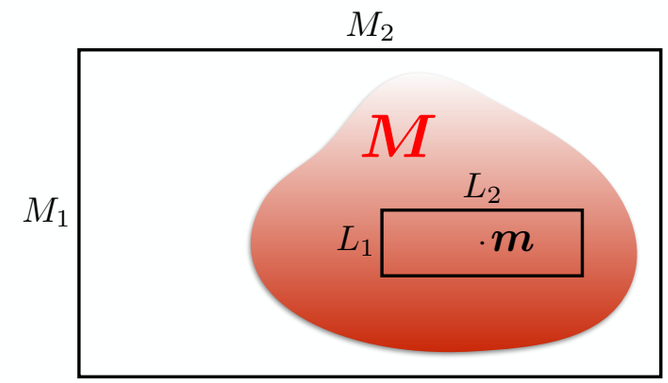

  - Example with operator: undecimated isotropic Simoncelli's dyadic wavelets [Portilla2000] applied to all image positions $\boldsymbol{m} \in \mathbb{R}^{M_1 \times M_2}$

$$\hat{g}_1(\rho) = \begin{cases} \cos\left(\frac{\pi}{2}\log_2\left(\frac{2\rho}{\pi}\right)\right), & \frac{\pi}{4} < \rho \leq \pi \\ 0, & \text{otherwise.} \end{cases}$$

$$\hat{g}_2(\rho) = \begin{cases} \cos\left(\frac{\pi}{2}\log_2\left(\frac{4\rho}{\pi}\right)\right), & \frac{\pi}{8} < \rho \leq \frac{\pi}{2} \\ 0, & \text{otherwise.} \end{cases}$$

$$\widehat{g_{1,2}(f(\rho,\phi))} = \hat{g}_{1,2}(\rho,\phi) \cdot \hat{f}(\rho,\phi)$$

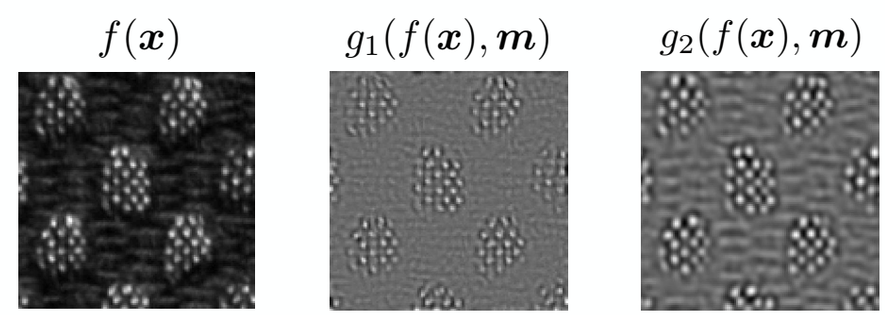

  - Operators' responses are averaged over $\boldsymbol{M}$

original image $f(\boldsymbol{x})$ with regions $\boldsymbol{M}_a, \boldsymbol{M}_b, \boldsymbol{M}_c$

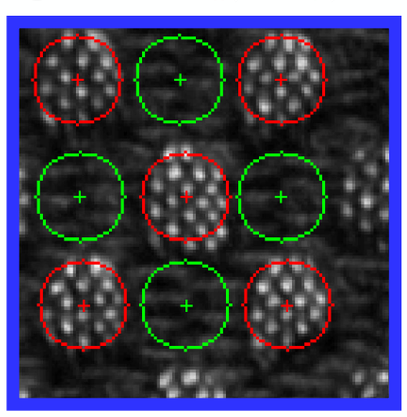

feature space

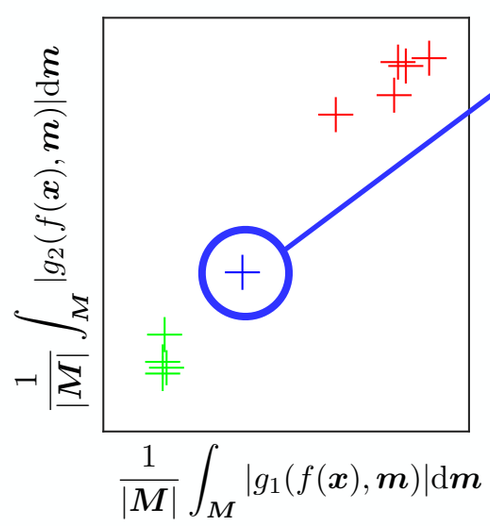

The averaged responses over the entire image does not correspond to anything visually!

MULTISCALE TEXTURE OPERATORS

- How large must be the region of interest $\boldsymbol{M}$?
  - No more than enough to evaluate texture stationarity in terms of human perception / tissue biology

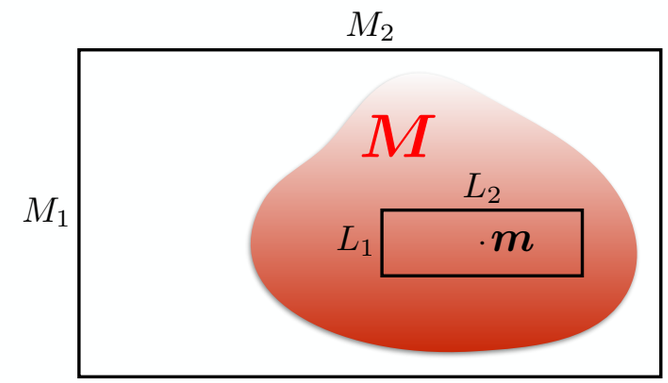

  - Example with operator: undecimated isotropic Simoncelli's dyadic wavelets [Portilla2000] applied to all image positions $\boldsymbol{m} \in \mathbb{R}^{M_1 \times M_2}$

$$\hat{g}_1(\rho) = \begin{cases} \cos\left(\frac{\pi}{2}\log_2\left(\frac{2\rho}{\pi}\right)\right), & \frac{\pi}{4} < \rho \leq \pi \\ 0, & \text{otherwise.} \end{cases}$$

$$\hat{g}_2(\rho) = \begin{cases} \cos\left(\frac{\pi}{2}\log_2\left(\frac{4\rho}{\pi}\right)\right), & \frac{\pi}{8} < \rho \leq \frac{\pi}{2} \\ 0, & \text{otherwise.} \end{cases}$$

$$\widehat{g_{1,2}(f(\rho,\phi))} = \hat{g}_{1,2}(\rho,\phi) \cdot \hat{f}(\rho,\phi)$$

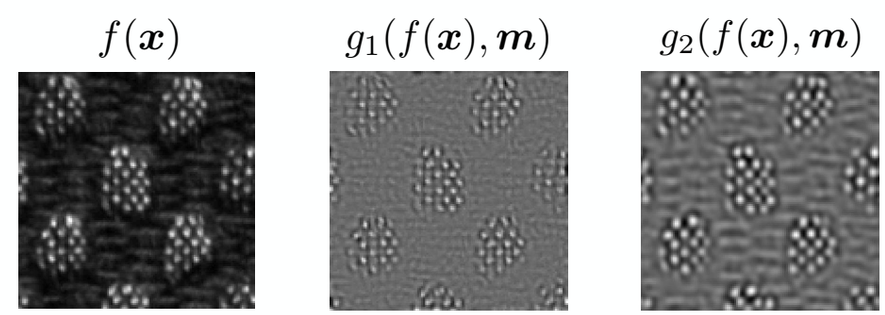

  - Operators' responses are averaged over $\boldsymbol{M}$

original image $f(\boldsymbol{x})$ with regions $\boldsymbol{M}_a, \boldsymbol{M}_b, \boldsymbol{M}_c$

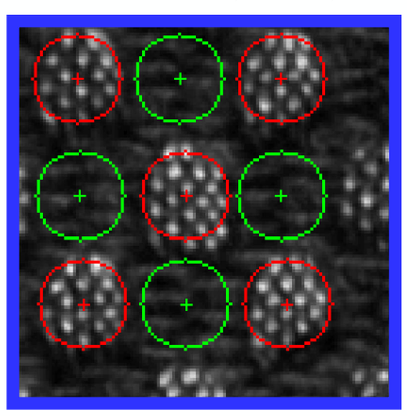

feature space

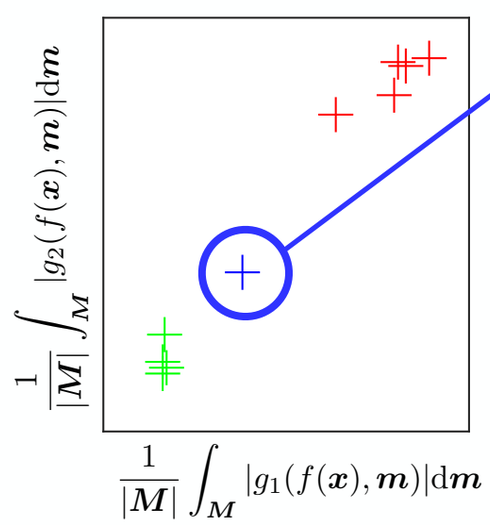

The averaged responses over the entire image does not correspond to anything visually!

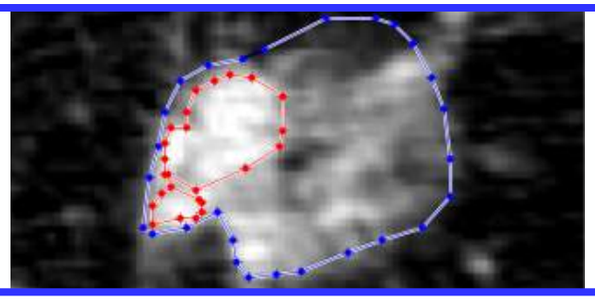

Nor biologically!

MULTISCALE TEXTURE OPERATORS

- How large must be the region of interest $\boldsymbol{M}$?
  - No more than enough to evaluate texture stationarity in terms of human perception / tissue biology

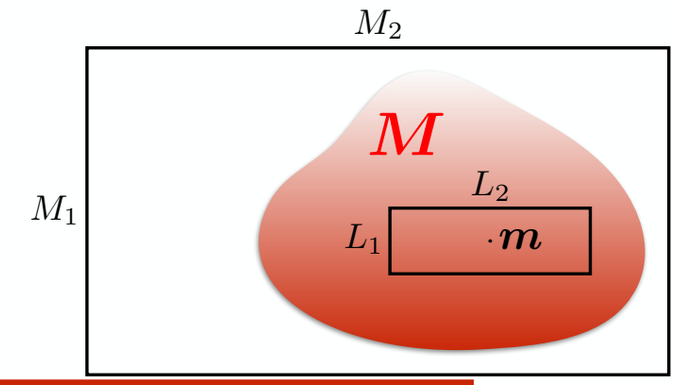

  - E … lets [

Define regions that are homogeneous in terms of operators' responses

(e.g., pixelwise clustering, graph cuts [Malik2001], Pott's model [Storath2014])

  - C … onses over the entire image does not correspond to anything visually!

regions $\boldsymbol{M}_a, \boldsymbol{M}_b, \boldsymbol{M}_c$

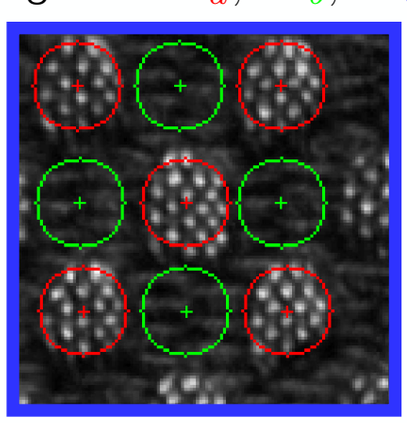

feature space

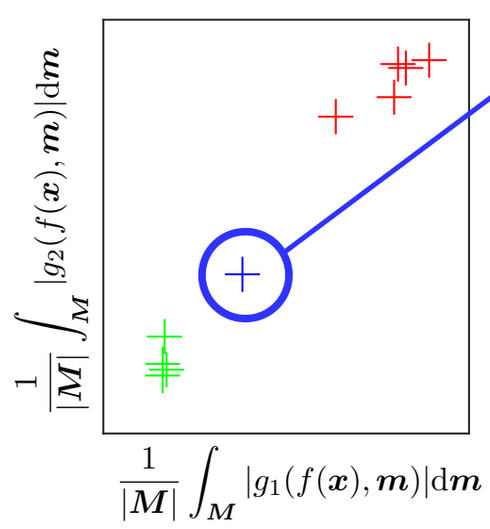

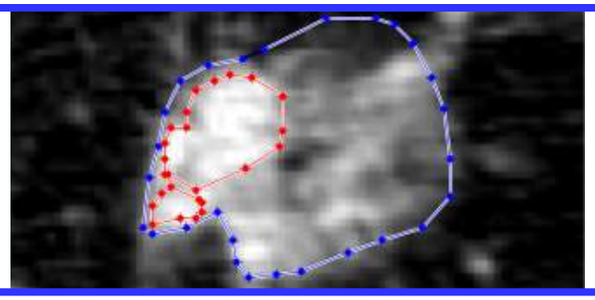

Nor biologically!

MULTISCALE TEXTURE OPERATORS

- How large must be the region of interest $\boldsymbol{M}$?
  - Example: supervised texture segmentation with undecimated isotropic Simoncelli's wavelets and linear support vector machines (SVM)

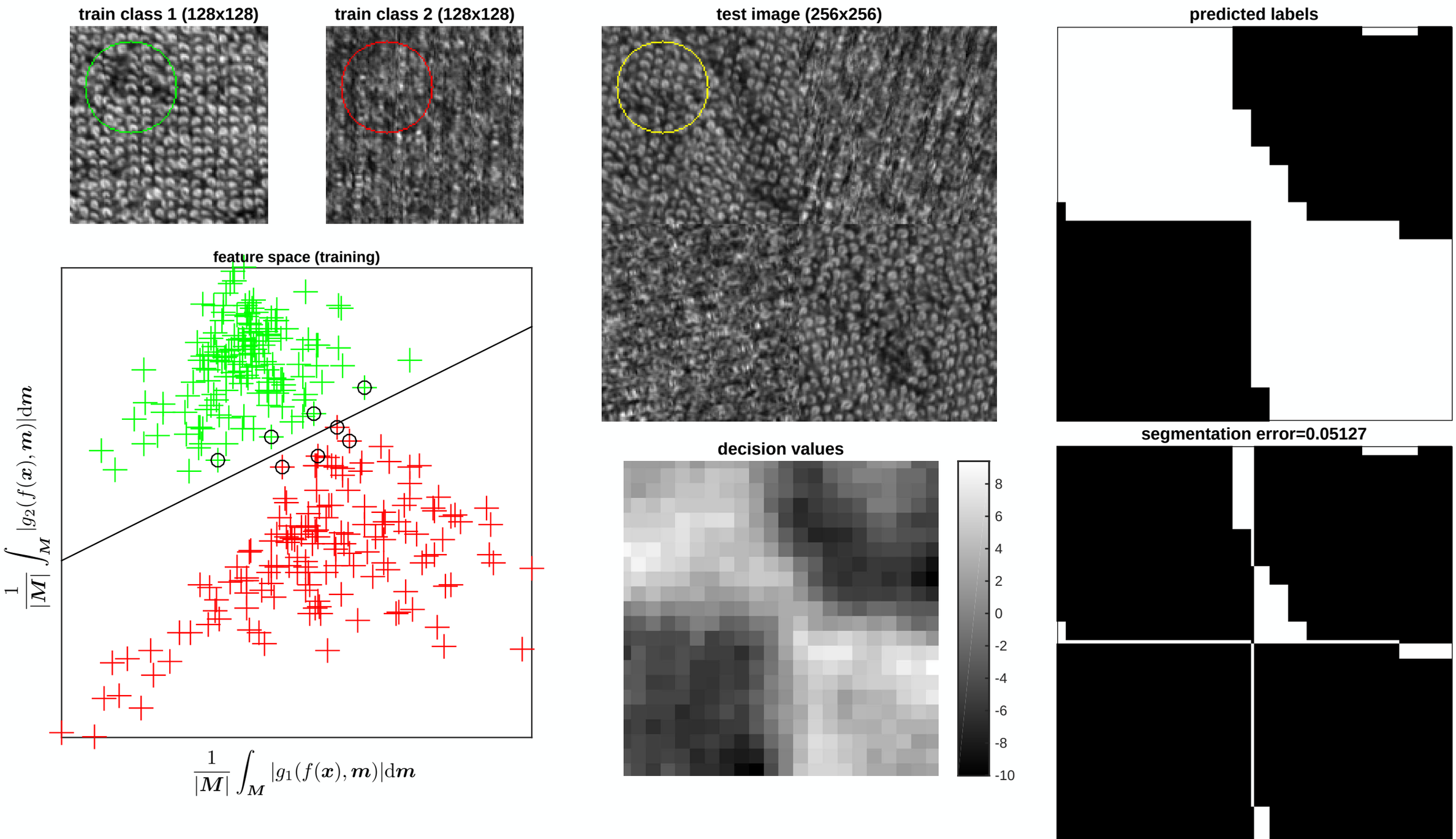

MULTISCALE TEXTURE OPERATORS

- How large must be the region of interest $\boldsymbol{M}$?
  - Example: supervised texture segmentation with undecimated isotropic Simoncelli's wavelets and linear support vector machines (SVM)

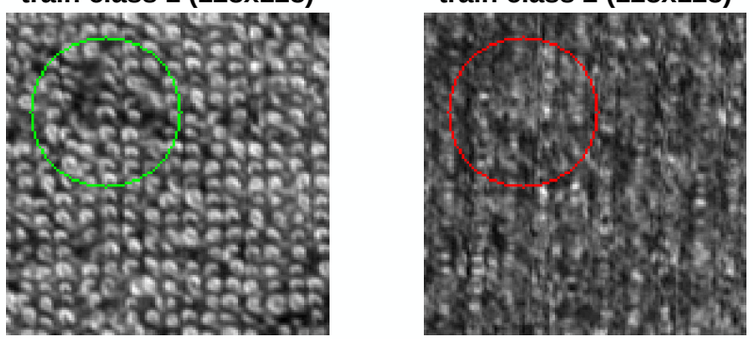

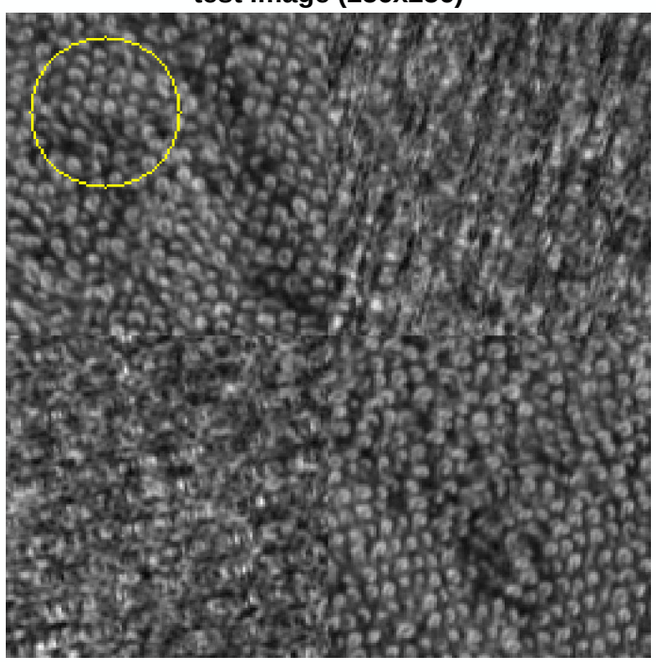

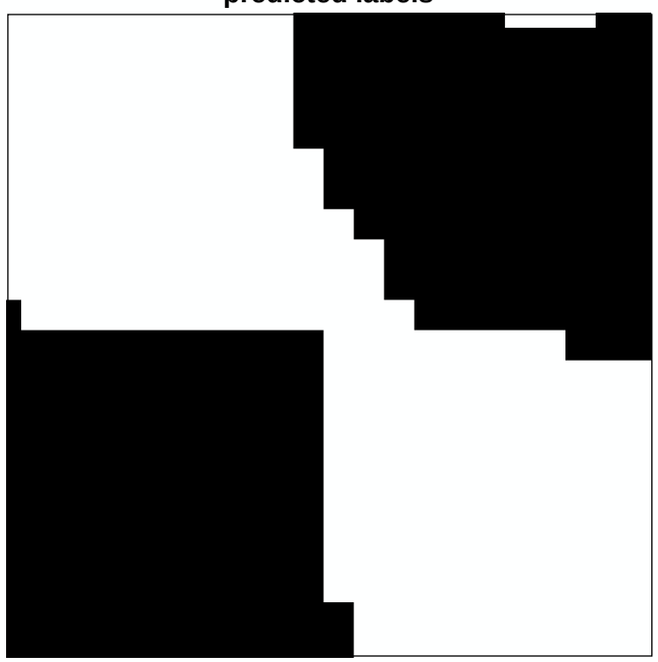

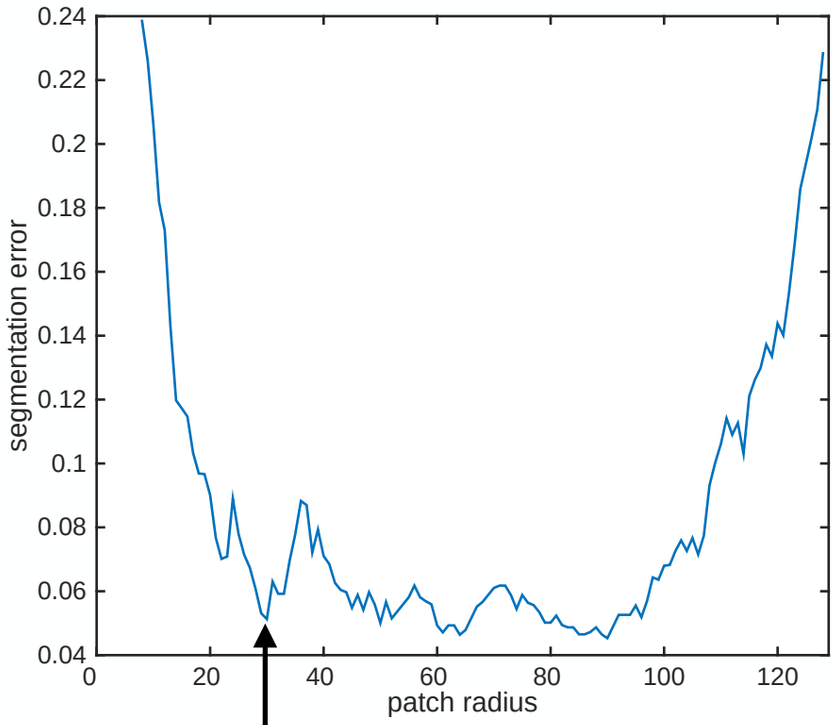

$\boldsymbol{M}$: circular patch with $r = 30$

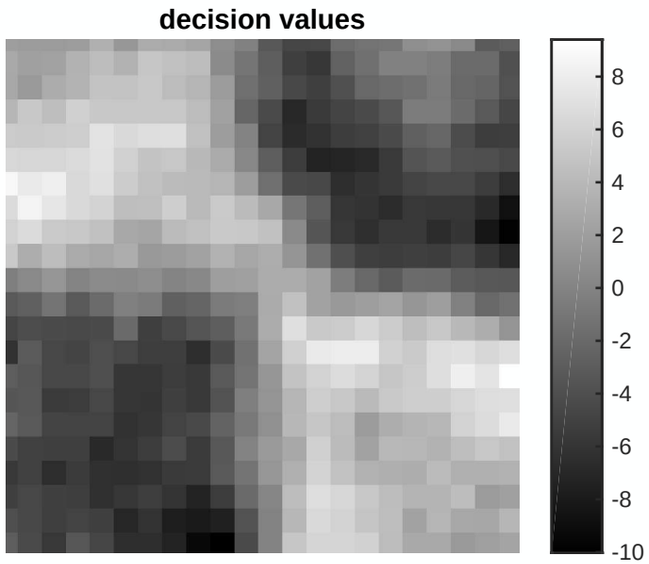

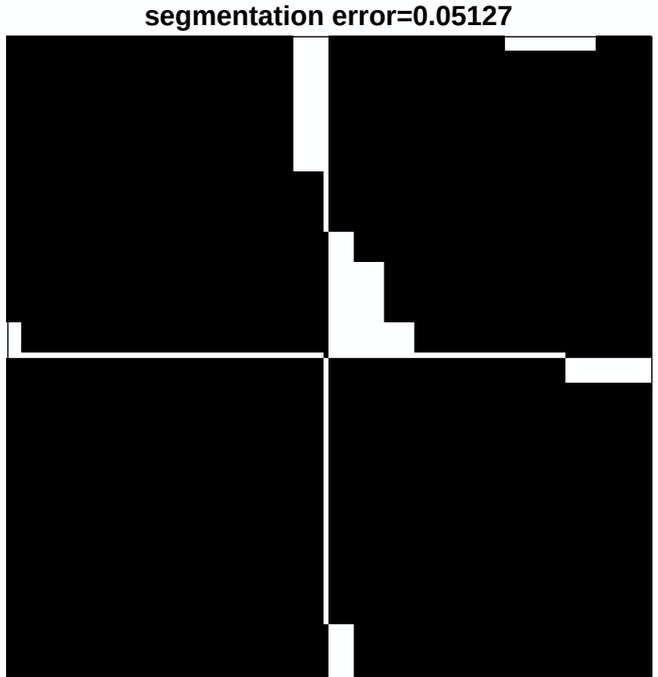

MULTISCALE TEXTURE OPERATORS

- How large must be the region of interest $\boldsymbol{M}$?
  - Example: supervised texture segmentation with undecimated isotropic Simoncelli's wavelets and linear support vector machines (SVM)

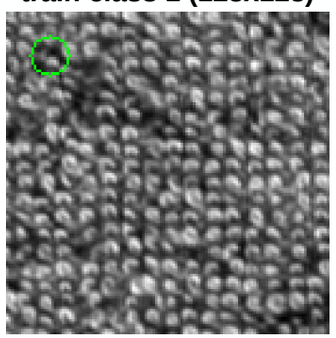

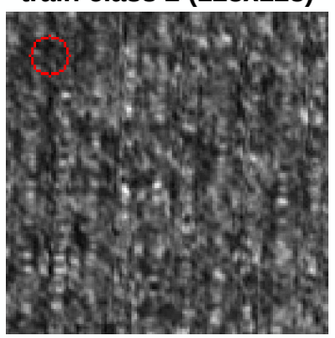

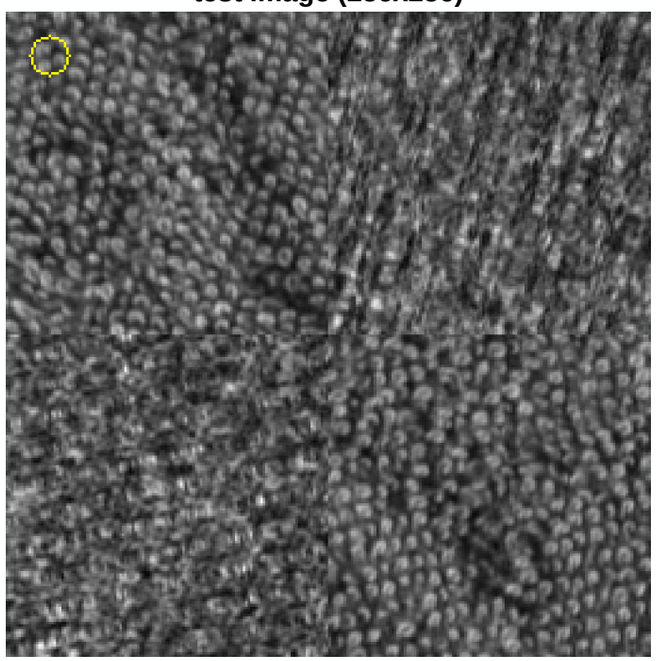

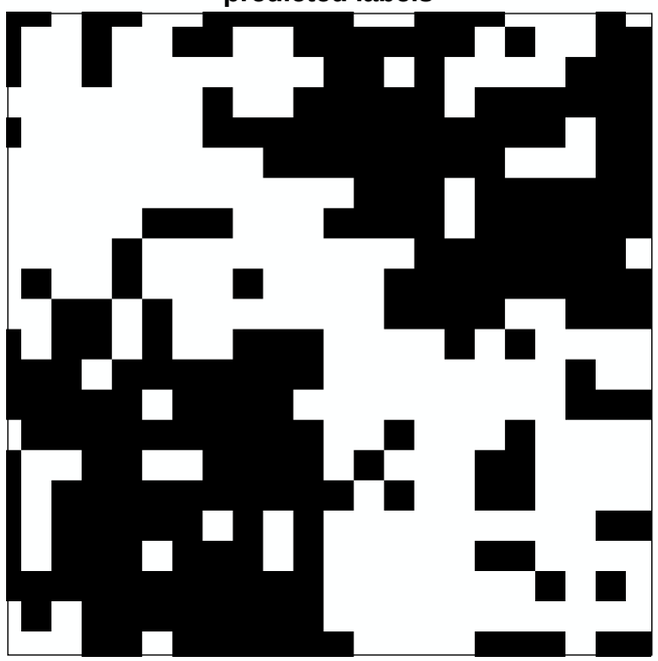

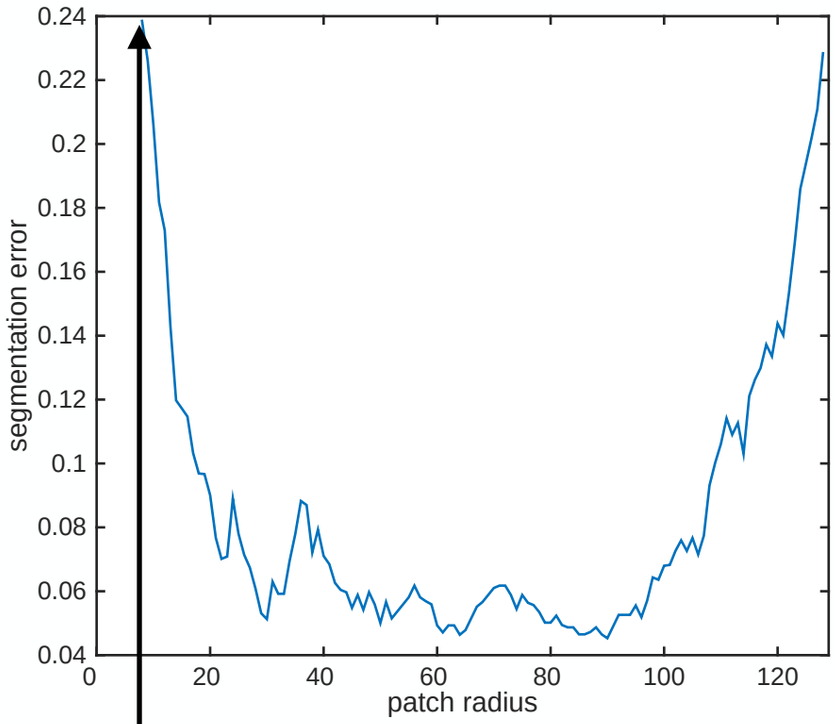

$\boldsymbol{M}$: circular patch with $r = 8$

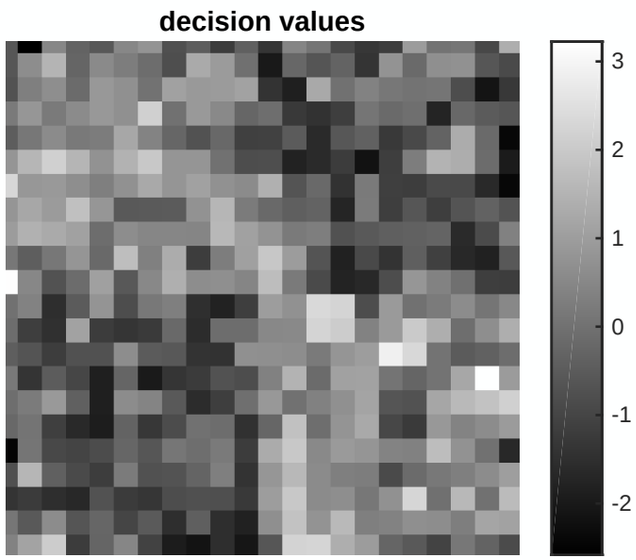

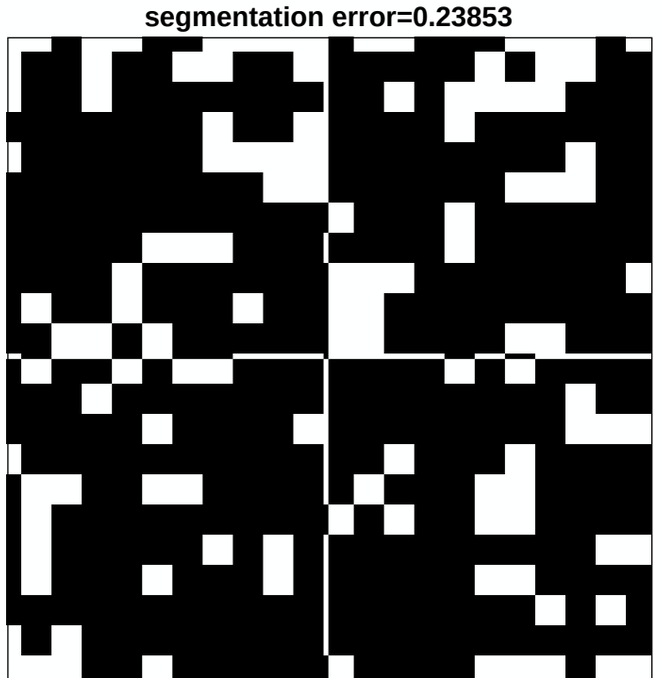

MULTISCALE TEXTURE OPERATORS

- How large must be the region of interest $\boldsymbol{M}$?
  - Example: supervised texture segmentation with undecimated isotropic Simoncelli's wavelets and linear support vector machines (SVM)

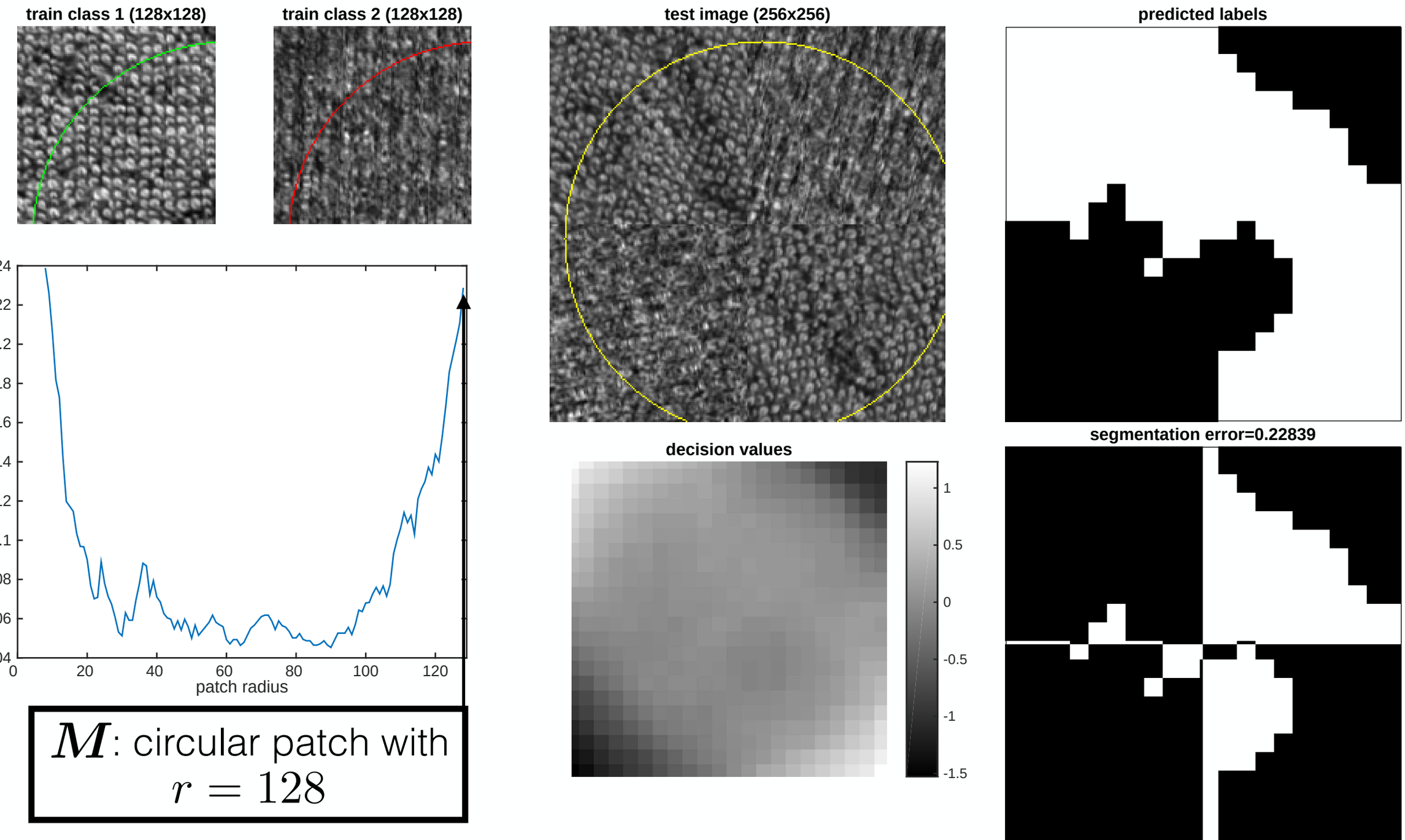

$\boldsymbol{M}$: circular patch with $r = 128$

Multiscale texture operators

- How large must be the region of interest $\boldsymbol{M}$?
  - Tissue properties are not homogeneous (i.e., non-stationary) over the entire organ

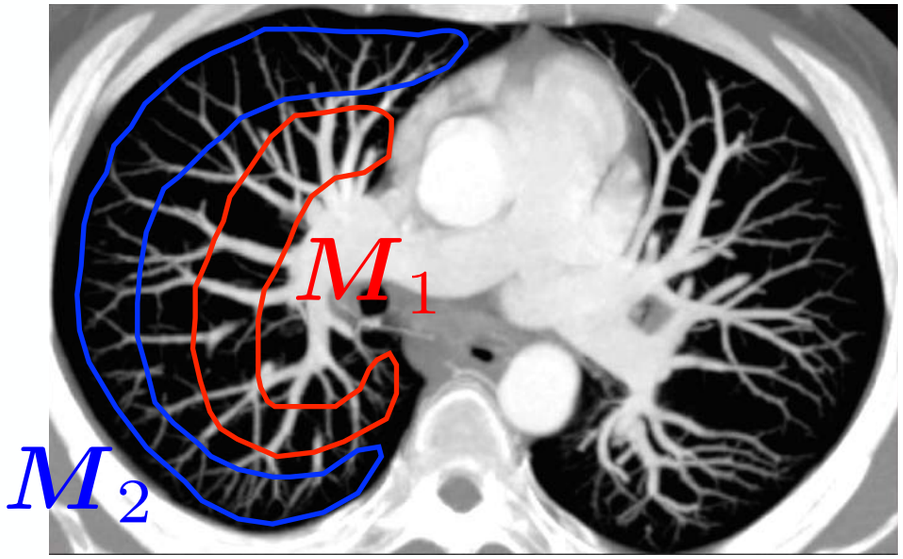

  - Importance of building tissue atlases and digital phenotypes [Depeursinge2015b]

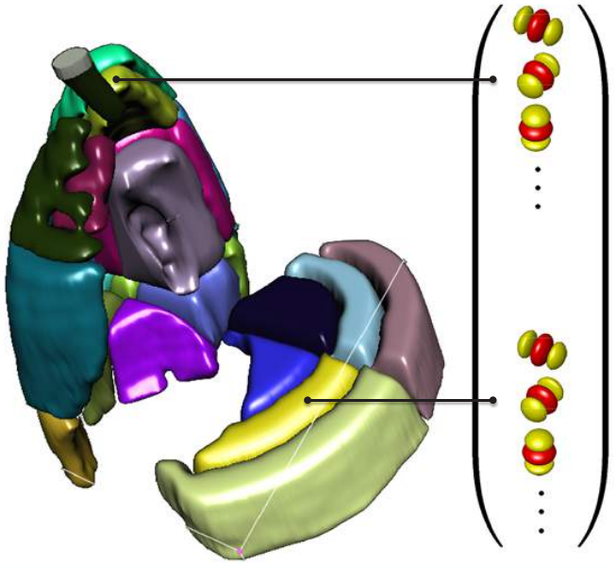

$$= \mu_{\boldsymbol{M}_{1,\ldots,S}}$$

OUTLINE

- Biomedical texture analysis: background
- Defining texture processes
  - Notations, sampling and texture functions
- Texture operators, primitives and invariances
  - Multiscale analysis
    - Operator scale and uncertainty principle
    - Region of interest and operator aggregation
  - Multidirectional analysis
    - Isotropic versus directional operators
    - Importance of the local organization of image directions
- Conclusions
- References

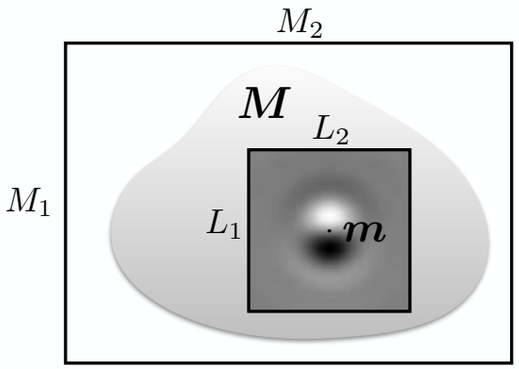

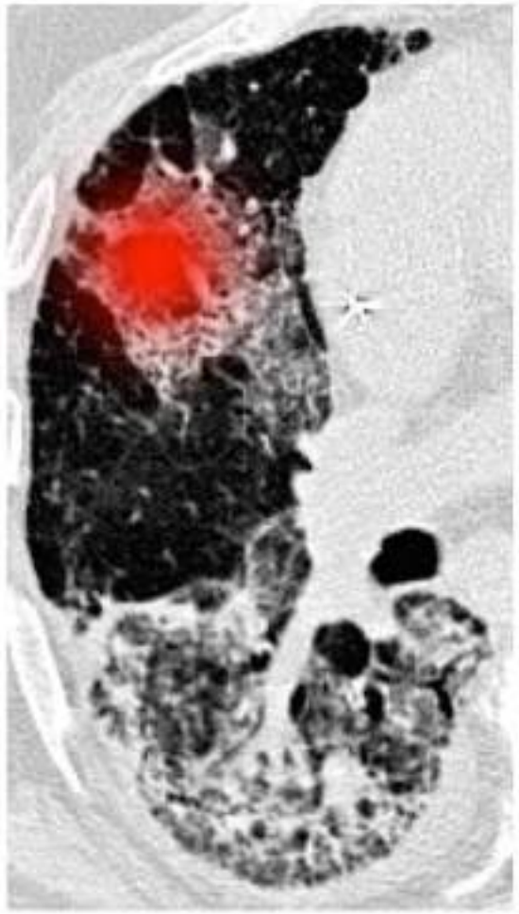

Hes·so VALAIS WALLIS
School of Management & Tourism

MULTIDIRECTIONAL TEXTURE OPERATORS

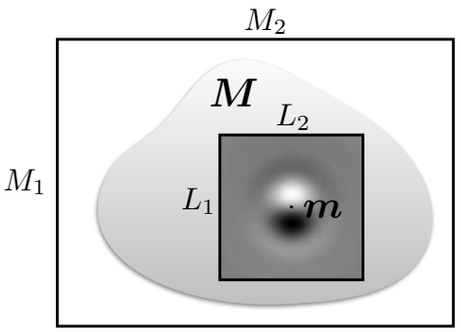

- Which directions for texture measurements?
  - Isotropic operators: insensitive to image directions

$$g_n(r, \cancel{\theta}, \boldsymbol{m}) \mapsto g_n(r, \boldsymbol{m})$$

    - Linear:

2D Gaussian filter

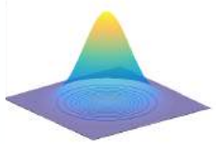

2D isotropic wavelets [Portilla2000]

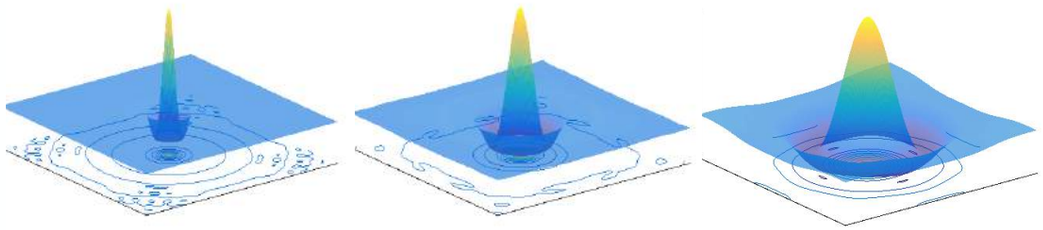

    - Non-linear: e.g., median filter
  - Directional operators
    - Linear:

2D Gaussian derivatives (e.g., Riesz wavelets [Unser2011])

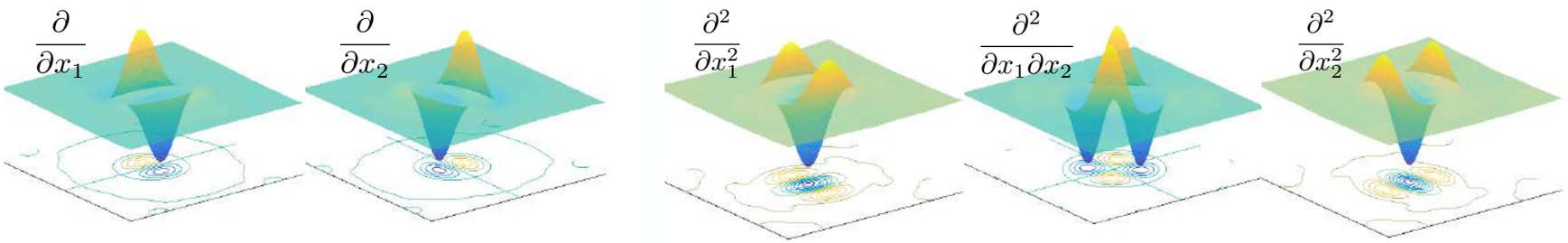

Other: e.g., Fourier, circular and spherical harmonics [Unser2013, Ward2014], MR8 [Varma2005], HOG [Dalal2005], Simoncelli's pyramid [Simoncelli1995], curvelets [Candes2000]

    - Non-linear:

2D GLCMs

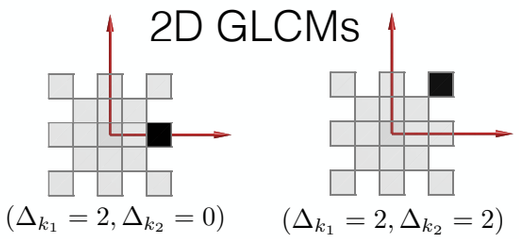

2D LBPs [Ojala2002]

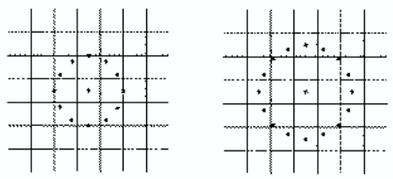

Other: e.g., RLE [Galloway1975]

Multidirectional texture operators

- Which directions for texture measurements?
  - Is directional information important for texture discrimination?

$f(\boldsymbol{x})$

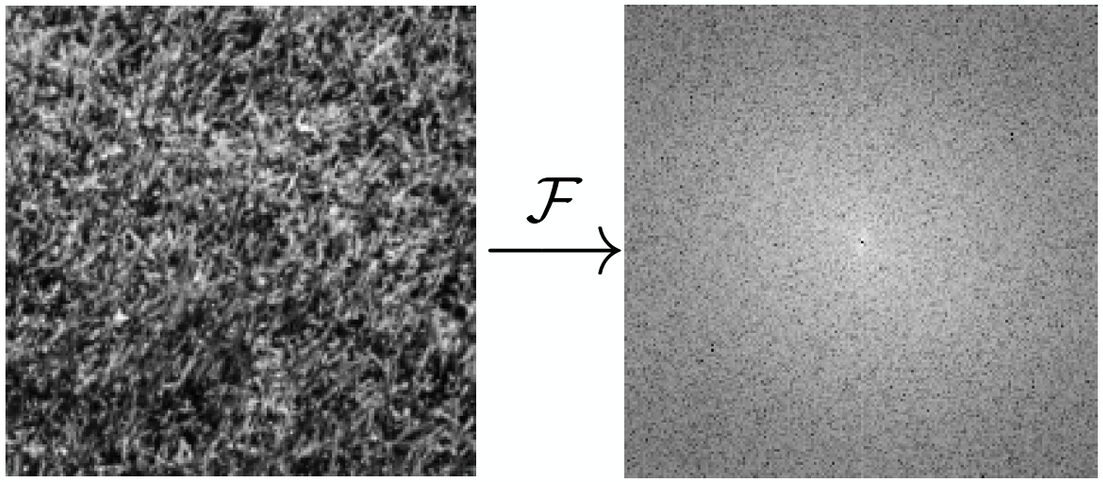

$\xrightarrow{\mathcal{F}}$

$\hat{f}(\boldsymbol{\omega})$

$f(\boldsymbol{x})$

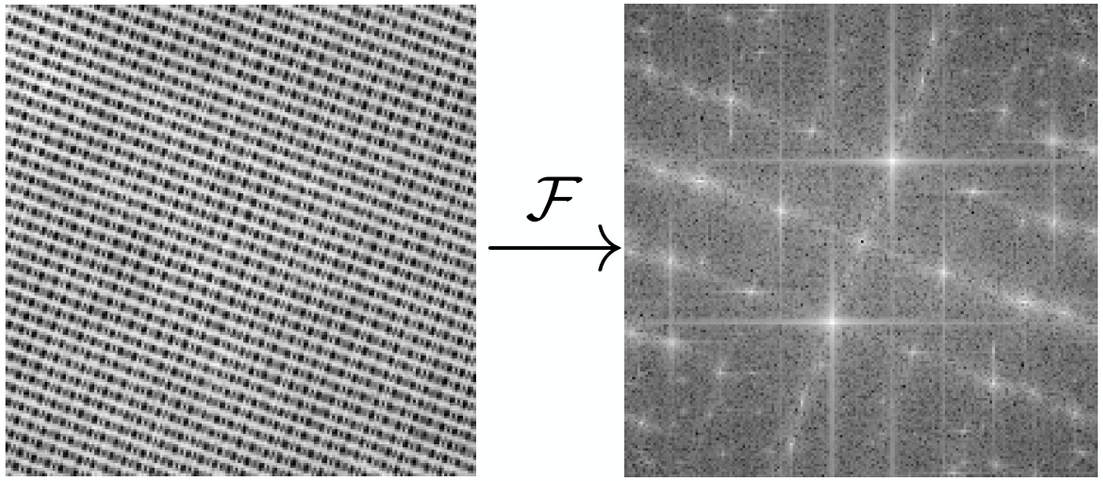

$\xrightarrow{\mathcal{F}}$

$\hat{f}(\boldsymbol{\omega})$

MULTIDIRECTIONAL TEXTURE OPERATORS

- Which directions for texture measurements?
  - Importance of the local organization of image directions (LOID)

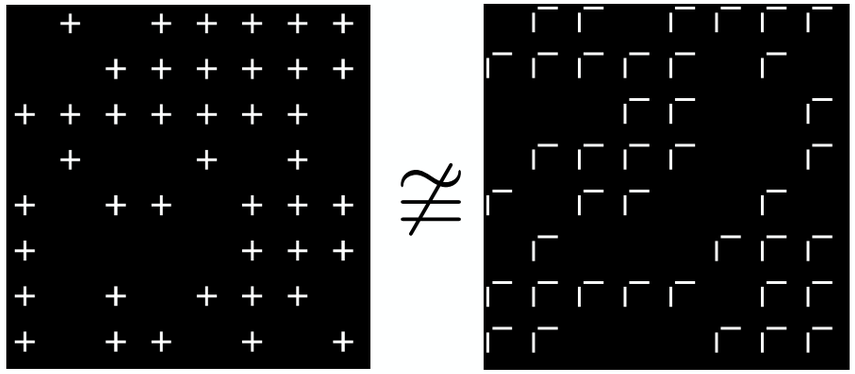

  - i.e., how directional structures intersect

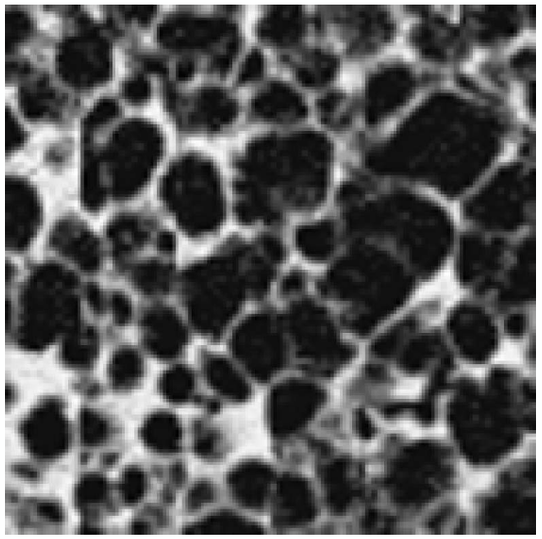

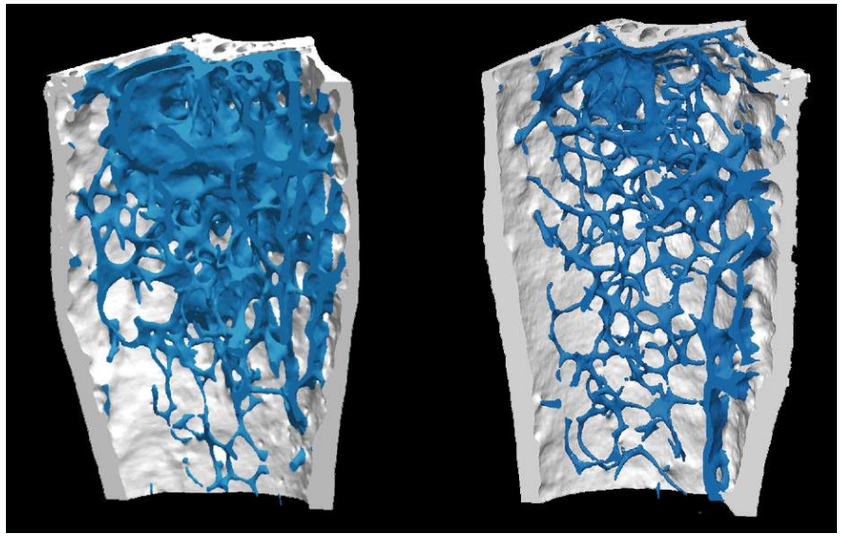

MULTIDIRECTIONAL TEXTURE OPERATORS

- Which directions for texture measurements?
  - Isotropic and unidirectional operators can hardly characterize the LOIDs, especially when aggregated over a region $\boldsymbol{M}$ [Sifre2014, Depeursinge2014b]

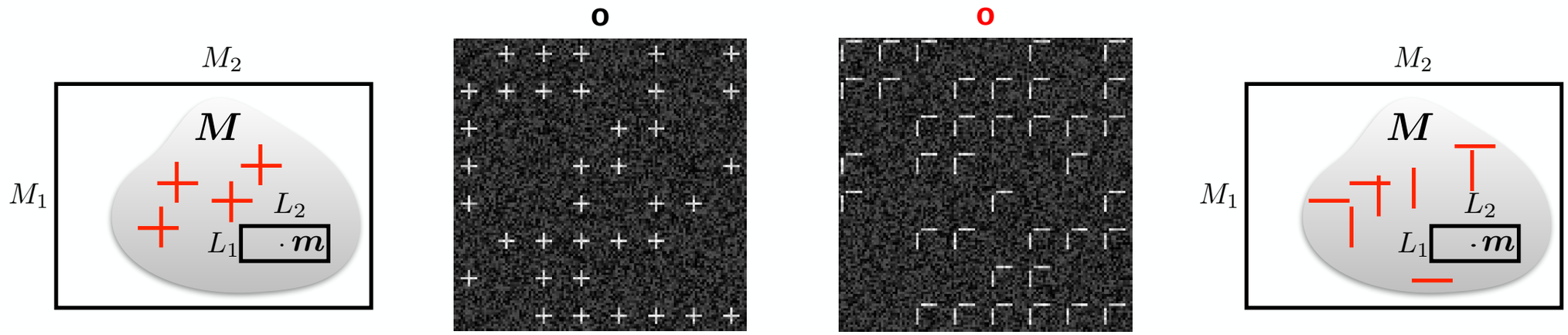

  - Example of feature representation when integrated over $\boldsymbol{M} \equiv$ entire image

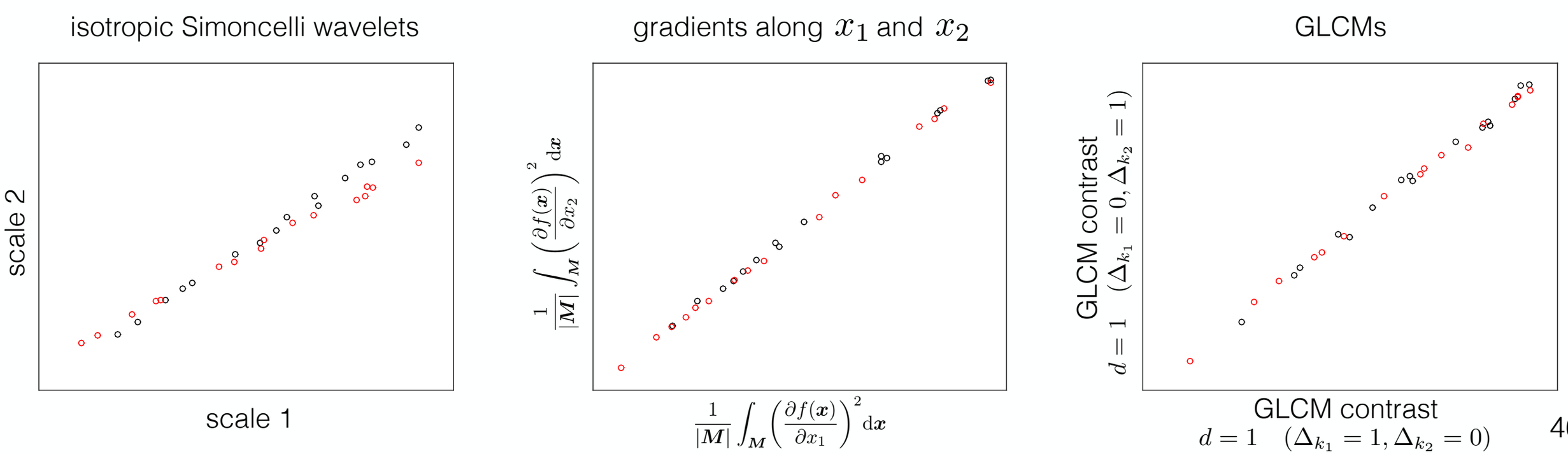

MULTIDIRECTIONAL TEXTURE OPERATORS

- Which directions for texture measurements?
  - Isotropic and unidirectional operators can hardly characterize the LOIDs, especially when aggregated over a region $\boldsymbol{M}$ [Sifre2014, Depeursinge2014b]

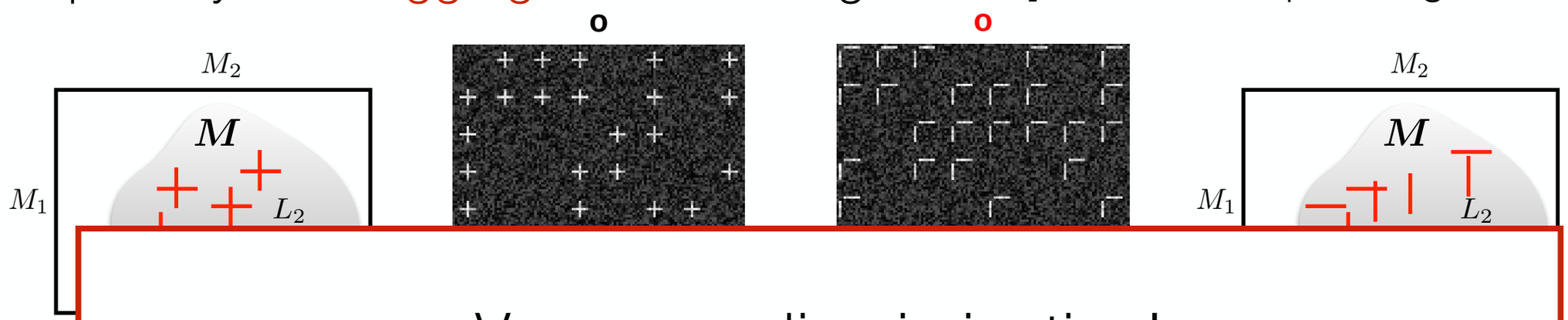

Very poor discrimination!
Solutions proposed in a few slides…

- Ex age

isotropic S

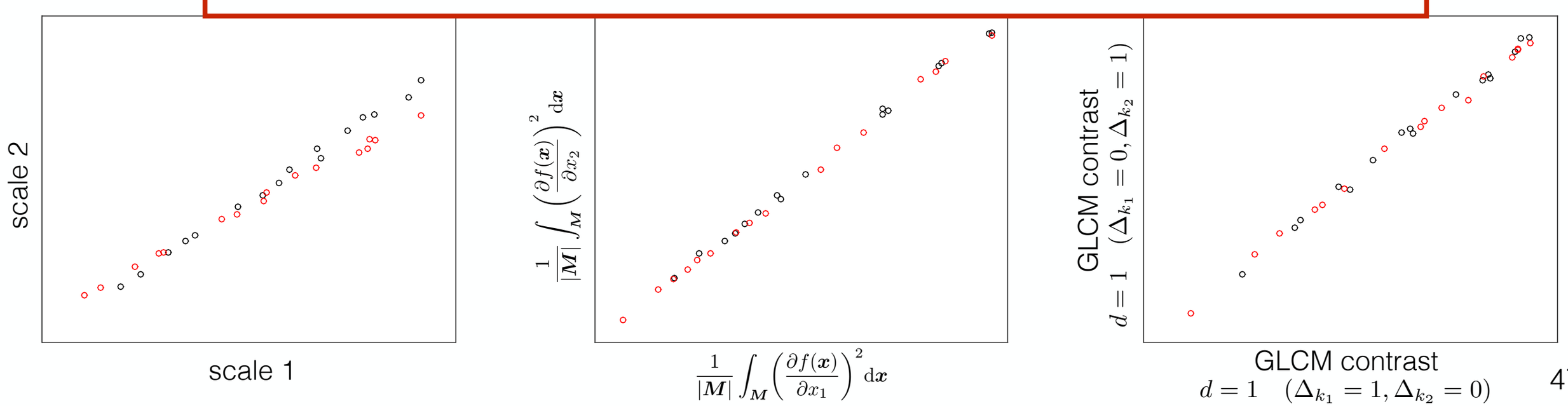

MULTIDIRECTIONAL TEXTURE OPERATORS

- Locally rotation-invariant operators over $L_1 \times L_2$

$$g(f(\boldsymbol{x}), \boldsymbol{m}) = g(f(\boldsymbol{R}_{\theta_0}\boldsymbol{x}), \boldsymbol{m}), \quad \forall \theta_0 \in [0, 2\pi), \quad \forall \boldsymbol{x} \in \mathbb{R}^{L_1 \times L_2}$$

- Isotropic operators:
  - By definition

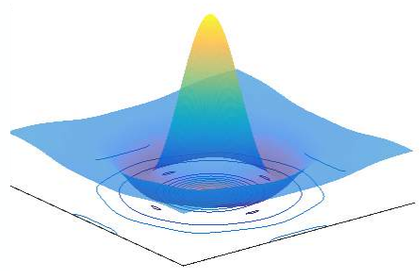

- Directional:
  - Averaging operators' responses over all directions:

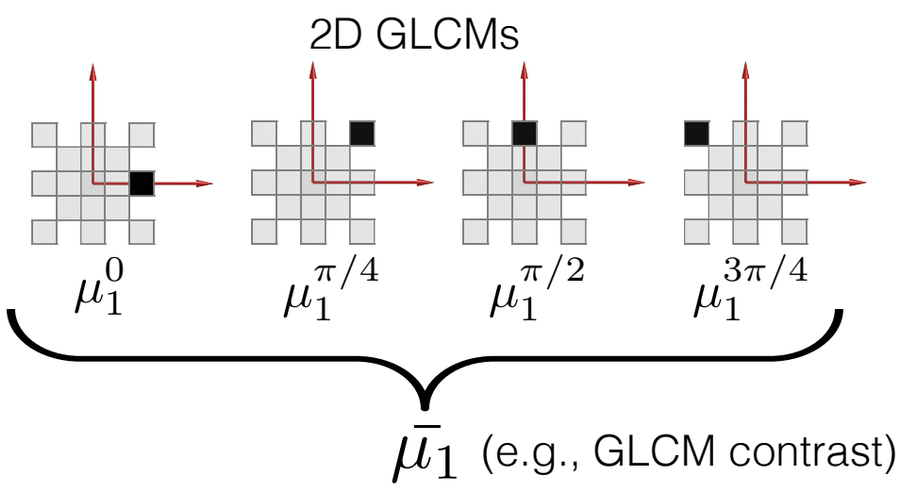

No characterization of image directions!

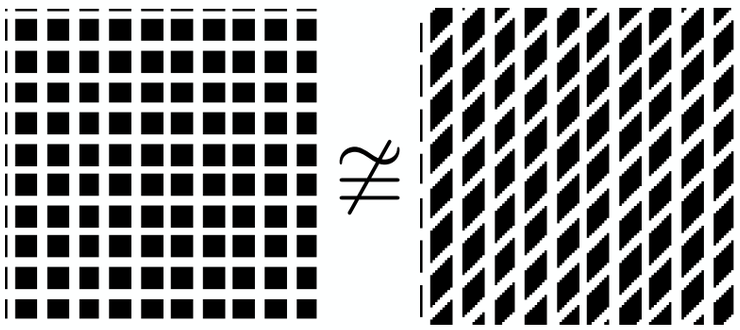

MULTIDIRECTIONAL TEXTURE OPERATORS

- Locally rotation-invariant operators over $L_1 \times L_2$

$$g(f(\boldsymbol{x}), \boldsymbol{m}) = g(f(\boldsymbol{R}_{\theta_0}\boldsymbol{x}), \boldsymbol{m}), \quad \forall \theta_0 \in [0, 2\pi), \quad \forall \boldsymbol{x} \in \mathbb{R}^{L_1 \times L_2}$$

- Locally "aligning" directional operators
  - MR8 filterbank [Varma2005]
  - Rotation-invariant LBP [Ojala2002, Ahonen2009]
  - Steerable Riesz wavelets [Unser2013, Depeursinge2014b]

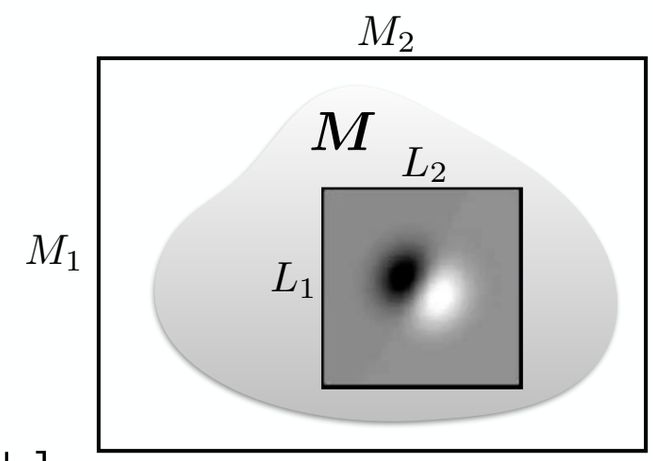

MULTIDIRECTIONAL TEXTURE OPERATORS

- Locally rotation-invariant operators over $L_1 \times L_2$

$$g(f(\boldsymbol{x}), \boldsymbol{m}) = g(f(\boldsymbol{R}_{\theta_0}\boldsymbol{x}), \boldsymbol{m}), \quad \forall \theta_0 \in [0, 2\pi), \quad \forall \boldsymbol{x} \in \mathbb{R}^{L_1 \times L_2}$$

- Locally "aligning" directional operators
  - Maximum response 8 (MR8) filterbank [Varma2005]

isotropic

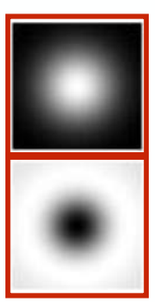

mutliscale oriented gradients

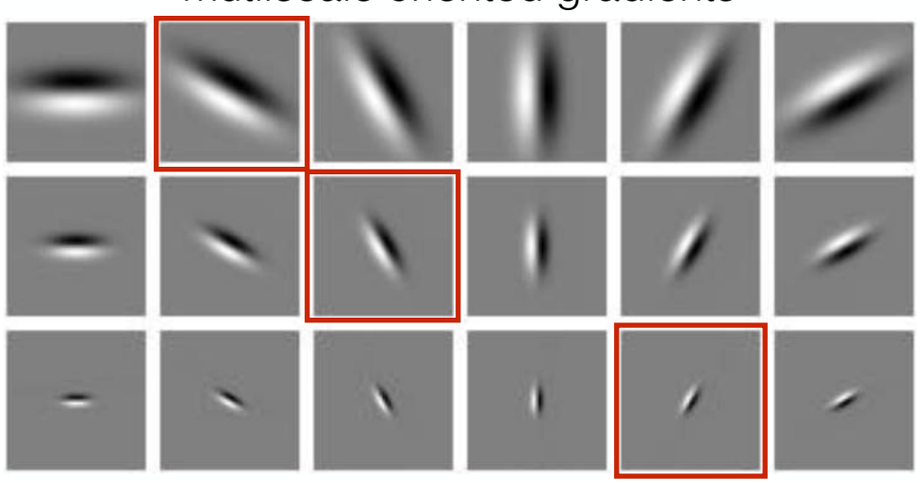

multiscale oriented Laplacians

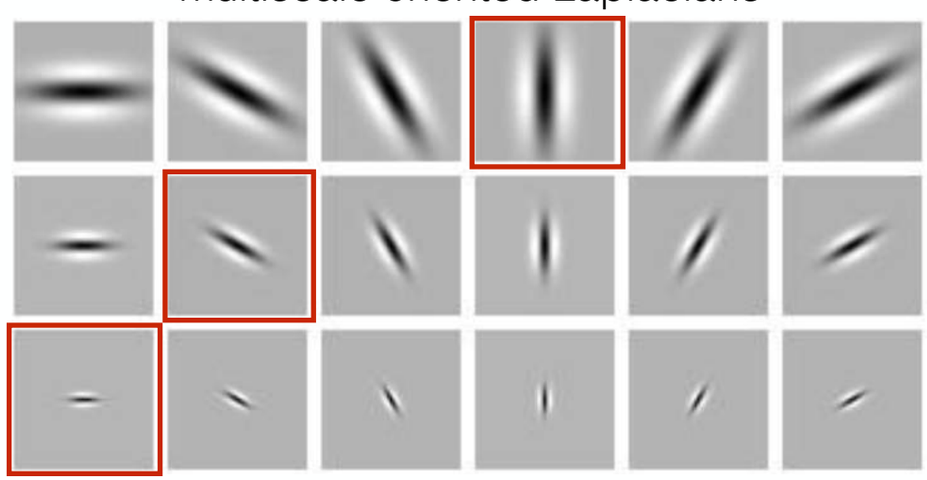

  - Filter responses are obtained for each pixel from the convolution of the filter and the image
  - For each position $\boldsymbol{m}$, only the maximum responses among gradient and Laplacian filters are kept

MULTIDIRECTIONAL TEXTURE OPERATORS

- Locally rotation-invariant operators over $L_1 \times L_2$

$$g(f(\boldsymbol{x}), \boldsymbol{m}) = g(f(\boldsymbol{R}_{\theta_0}\boldsymbol{x}), \boldsymbol{m}), \quad \forall \theta_0 \in [0, 2\pi), \quad \forall \boldsymbol{x} \in \mathbb{R}^{L_1 \times L_2}$$

- Locally "aligning" directional operators
  - Maximum response 8 (MR8) filterbank [Varma2005]

isotropic

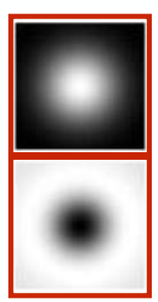

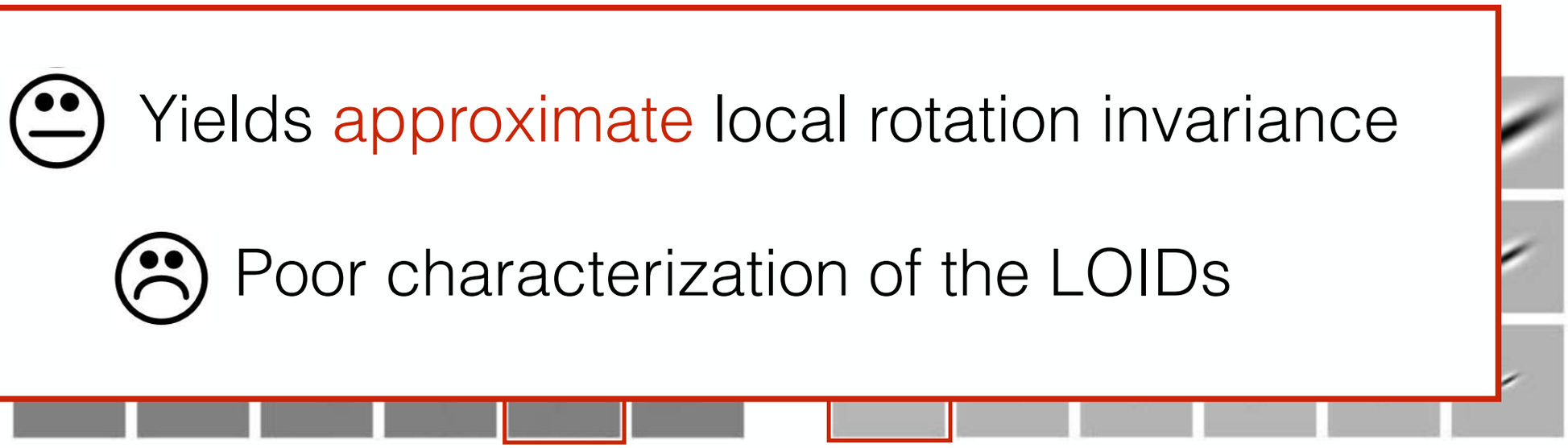

😐 Yields approximate local rotation invariance

☹ Poor characterization of the LOIDs

  - Filter responses are obtained for each pixel from the convolution of the filter and the image
  - For each position $\boldsymbol{m}$, only the maximum responses among gradient and Laplacian filters are kept

MULTIDIRECTIONAL TEXTURE OPERATORS

- Locally rotation-invariant operators over $L_1 \times L_2$

$$g(f(\boldsymbol{x}), \boldsymbol{m}) = g(f(\boldsymbol{R}_{\theta_0}\boldsymbol{x}), \boldsymbol{m}), \quad \forall \theta_0 \in [0, 2\pi), \quad \forall \boldsymbol{x} \in \mathbb{R}^{L_1 \times L_2}$$

- Locally "aligning" directional operators

  - Local binary patterns (LBP) [Ojala2002]

1) define a circular neighborhood

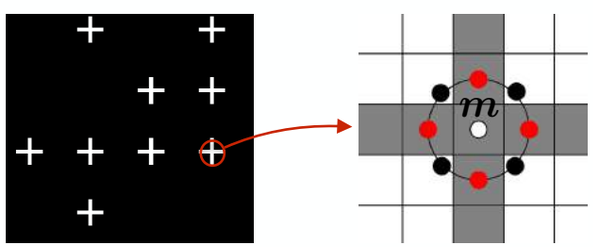

2) Binarize and build a number that encode the LOIDs

$$\Rightarrow \quad U_8(1,0) = 10101010 = 170$$

3) Aggregate over the entire image and count code occurrences

$$\mu_{0,p} = h_I(U_8(1,0))$$

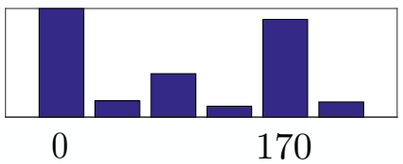

  - Rotation-invariant LBP [Ahonen2009]

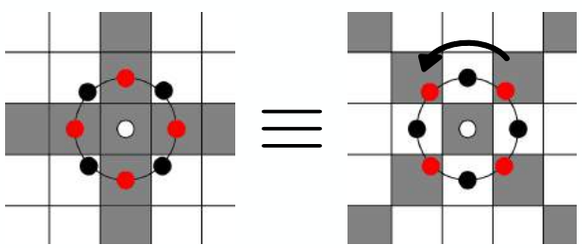

4) make codes invariant to circular shifts

$$\left.\begin{aligned} U_8(1,\boxed{0}) &= 10101010 \\ U_8(1,\boxed{1}) &= 01010101 \end{aligned}\right\}$$

rotation r

discrete Fourier transform

$$H_8(1,u) = \sum_{r=0}^{7} h_I(U_8(1,r))e^{-j2\pi ur/8}$$

$\Rightarrow$ The new measures $\mu_p = |H_8(1,u)|$ are independent of the rotation r

MULTIDIRECTIONAL TEXTURE OPERATORS

- Locally rotation-invariant operators over $L_1 \times L_2$

$$g(f(\boldsymbol{x}), \boldsymbol{m}) = g(f(\boldsymbol{R}_{\theta_0}\boldsymbol{x}), \boldsymbol{m}), \quad \forall \theta_0 \in [0, 2\pi), \quad \forall \boldsymbol{x} \in \mathbb{R}^{L_1 \times L_2}$$

- Locally "aligning" directional operators
  - L
    1) d
  - R

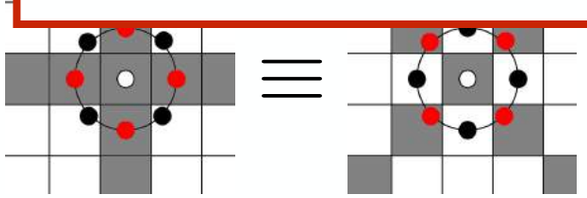

$$U_8(1,1) = 01010101$$

rotation r

$$H_8(1,u) = \sum_{r=0} h_I(U_8(1,r))e^{-j2\pi ur/8}$$

ntire image
rrences
$,0))$
sform

☺ Encodes the LOIDs independently from their local orientations!

☹ Requires binarization…

☹ Spherical sequences are undefined in 3D…

$\Rightarrow$ The new measures $\mu_p = |H_8(1,u)|$ are independent of the rotation r

MULTIDIRECTIONAL TEXTURE OPERATORS

- Locally rotation-invariant operators over $L_1 \times L_2$

$$g(f(\boldsymbol{x}), \boldsymbol{m}) = g(f(\boldsymbol{R}_{\theta_0}\boldsymbol{x}), \boldsymbol{m}), \quad \forall \theta_0 \in [0, 2\pi), \quad \forall \boldsymbol{x} \in \mathbb{R}^{L_1 \times L_2}$$

- Locally "aligning" directional operators
  - Steerable Riesz wavelets [Unser2013, Depeursinge2014b]
    - Operators: Nth-order multi-scale image derivatives

$N = 1$

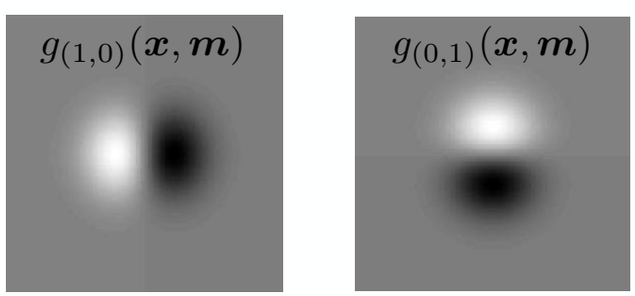

input image $f(\boldsymbol{x})$

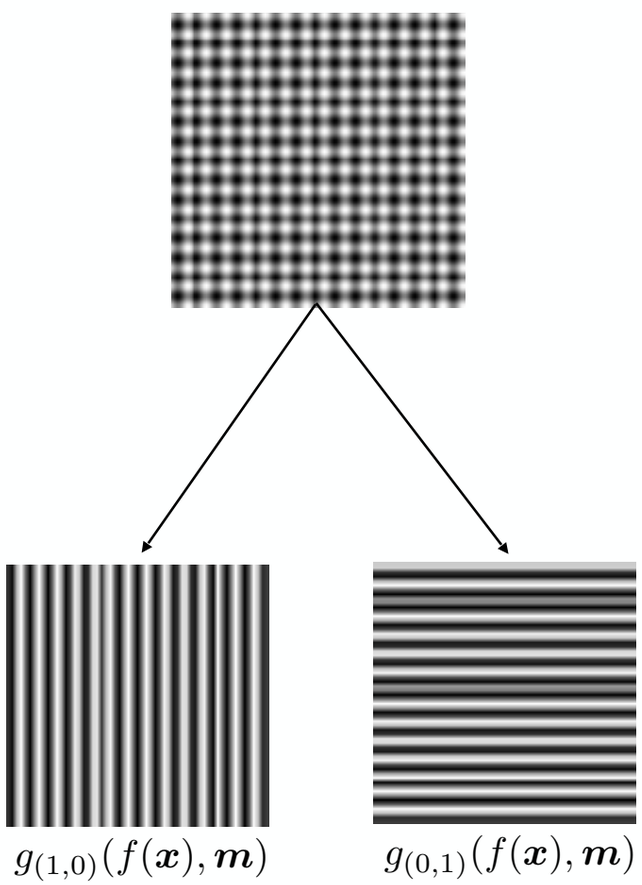

ÉCOLE POLYTECHNIQUE FÉDÉRALE DE LAUSANNE

MULTIDIRECTIONAL TEXTURE OPERATORS

- Locally rotation-invariant operators over $L_1 \times L_2$

$$g(f(\boldsymbol{x}), \boldsymbol{m}) = g(f(\boldsymbol{R}_{\theta_0}\boldsymbol{x}), \boldsymbol{m}), \quad \forall \theta_0 \in [0, 2\pi), \quad \forall \boldsymbol{x} \in \mathbb{R}^{L_1 \times L_2}$$

- Locally "aligning" directional operators
  - Steerable Riesz wavelets [Unser2013, Depeursinge2014b]
    - Operators: Nth-order multi-scale image derivatives

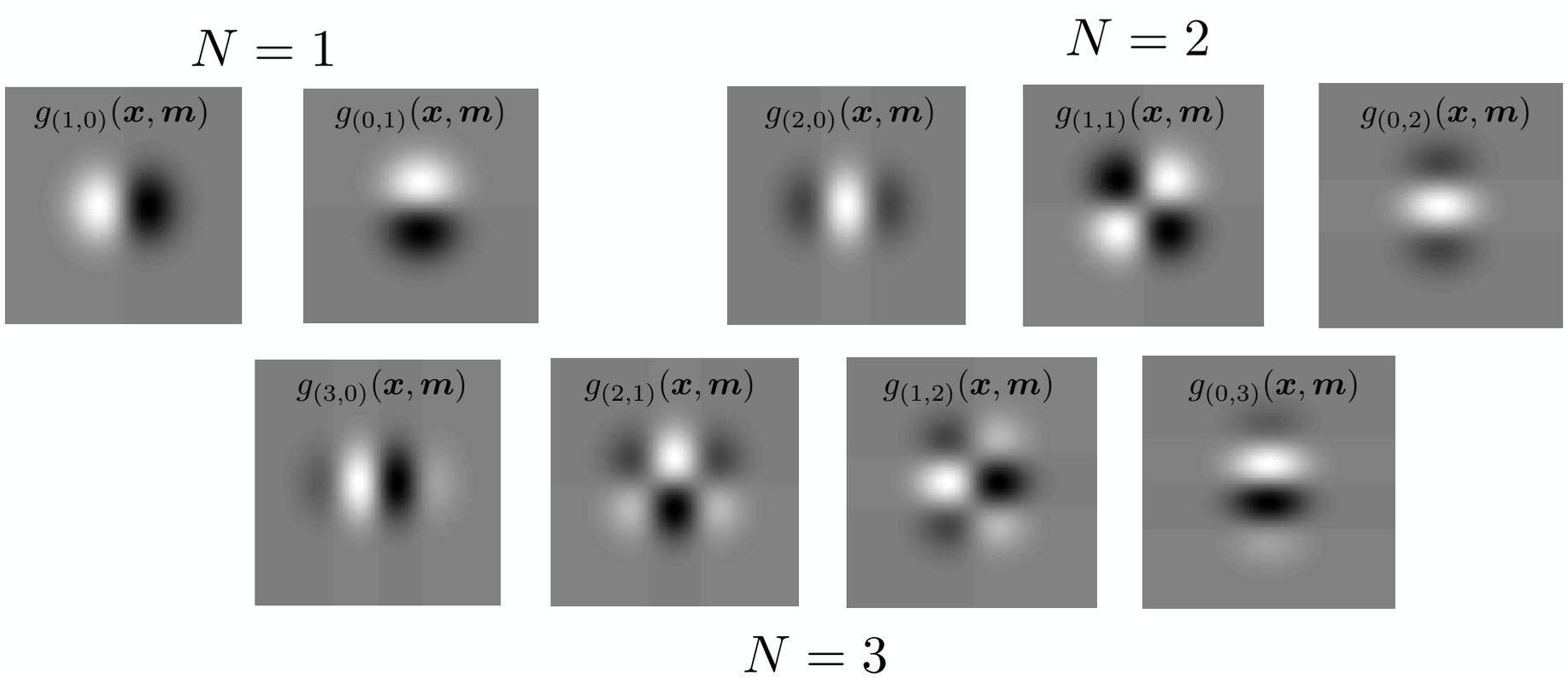

ÉCOLE POLYTECHNIQUE FÉDÉRALE DE LAUSANNE

MULTIDIRECTIONAL TEXTURE OPERATORS

- Locally rotation-invariant operators over $L_1 \times L_2$

$$g(f(\boldsymbol{x}), \boldsymbol{m}) = g(f(\boldsymbol{R}_{\theta_0}\boldsymbol{x}), \boldsymbol{m}), \quad \forall \theta_0 \in [0, 2\pi), \quad \forall \boldsymbol{x} \in \mathbb{R}^{L_1 \times L_2}$$

- Locally "aligning" directional operators
  - Steerable Riesz wavelets [Unser2013, Depeursinge2014b]
    - Steerability:

$$g_{(1,0)}(\boldsymbol{R}_{\theta_0}\boldsymbol{x}, \boldsymbol{0}) = \cos\theta_0 \, g_{(1,0)}(\boldsymbol{x}, \boldsymbol{0}) \; + \; \sin\theta_0 \, g_{(0,1)}(\boldsymbol{x}, \boldsymbol{0})$$

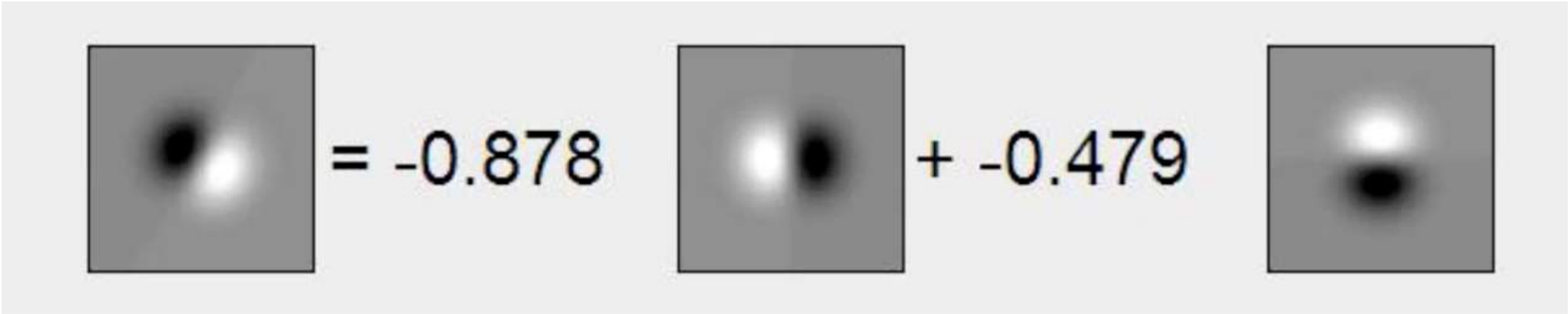

MULTIDIRECTIONAL TEXTURE OPERATORS

- Locally rotation-invariant operators over $L_1 \times L_2$

$$g(f(\boldsymbol{x}), \boldsymbol{m}) = g(f(\boldsymbol{R}_{\theta_0}\boldsymbol{x}), \boldsymbol{m}), \quad \forall \theta_0 \in [0, 2\pi), \quad \forall \boldsymbol{x} \in \mathbb{R}^{L_1 \times L_2}$$

- Locally "aligning" directional operators
  - Steerable Riesz wavelets [Unser2013, Depeursinge2014b]
    - Local rotation-invariance:

$$\theta_{\max}(\boldsymbol{m}) := \underset{\theta_0 \in [0,2\pi)}{\arg\max} \Big(\cos\theta_0 \, g_{(1,0)}(f(\boldsymbol{x}), \boldsymbol{m}) \; + \; \sin\theta_0 \, g_{(0,1)}(f(\boldsymbol{x}), \boldsymbol{m}) \Big)$$

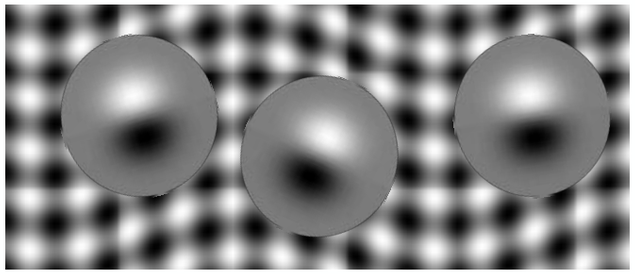

$$\Rightarrow \quad \mu_{\boldsymbol{M}} = \frac{1}{|\boldsymbol{M}|} \int_{\boldsymbol{M}} \Big(g_{(1,0)}(f(\boldsymbol{R}_{\theta_{\max}(\boldsymbol{m})} \, \boldsymbol{x}), \boldsymbol{m}) \Big)^2 \mathrm{d}\boldsymbol{m}$$

MULTIDIRECTIONAL TEXTURE OPERATORS

- Locally rotation-invariant operators over $L_1 \times L_2$

$$g(f(\boldsymbol{x}), \boldsymbol{m}) = g(f(\boldsymbol{R}_{\theta_0}\boldsymbol{x}), \boldsymbol{m}), \quad \forall \theta_0 \in [0, 2\pi), \quad \forall \boldsymbol{x} \in \mathbb{R}^{L_1 \times L_2}$$

- Locally "aligning" directional operators

☺ Encodes the LOIDs independently from their local orientations!

☺ No binarization required!

☺ Available in 3D [Chenouard2012, Depeursinge2015a], and combined with feature learning [Depeursinge2014b].

MULTIDIRECTIONAL TEXTURE OPERATORS

- Operators characterizing the LOIDs

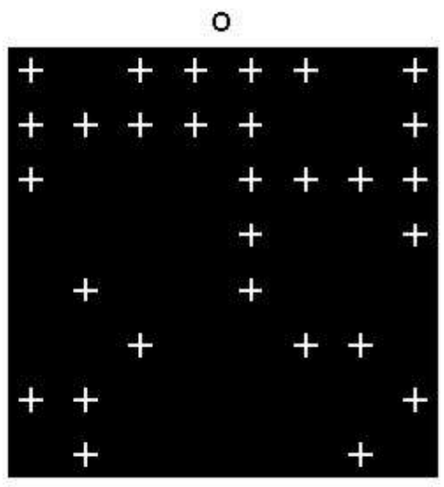

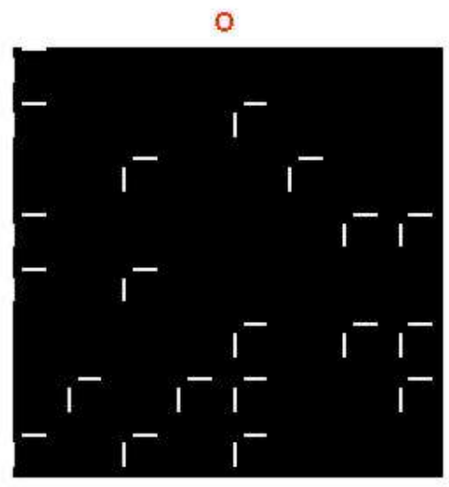

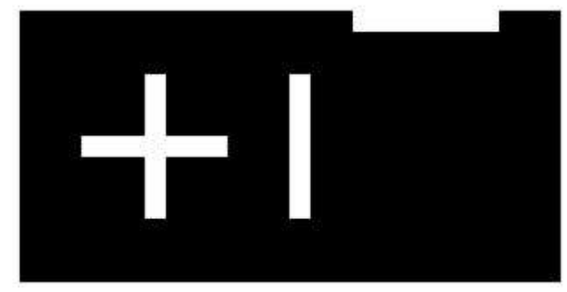

GLCMs

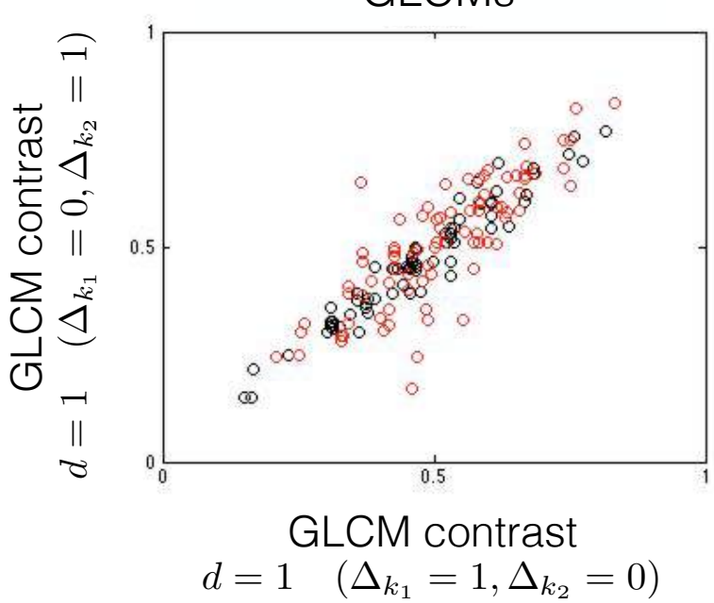

Riesz wavelets ($N = 2$)

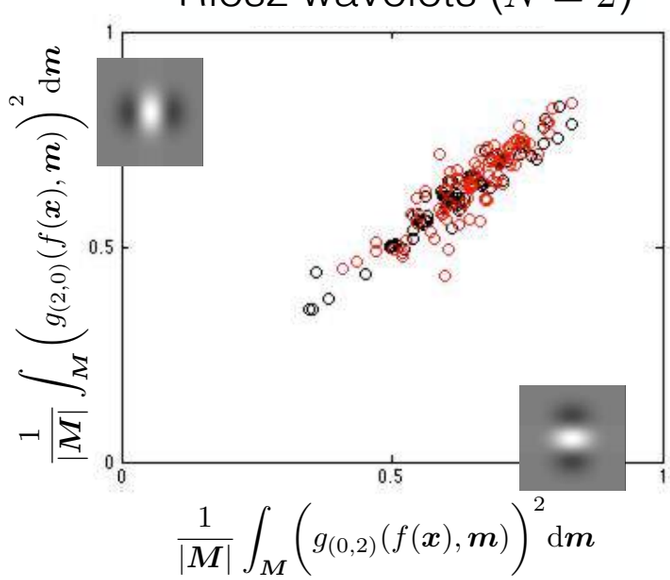

aligned Riesz wavelets ($N = 2$)

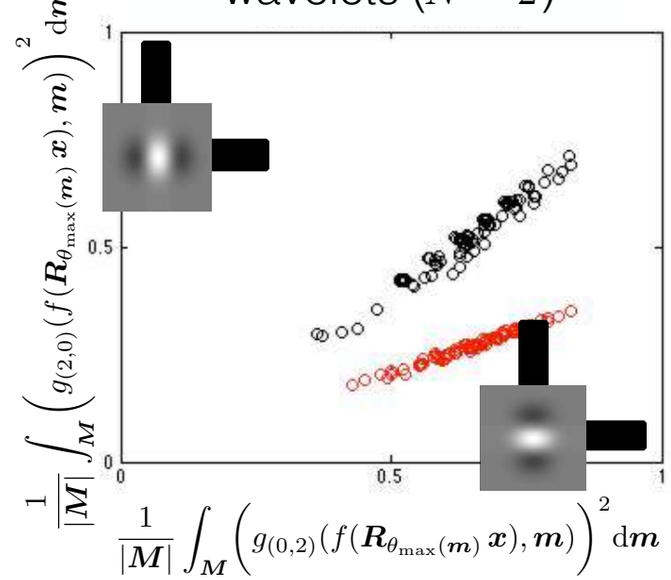

ÉCOLE POLYTECHNIQUE FÉDÉRALE DE LAUSANNE

Hes·so VALAIS WALLIS School of Management & Tourism

MULTIDIRECTIONAL TEXTURE OPERATORS

- Operators characterizing the LOIDs

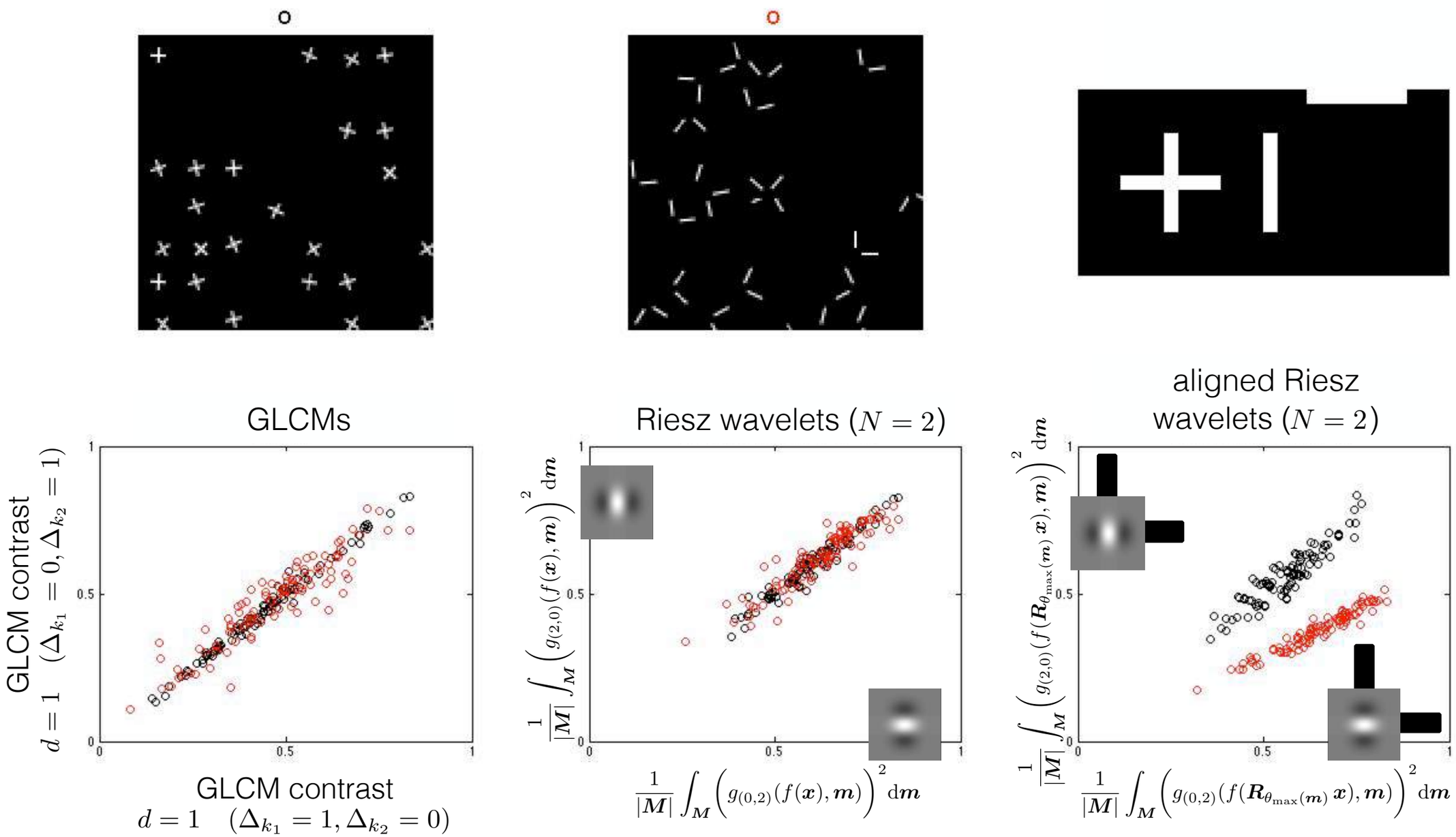

MULTIDIRECTIONAL TEXTURE OPERATORS

- Isotropic or directional analysis? [Depeursinge2014b]
  - Outex [Ojala2002]: 24 classes, 180 images/class, 9 rotation angles in $[0°; 90°]$

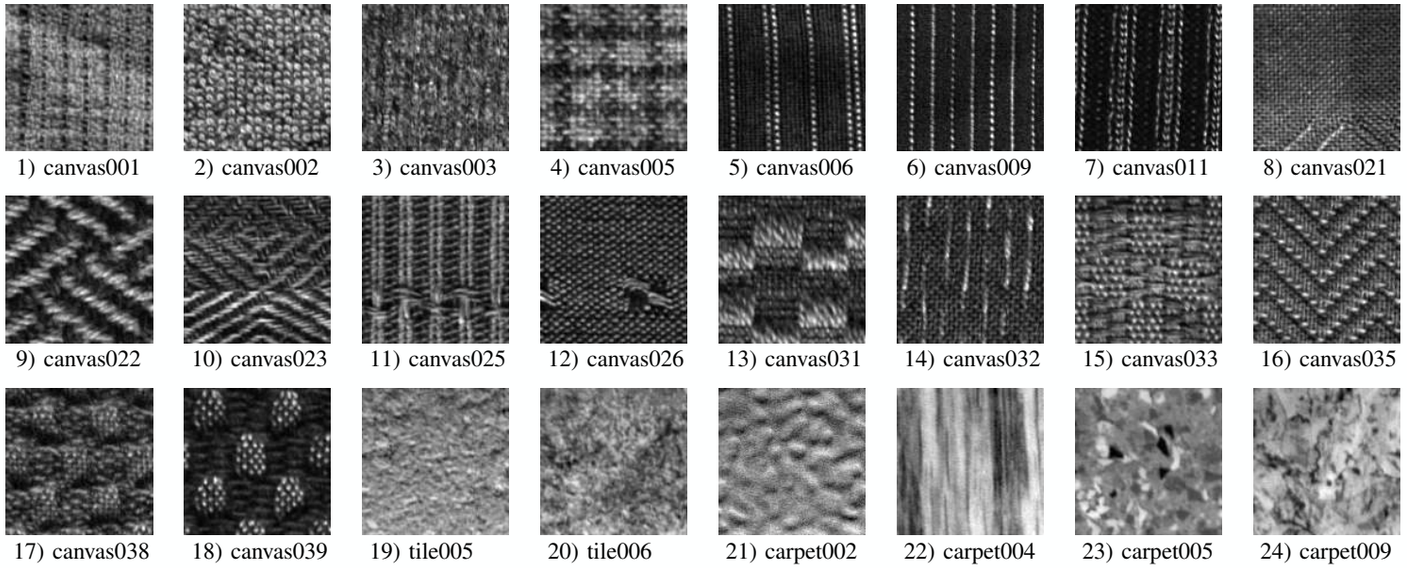

  - Texture classification: linear SVMs trained with unrotated images only

ÉCOLE POLYTECHNIQUE FÉDÉRALE DE LAUSANNE

Hes·so VALAIS WALLIS School of Management & Tourism

MULTIDIRECTIONAL TEXTURE OPERATORS

- Isotropic or directional analysis? [Depeursinge2014b]
  - Outex [Ojala2002]: 24 classes, 180 images/class, 9 rotation angles in $[0°; 90°]$

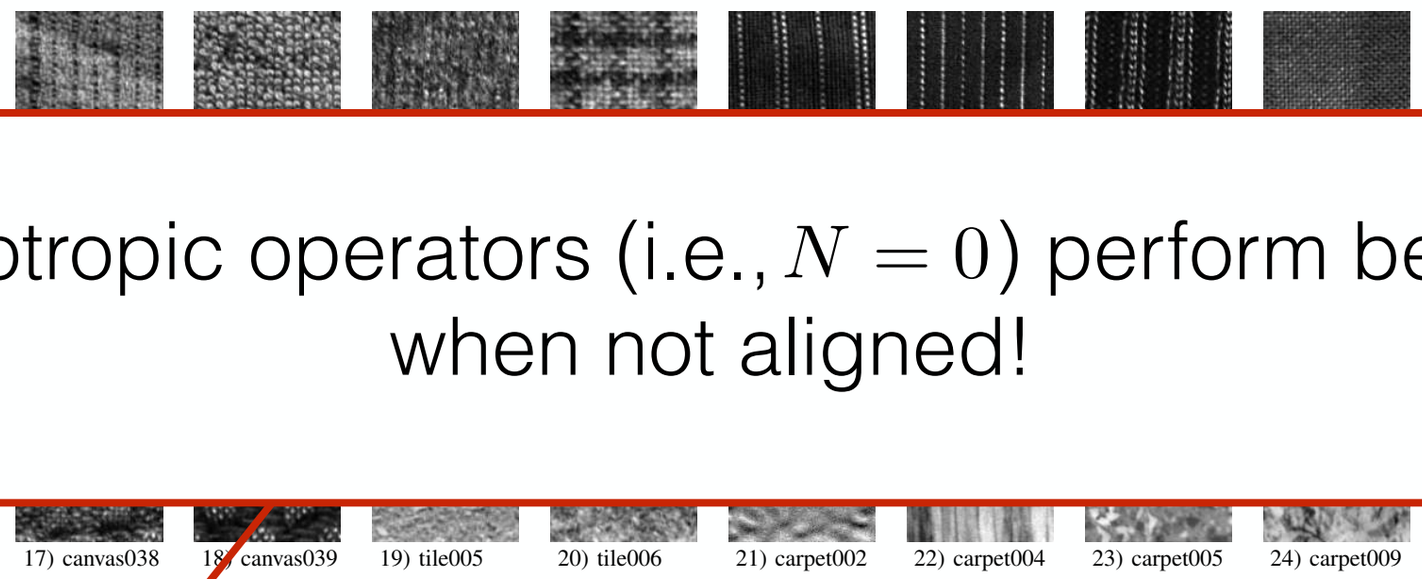

Isotropic operators (i.e., $N = 0$) perform best when not aligned!

  - Texture classification: linear SVMs trained with unrotated images only

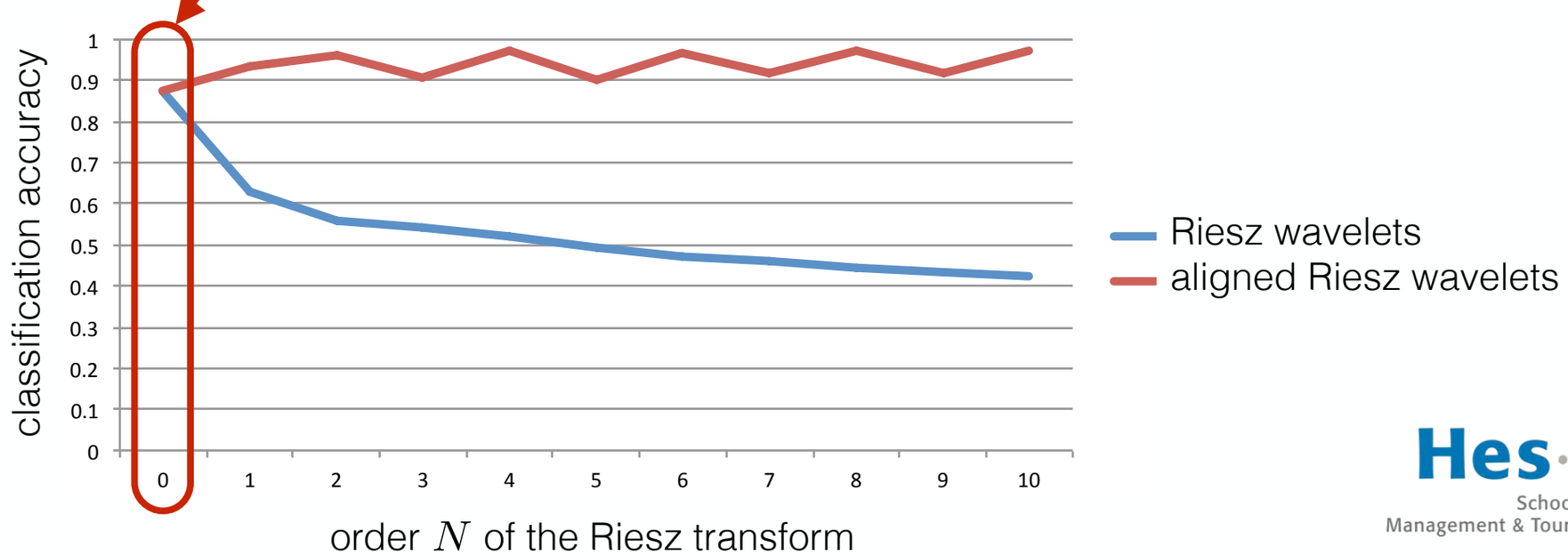

ÉCOLE POLYTECHNIQUE FÉDÉRALE DE LAUSANNE

Hes·so VALAIS WALLIS School of Management & Tourism

OUTLINE

- Biomedical texture analysis: background
- Defining texture processes
  - Notations, sampling and texture functions
- Texture operators, primitives and invariances
  - Multiscale analysis
    - Operator scale and uncertainty principle
    - Region of interest and operator aggregation
  - Multidirectional analysis
    - Isotropic versus directional operators
    - Importance of the local organization of image directions
- Conclusions
- References

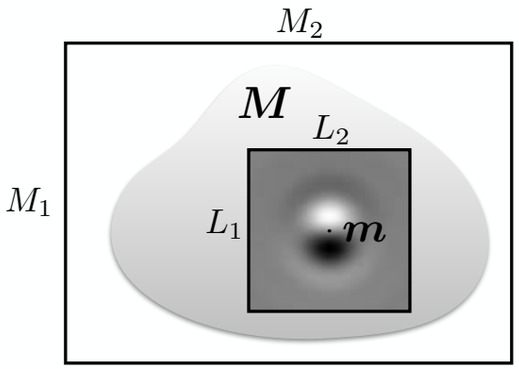

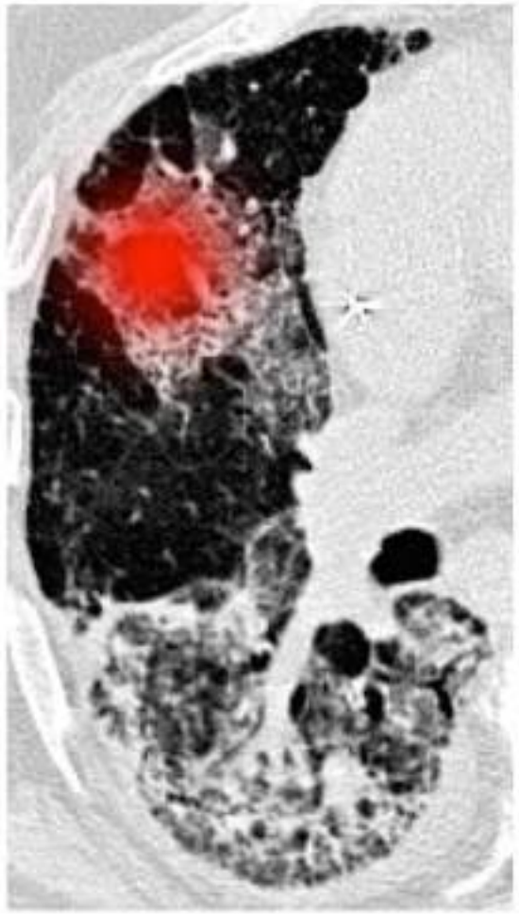

Hes·so VALAIS WALLIS
School of Management & Tourism

Conclusions

- We presented a general framework to describe and analyse texture information in 2D and 3D

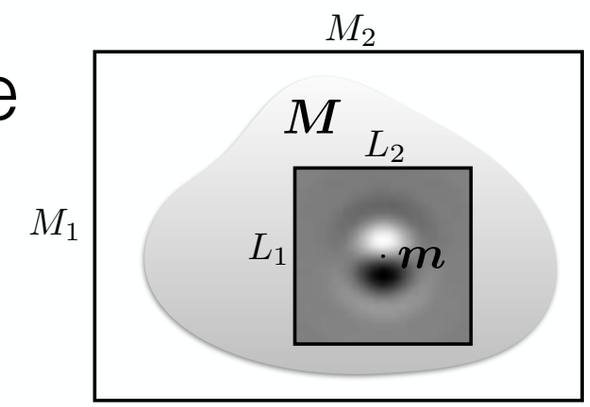

- Tissue structures in 2D/3D medical images contain extremely rich and valuable information to optimize personalized medicine in a non-invasive way

- Invisible to the naked eye!

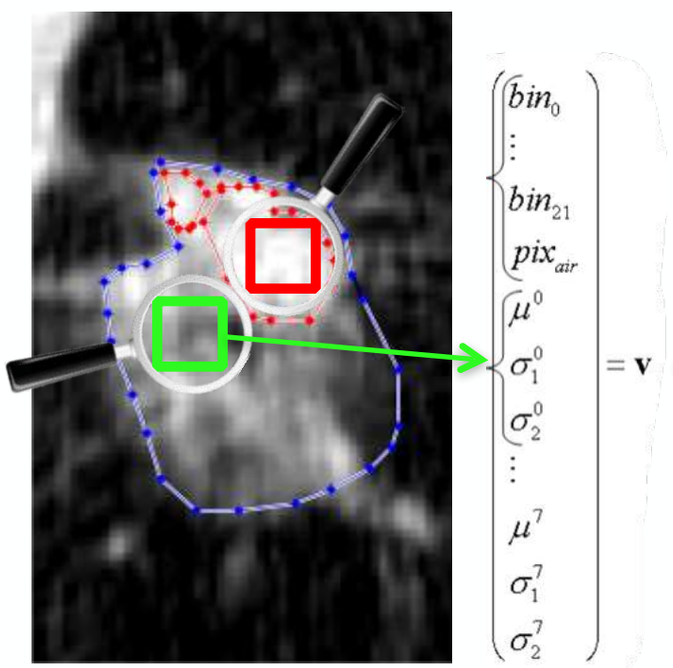

$$\begin{Bmatrix} bin_0 \\ \vdots \\ bin_{21} \\ pix_{air} \\ \mu^0 \\ \sigma_1^0 \\ \sigma_2^0 \\ \vdots \\ \mu^7 \\ \sigma_1^7 \\ \sigma_2^7 \end{Bmatrix} = \mathbf{v}$$

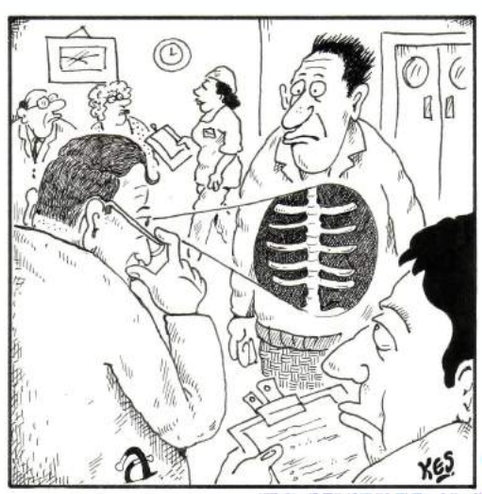

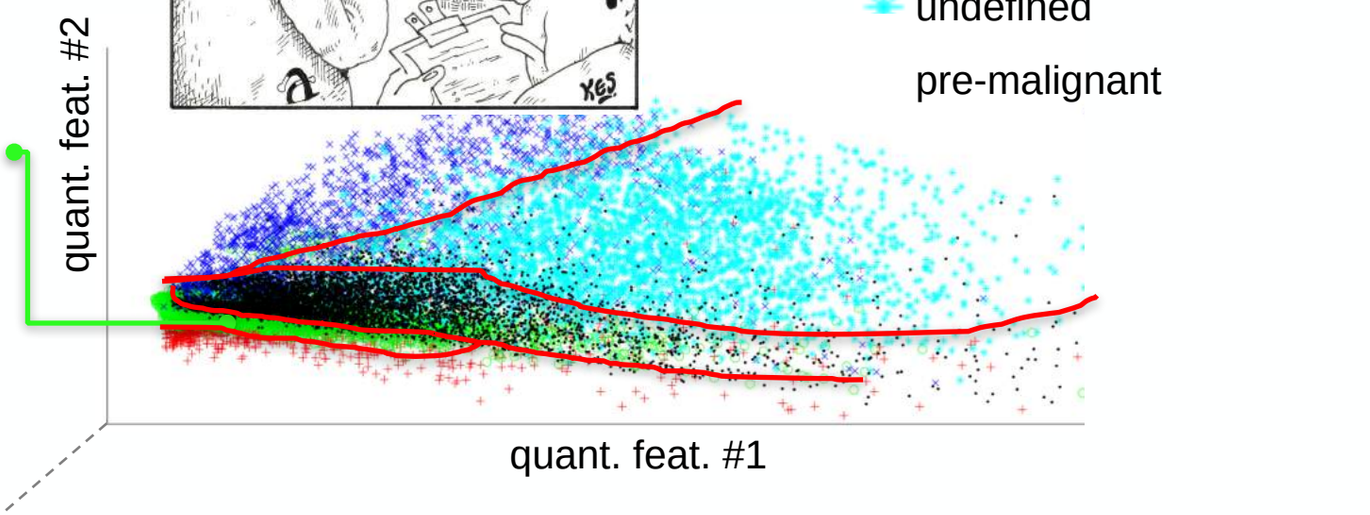

CONCLUSIONS

- Biomedical textures are realizations of complex non-stationary spatial stochastic processes
- General-purpose image operators are necessary to identify data-specific discriminative scales and directions

	texture operators	region of interest and aggregation
scales	uncertainty principle 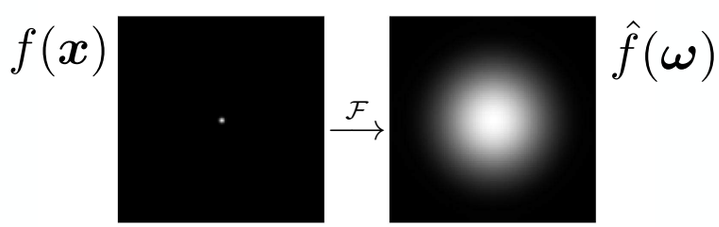	averaging operators' responses 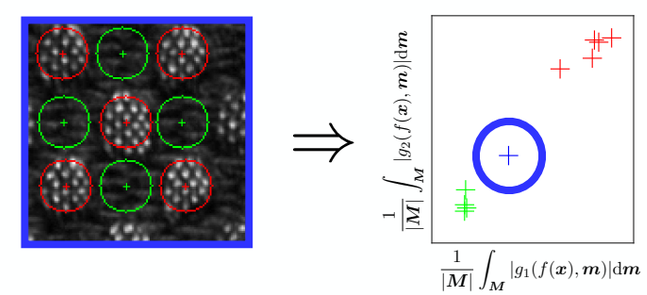
directions	isotropic versus directional 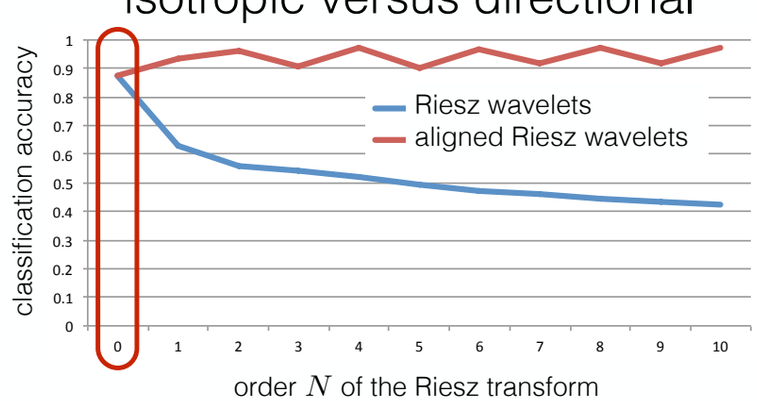	importance of LOIDs 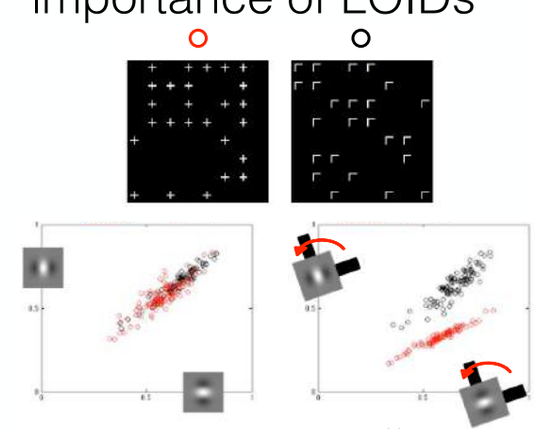

THANKS !

Source code and data available!
https://sites.google.com/site/btamiccai2015/
adrien.depeursinge@epfl.ch

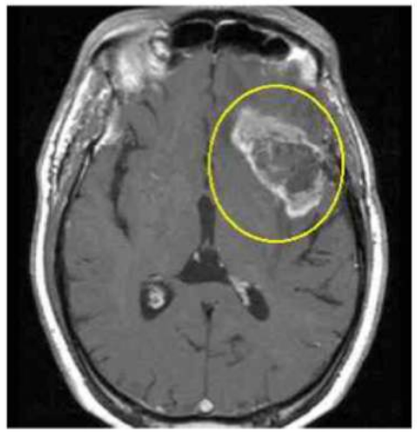

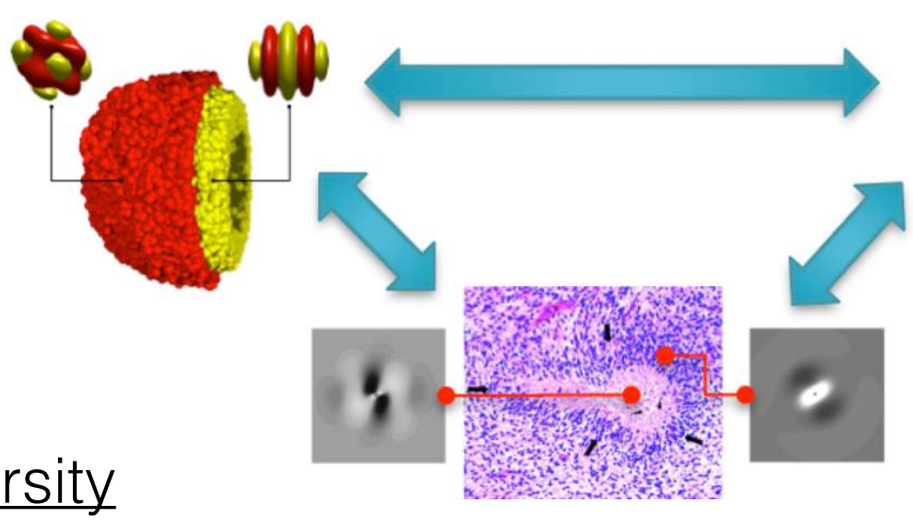

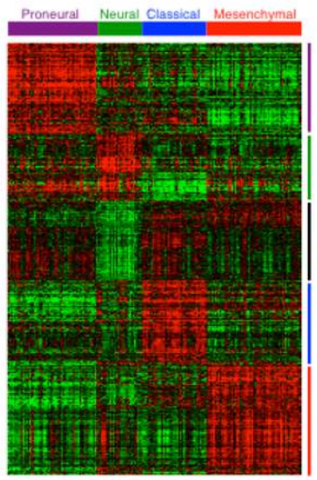

BIG @ EPFL
Michael Unser
Julien Fageot
Arash Amini
and all members

MedGIFT @ HES-SO
Henning Müller
Yashin Dicente
Roger Schaer
Ranveer Joyseree
Oscar Jimenez
Manfredo Atzori

Stanford University
Daniel Rubin
Olivier Gevaert
Ann Leung

Dimitri Van de Ville, UNIGE
Camille Kurtz, Paris Descartes
Pierre-Alexandre Poletti, HUG
John-Paul Ward, UCF

MICCAI'15 MUNICH

EPFL ÉCOLE POLYTECHNIQUE FÉDÉRALE DE LAUSANNE

[BIG]

FNSNF SWISS NATIONAL SCIENCE FOUNDATION

STANFORD SCHOOL OF MEDICINE
Stanford University Medical Center

HUG Hôpitaux Universitaires de Genève

Hes·so VALAIS WALLIS School of Management & Tourism

References (sorting in alphabetical order)

[Ahonen2009] Ahonen, T.; Matas, J.; He, C. & Pietikäinen, M.
Salberg, A.-B.; Hardeberg, J. & Jenssen, R. (Eds.)
Rotation Invariant Image Description with Local Binary Pattern Histogram Fourier Features
Image Analysis, Springer Berlin Heidelberg, 2009, 5575, 61-70

[Aerts2014] Aerts, H. J. W. L.; Velazquez, E. R.; Leijenaar, R. T. H.; Parmar, C.; Grossmann, P.; Carvalho, S.; Bussink, J.; Monshouwer, R.; Haibe-Kains, B.; Rietveld, D.; Hoebers, F.; Rietbergen, M. M.; Leemans, C. R.; Dekker, A.; Quackenbush, J.; Gillies, R. J. & Lambin, P.
Decoding Tumour Phenotype by Noninvasive Imaging Using a Quantitative Radiomics Approach
Nature Communications, Nature Publishing Group, a division of Macmillan Publishers Limited. All Rights Reserved, 2014, 5

[Blakemore1969] Blakemore, C. & Campbell, F. W.
On the Existence of Neurones in the Human Visual System Selectively Sensitive to the Orientation and Size of Retinal Images
The Journal of Physiology, 1969, 203, 237-260

[Candes2000] Candès, E. J. & Donoho, D. L.
Curvelets - A Surprisingly Effective Nonadaptive Representation For Objects with Edges
Curves and Surface Fitting, Vanderbilt University Press, 2000, 105-120

[Chenouard2011] Chenouard, N. & Unser, M.
3D Steerable Wavelets and Monogenic Analysis for Bioimaging
2011 IEEE International Symposium on Biomedical Imaging: From Nano to Macro, 2011, 2132-2135

[Chenouard2012] Chenouard, N. & Unser, M.
3D Steerable Wavelets in Practice
IEEE Transactions on Image Processing, 2012, 21, 4522-4533

References (sorting in alphabetical order)

[Dalal2005] Dalal, N. & Triggs, B.
Histograms of Oriented Gradients for Human Detection
Proceedings of the 2005 IEEE Computer Society Conference on Computer Vision and Pattern Recognition (CVPR'05), IEEE Computer Society, 2005, 1, 886-893

[Depeursinge2012a] Depeursinge, A.; Foncubierta-Rodrguez, A.; Van De Ville, D. & Müller, H.
Multiscale Lung Texture Signature Learning Using The Riesz Transform
Medical Image Computing and Computer-Assisted Intervention MICCAI 2012, Springer Berlin / Heidelberg, 2012, 7512, 517-524

[Depeursinge2012b] Depeursinge, A.; Van De Ville, D.; Platon, A.; Geissbuhler, A.; Poletti, P.-A. & Müller, H.
Near-Affine-Invariant Texture Learning for Lung Tissue Analysis Using Isotropic Wavelet Frames
IEEE Transactions on Information Technology in BioMedicine, 2012, 16, 665-675

[Depeursinge2014a] Depeursinge, A.; Foncubierta-Rodrguez, A.; Van De Ville, D. & Müller, H.
Three-Dimensional Solid Texture Analysis and Retrieval in Biomedical Imaging: Review and Opportunities
Medical Image Analysis, 2014, 18, 176-196

[Depeursinge2014b] Depeursinge, A.; Foncubierta-Rodrguez, A.; Van De Ville, D. & Müller, H.
Rotation-Covariant Texture Learning Using Steerable Riesz Wavelets
IEEE Transactions on Image Processing, 2014, 23, 898-908

[Depeursinge2015a] Depeursinge, A.; Pad, P.; Chin, A. C.; Leung, A. N.; Rubin, D. L.; Müller, H. & Unser, M.
Optimized Steerable Wavelets for Texture Analysis of Lung Tissue in 3-D CT: Classification of Usual Interstitial Pneumonia
IEEE 12th International Symposium on Biomedical Imaging, IEEE, 2015, 403-406

[Depeursinge2015b] Depeursinge, A.; Chin, A. C.; Leung, A. N.; Terrone, D.; Bristow, M.; Rosen, G. & Rubin, D. L.
Automated Classification of Usual Interstitial Pneumonia Using Regional Volumetric Texture Analysis in High-Resolution CT
Investigative Radiology, 2015, 50, 261-267

References (sorting in alphabetical order)

[Dumas2009] Dumas, A.; Brigitte, M.; Moreau, M.; Chrétien, F.; Baslé, M. & Chappard, D.
Bone Mass and Microarchitecture of Irradiated and Bone Marrow-Transplanted Mice: Influences of the Donor Strain
Osteoporosis International, Springer-Verlag, 2009, 20, 435-443

[Galloway1975] Galloway, M. M.
Texture Analysis Using Gray Level Run Lengths
Computer Graphics and Image Processing, 1975, 4, 172-179
(Gal1975)

[Gerlinger2012] Gerlinger, M.; Rowan, A. J.; Horswell, S.; Larkin, J.; Endesfelder, D.; Gronroos, E.; Martinez, P.; Matthews, N.; Stewart, A.; Tarpey, P.; Varela, I.; Phillimore, B.; Begum, S.; McDonald, N. Q.; Butler, A.; Jones, D.; Raine, K.; Latimer, C.; Santos, C. R.; Nohadani, M.; Eklund, A. C.; Spencer-Dene, B.; Clark, G.; Pickering, L.; Stamp, G.; Gore, M.; Szallasi, Z.; Downward, J.; Futreal, P. A. & Swanton, C.
Intratumor Heterogeneity and Branched Evolution Revealed by Multiregion Sequencing
New England Journal of Medicine, 2012, 366, 883-892

[Gurcan2009] Gurcan, M. N.; Boucheron, L. E.; Can, A.; Madabhushi, A.; Rajpoot, N. M. & Yener, B.
Histopathological Image Analysis: A Review
IEEE Reviews in Biomedical Engineering, 2009, 2, 147-171

[Haidekker2011] Haidekker, M. A.
Texture Analysis
Advanced Biomedical Image Analysis, John Wiley & Sons, Inc., 2010, 236-275

[Haralick1979] Haralick, R. M.
Statistical and Structural Approaches to Texture
Proceedings of the IEEE, 1979, 67, 786-804

References (sorting in alphabetical order)

[Khan2013] Khan, A. M.; El-Daly, H.; Simmons, E. & Rajpoot, N. M.
HyMaP: A Hybrid Magnitude-Phase Approach to Unsupervised Segmentation of Tumor Areas in Breast Cancer Histology Images
Journal of pathology informatics, Medknow Publications, 2013, 4

[Kumar2012] Kumar, V.; Gu, Y.; Basu, S.; Berglund, A.; Eschrich, S. A.; Schabath, M. B.; Forster, K.; Aerts, H. J. W. L.; Dekker, A.; Fenstermacher, D.; Goldgof, D. B.; Hall, L. O.; Lambin, P.; Balagurunathan, Y.; Gatenby, R. A. & Gillies, R. J.
Radiomics: The Process and the Challenges
Magnetic Resonance Imaging, 2012, 30, 1234-1248

[Lazebnik2005] Lazebnik, S.; Schmid, C. & Ponce, J.
A Sparse Texture Representation Using Local Affine Regions
IEEE Transactions on Pattern Analysis and Machine Intelligence, IEEE Computer Society, 2005, 27, 1265-1278

[Malik2001] Malik, J.; Belongie, S.; Leung, T. & Shi, J.
Contour and Texture Analysis for Image Segmentation
International Journal of Computer Vision, Kluwer Academic Publishers, 2001, 43, 7-27

[Mosquera2015] Mosquera-Lopez, C.; Agaian, S.; Velez-Hoyos, A. & Thompson, I.
Computer-Aided Prostate Cancer Diagnosis From Digitized Histopathology: A Review on Texture-Based Systems
IEEE Reviews in Biomedical Engineering, 2015, 8, 98-113

[Ojala2002] Ojala, T.; Pietikäinen, M. & Mäenpää, T.
Multiresolution Gray-Scale and Rotation Invariant Texture Classification with Local Binary Patterns
IEEE Transactions on Pattern Analysis and Machine Intelligence, 2002, 24, 971-987

References (sorting in alphabetical order)

[Petrou2006] Petrou, M. & Garcia Sevilla, P.
Image Processing: Dealing with Texture
Wiley, 2006

[Petrou2011] Petrou, M.
Deserno, T. M. (Ed.)
Texture in Biomedical Images
Biomedical Image Processing, Springer-Verlag Berlin Heidelberg, 2011, 157-176

[Portilla2000] Portilla, J. & Simoncelli, E. P.
A Parametric Texture Model Based on Joint Statistics of Complex Wavelet Coefficients
International Journal of Computer Vision, Kluwer Academic Publishers, 2000, 40, 49-70

[Romeny2011] ter Haar Romeny, B. M.
Deserno, T. M. (Ed.)
Multi-Scale and Multi-Orientation Medical Image Analysis
Biomedical Image Processing, Springer-Verlag Berlin Heidelberg, 2011, 177-196

[Sifre2014] Sifre, L. & Mallat, S.
Rigid-Motion Scattering for Texture Classification
Submitted to International Journal of Computer Vision, 2014, abs/1403.1687, 1-19

[Simoncelli1995] Simoncelli, E. P. & Freeman, W. T.
The Steerable Pyramid: A Flexible Architecture for Multi-Scale Derivative Computation
Proceedings of International Conference on Image Processing, 1995, 3, 444-447

[Storath2014] Storath, M.; Weinmann, A. & Unser, M.
Unsupervised Texture Segmentation Using Monogenic Curvelets and the Potts Model
IEEE International Conference on Image Processing (ICIP), 2014, 4348-4352

References (sorting in alphabetical order)

[Unser2011] Unser, M.; Chenouard, N. & Van De Ville, D.
Steerable Pyramids and Tight Wavelet Frames in $L_2(\mathbb{R}^d)$
IEEE Transactions on Image Processing, 2011, 20, 2705-2721

[Unser2013] Unser, M. & Chenouard, N.
A Unifying Parametric Framework for 2D Steerable Wavelet Transforms
SIAM Journal on Imaging Sciences, 2013, 6, 102-135

[Varma2005] Varma, M. & Zisserman, A.
A Statistical Approach to Texture Classification from Single Images
International Journal of Computer Vision, Kluwer Academic Publishers, 2005, 62, 61-81

[Ward2014] Ward, J. & Unser, M.
Harmonic Singular Integrals and Steerable Wavelets in $L_2(\mathbb{R}^d)$
Applied and Computational Harmonic Analysis, 2014, 36, 183-197

[Ward2015] Ward, J.; Pad, P. & Unser, M.
Optimal Isotropic Wavelets for Localized Tight Frame Representations
IEEE Signal Processing Letters, 2015, 22, 1918-1921

[Xu2012] Xu, J.; Napel, S.; Greenspan, H.; Beaulieu, C. F.; Agrawal, N. & Rubin, D.
Quantifying the Margin Sharpness of Lesions on Radiological Images for Content-Based Image Retrieval
Medical Physics, 2012, 39, 5405-5418